Dissertations in Health Sciences

UNIVERSITY OF
EASTERN FINLAND

JONNA TENHUNEN

Exploring SIRT6 modulators and an indirect approach to regulate sirtuin activity

EXPLORING SIRT6 MODULATORS AND AN INDIRECT APPROACH TO REGULATE SIRTUIN ACTIVITY

Jonna Tenhunen

EXPLORING SIRT6 MODULATORS AND AN INDIRECT APPROACH TO REGULATE SIRTUIN ACTIVITY

To be presented by permission of the Faculty of Health Sciences,
University of Eastern Finland for public examination in MD100 Auditorium,
Kuopio
on December 5th, 2020, at 12 o'clock noon

Author's address: School of Pharmacy
                       University of Eastern Finland
                       KUOPIO
                       FINLAND

Doctoral programme: Doctoral Programme in Drug Discovery

Supervisors: Docent Maija Lahtela-Kakkonen, Ph.D.
                       School of Pharmacy
                       University of Eastern Finland
                       KUOPIO
                       FINLAND

                       Minna Rahnasto-Rilla, Ph.D.
                       School of Pharmacy
                       University of Eastern Finland
                       KUOPIO
                       FINLAND

                       Jenni Küblbeck, Ph.D.
                       A.I. Virtanen Institute for Molecular Sciences
                       University of Eastern Finland
                       KUOPIO
                       FINLAND

Reviewers: Associate Professor Katarina Nikolić, Ph.D.
                       Department of Pharmaceutical Chemistry
                       University of Belgrade
                       BELGRADE
                       SERBIA

                       Docent Henri Xhaard, Ph.D.
                       Division of Pharmaceutical Chemistry and Technology
                       University of Helsinki
                       HELSINKI
                       FINLAND

Opponent: Professor Outi Salo-Ahen, Ph.D.
                       Department of Biosciences
                       Åbo Akademi
                       TURKU
                       FINLAND

ABSTRACT

A drug development process often starts with the identification of a disease-related target that is most often a protein. The target must have a site where a drug-like molecule (DLM) can bind and undergo interactions to alter the activity of the target. Several computational DLM binding site prediction tools, such as SiteMap, have been developed; these are especially important if no ligands or their binding sites for the target have been reported. Should there be a known DLM that modulates the target, then the binding site can be detected by co-crystallising the DLM with the target, or by using other experimental methods.

Sirtuins (SIRTs) are class III histone deacetylases (HDACs) that can deacetylate lysine residues of several proteins and thus control gene expression as well as various cellular pathways. The most widely studied SIRTs have been SIRT1–3 while SIRT6 has been less extensively investigated. SIRT6 is a possible drug development target in many age-related diseases, for example in cancer, where it can act as either a tumour suppressor or promotor. Thus, SIRT6 should be either activated or inhibited depending on the type of the cancer. While some structures of SIRT6 inhibitors have been published, only a few activators have been described so far. Overall, developing SIRT activators is challenging, as the location of activator binding site is still a matter of debate.

In this work, novel and potent SIRT6 modulators were discovered experimentally and their binding pockets and interactions were predicted with computational molecular modelling methods. The inhibitors were predicted to bind to sites where they would either disturb the binding of substrate or the co-factor of the deacetylation reaction. Two possible activator binding sites were investigated with computational method, but SIRT6 might have other activator binding sites that should be also examined.

As SIRT activators are difficult to develop, an alternative approach to modulating SIRT activity was also investigated. Inhibition of bromodomain and extraterminal proteins (BETs), that are also involved in histone lysine acetylation, was shown to modulate SIRT1 protein levels. All in all, this work gives new tools to investigate

SIRT6-related diseases and develop more potent SIRT6 modulators and alternative experimental methods to affect SIRT activity.

TIIVISTELMÄ

Lääkekehitys alkaa usein sairauteen liittyvän kohteen tunnistamisella. Kohde on yleensä proteiini, johon lääkeaineen kaltainen molekyyli (ligandi) voi sitoutua ja muodostaa vuorovaikutuksia siten, että kohteen aktiivisuus muuttuu. Nämä sitoutumispaikat sijaitsevat yleensä proteiinien onkalomaisissa rakenteissa, ja niiden sijainnin ennustamiseen on kehitetty useita tietokoneavusteisia menetelmiä, kuten esimerkiksi SiteMap. Nämä menetelmät ovat hyödyllisiä varsinkin silloin, jos kohteeseen sitoutuvia ligandeja tai niiden sitoutumispaikkoja proteiinissa ei tiedetä. Jos kohdetta säätelevä ligandi tunnetaan, sitoutumiskohta voidaan selvittää kiteyttämällä ligandi yhdessä kohteen kanssa tai käyttämällä muita kokeellisia menetelmiä.

Sirtuiinit ovat luokan III histonideasetylaaseja (HDAC), jotka voivat deasetyloida proteiinien lysiinejä ja siten kontrolloida geeniekspressiota ja erilaisia säätelyreittejä soluissa. Ihmisten sirtuiineista (SIRT1-7) eniten tutkittuja ovat SIRT1–3, kun taas SIRT6:a on tutkittu vielä vähän. SIRT6 on mahdollinen lääkekehityksen kohde syövässä ja muissa ikääntymiseen liittyvissä sairauksissa. Syövässä SIRT6 voi toimia tuumorisuppressorina tai -promoottorina ja täten SIRT6:a pitäisi estää tai aktivoida riippuen syövästä. Joitain SIRT6-inhibiittoreita on julkaistu, mutta toistaiseksi aktivaattoreita tunnetaan vähän. SIRT-aktivaattorien kehittäminen on yleisestikin vaikeaa, koska niiden sitoutumiskohdan sijannista ei ole varmuutta.

Tässä työssä tunnistettiin kokeellisesti uusia ja tehokkaita SIRT6-säätelijöitä ja niiden sitoutumistaskuja ja vuorovaikutuksia ennustettiin laskennallisten molekyylimallinnustyökalujen avulla. Inhibiittorien ennustettiin sitoutuvan siten, että ne häiritsevät substraatin tai deasetylaatioreaktion kofaktorin sitoutumista. Kahta mahdollista aktivaattorien sitoutumiskohtaa tutkittiin, mutta SIRT6:lla voi olla myös muita aktivaattorin sitoutumiskohtia, joita tulisi myös tutkia.

Koska SIRT-aktivaattoreita on vaikea kehittää, myös vaihtoehtoista tapaa säädellä SIRT:ien aktiivisuutta tutkittiin. Histonien lysiininen asetylaation liittyvien BET-proteiinien estäminen vaikutti SIRT1-proteiinitasoihin. Kokonaisuudessaan tämä työ antaa uusia työkaluja tutkia SIRT6:een liittyviä sairauksia ja kehittää tehokkaampia SIRT6-säätelijöitä sekä vaihtoehtoisia menetelmiä SIRT-aktiivisuuden säätelyyn.

If it's not Here, that means it's out There.

- Winnie the Pooh

ACKNOWLEDGEMENTS

I would like to first thank my supervisors Maija Lahtela-Kakkonen, Minna Rahnasto-Rilla, and Jenni Küblbeck for the guidance during the studies. Maija, thank you for providing me the opportunities to visit all the training schools, conferences, and collaborating groups. Thank you also for having so much effort on figuring out my funding and being patient and appreciating my work especially when I was not satisfied to my results. Minna, thank you for all the discussions on our research topic and giving your time to work together with the manuscripts, especially helping to format difficult sentences. Thank you also for the tips for writing grant applications and guidance to the mysterious world of western blotting. Jenni, thank you for all the excellent comments for the thesis manuscript. The suggestions concerning the tables really improved the manuscript.

I thank Ewen McDonald for checking the language of the thesis. I also thank the thesis reviewers Katarina Nikolić and Henri Xhaard for taking the time to evaluate my thesis. The comments and suggestions for corrections were really useful. I also thank professor Outi Salo-Ahen for accepting the invitation to be the opponent.

I would like to thank Sari for guiding and helping me with the cell culturing and cell experiments already during my master's studies. I also thank all research collaborators and co-authors. Big thanks also for all the Pharmaceutical Chemistry group at UEF for creating a supporting working environment. Especially I would like to thank Tuomo for helping with software issues and in several modelling problems. Special thanks also to Prasanthi and Arun for all the tips and discussions related to modelling and everyday life. I am grateful also to all fellow PhD students that I have met and who have supported me during these years. I thank also Pekka and all the fellow lab teachers I have worked with during these years.

To my best friend Rosa: thank you for encouraging me during these studies. Thank you for showing interest on my work even though your field of expertise is somewhere else. I also thank my sisters Katri, Marika, and Elina. Katri: thank you for reviewing one of my working grant applications (the one that actually got accepted). Marika: thank you for all the scientific and philosophical conversations during these four years and also before that. Elina: It has been really important for me that you have lived close to me and that I have been able to visit you. Especially during the first academic years it meant a lot.

To my parents Ritva and Martti: thank you for all the support from the beginning of my life. You have raised four women, who all have had the opportunity to study

after high school and get education. Finally, I thank my husband Iiro, who has supported me (financially and emotionally) during all the years, reviewed a couple of grant applications and offered true IT support at home. I would have never made it without you.

20th of November 2020, Kuopio

Jonna Tenhunen

LIST OF ORIGINAL PUBLICATIONS

This dissertation is based on the following original publications:

I   Rahanasto-Rilla M[a], Tyni J[a,b], Huvoinen M, Jarho E, Kulikowicz T, Ravichandran S, Bohr VA, Ferrucci L, Lahtela-Kakkonen M, Moaddel R. Natural polyphenols as sirtuin 6 modulators. Sci Rep 8: 4163, 2018.

II   Heger V[a], Tyni J[a,b], Hunyadi A, Horáková L, Lahtela-Kakkonen M, Rahnasto-Rilla M. Quercetin based derivatives as sirtuin inhibitors. Biomed Pharmacother 111: 1326–1333, 2019.

III   Tenhunen J, Kučera T, Huovinen M, Küblbeck J, Bisenieks E, Vigante B, Ogle Z, Duburs G, Doležal M, Moaddel R, Lahtela-Kakkonen M, Rahnasto-Rilla M. Screening of SIRT6 modulators: impact of novel activator on breast cancer cells. Submitted.

IV   Tenhunen J, Kokkola T, Huovinen M, Rahnasto-Rilla M, Lahtela-Kakkonen M: Impact of structurally diverse BET inhibitors on SIRT1. Gene 741: 144558, 2020.

The publications were adapted with the permission of the copyright owners.

[a]Equal contribution.

[b]Jonna Tenhunen, née Tyni

The two main authors in publications I and II contributed equally to the work. In publication I and II JT designed and conducted the molecular modelling studies and analysed the results and the other main author performed *in vitro* studies. In publication III, TK conducted preliminary modelling studies and JT did further molecular modelling studies. In publication IV, JT designed and conducted all the experimental studies and analysed the results. JT participated in designing, writing, and editing the manuscript text and figures in all publications.

CONTENTS

ABBREVIATIONS

ADP	Adenosine diphosphate	I%	Inhibition percentage
ADPr	Adenosine diphosphate ribose	KAP1	KRAB-associated protein-1
BET	Bromodomain and extraterminal motif family	KRAB	Krüppel associated box
		LiF-MS	Ligand-footprinting mass spectrometry
BRD	Bromodomain	MD	Molecular dynamics
DLM	Drug-like molecule	MM-PBSA	Molecular mechanics with Poisson-Boltzmann and surface area continuum solvation
FA	Fold of activation		
FA_{max}	Maximal-fold of activation		
FEP	Free energy perturbation	MM-GBSA	Molecular mechanics with generalized Born and surface area continuum solvation
FOXO1	Forkhead box protein O1		
FoxO3α	Forkhead box protein O3	NAD^+	Nicotinamide adenine dinucleotide (oxidized form)
GCN5	General control non-repressed	NAM	Nicotinamide
GLUT-1	Glucose transporter type 1	NAMPT	Nicotinamide phosphoribosyl-transferase
HAT	Histone acetyl transferase	NMR	Nuclear magnetic resonance
HDAC	Histone deacetylase	*O*AADPr	*O*-acetylated adenosine diphosphate ribose
HPLC	High-performance liquid chromatography	PAL	Photo affinity labelling

PARP1	Poly [ADP-ribose] polymerase 1	RMSD	Root mean squared deviation
PCA	Principal component analysis	SDS-PAGE	Sodium dodecyl sulfate-polyacrylamide gel electrophoresis
PDB	Protein Data Bank		
PKM2	Pyruvate kinase M2	SDM	Site-directed mutagenesis
PPI	Protein-protein interaction	SIRT	Human sirtuin
PVDF	Polyvinylidene difluoride	SP	Standard precision
		TF	Transcription factor
PZA	Pyrazinamide	TNF-α	Tumor necrosis factor alpha
qPCR	Quantitative polymerase chain reaction		
		Twist1	Twist-related protein 1
RCSB PDB	Research Collaboratory for Structural Bioinformatics Protein Data Bank	XP	Extra precision

1 INTRODUCTION

Rational drug development often starts with the identification of a valid drug target. The target can be a human or pathogenic macromolecule, e.g. a protein or nucleic acid. In this thesis, the term target is used to refer to a protein as they are the most common drug targets (Overington et al. 2006, Santos et al. 2017). Once the target has been identified, it is important to evaluate if it is **druggable** as undruggability of a target is one of the major reasons why drug development processes often fail (Hingorani et al. 2019). The term druggable is defined as the ability of the target protein to interact with a drug-like molecule (DLM) with high enough affinity and to exert a therapeutic effect (Hopkins and Groom 2002, Edfeldt et al. 2011, Hussein et al. 2017). The term DLM is used in this thesis to refer to a drug-like small molecule that is not an endogenous ligand nor an approved drug, whereas the term ligand is used here to refer to any molecule that binds to a target.

Binding site prediction and detection is one way to assess the druggability of the target. The binding sites of drugs can be classified to orthosteric and allosteric sites (Wenthur et al. 2014). Orthosteric sites are the sites where endogenous ligands e.g. receptor agonists and antagonists or enzyme substrates bind. Allosteric sites are located distinct from the orthosteric site; a drug that binds to an allosteric site can change the protein's 3D conformation and thus, protein activity (Schwartz and Holst 2007, Wenthur et al. 2014, Lisi and Loria 2017). Protein-protein interaction (PPI) sites have also been proposed to be drug binding sites (Jin et al. 2014).

The identification of a drug-binding site is straightforward if a 3D structure of the protein has been crystallised with a drug. So far, approximately 171 000 macromolecular structures have been published in the Research Collaboratory for Structural Bioinformatics Protein Data Bank (RCSB PDB), but not all of them contain a co-crystallized drug (Berman et al. 2000, RCSB PDB 2020). However, structures that contain other ligands, e.g. enzyme substrates or cofactors, can be sometimes used in determining the DLM-binding site, as they show the orthosteric binding site.

If the target has not been crystallised with a ligand, the location of a possible binding site can be predicted and its druggability can be evaluated with computational modelling approaches (Dukka 2013, Roche et al. 2015, Zhao et al. 2020). These methods are based on the prior knowledge of the general properties of drug- and DLM-binding sites such as sequence, geometry, size, physicochemical properties, and possible interactions. In addition to molecular modelling methods, different *in vitro* applications can also be used in determining the binding sites (Smith and Collins 2015, Syson et al. 2016, Sirtori et al. 2018).

In recent years, epigenetic regulators have attracted interest in the field of drug research (Lanza et al. 2019, Lu et al. 2020a, Schiano et al. 2020). Epigenetic regulators can alter gene expression and affect phenotype without modifying genotype for example by controlling the post-translational modifications of histones and DNA. One of these post-translational modifications is histone lysine acetylation. The

acetylation of N-terminal lysines weakens the interaction between histones and DNA, leading to a less compact chromatin structure and subsequently activation of gene expression. The proteins that control the acetylation are histone acetyl transferases (HATs) and histone lysine deacetylases (HDACs) including human sirtuins (SIRTs) (Figure 1) (Filippakopoulos et al. 2010, Biswas and Rao 2018). Additionally, bromodomain (BRD) containing proteins can bind to acetylated lysines and serve as a binding platform for different transcription factors (TFs). Interestingly, some inhibitors of bromodomain containing proteins have been shown to potentiate the effects of certain HDAC inhibitors and thus, there might be a functional link between them (Kim et al. 2018, Meng et al. 2018, Cortiguera et al. 2019).
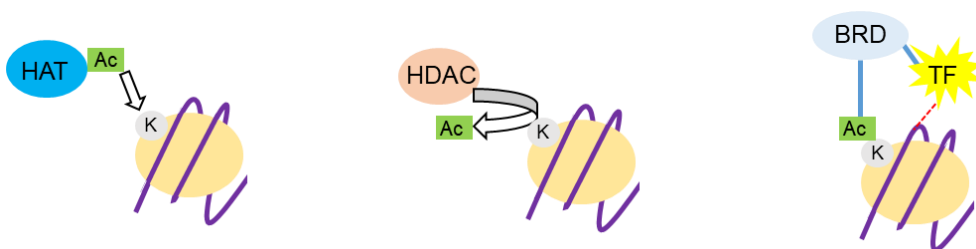
Figure 1. HATs, HDACs, and BRD-containing proteins are related to histone lysine (K) acetylation (Ac). Histones are presented with a peach colored shape that is surrounded by DNA (purple string). Transcription factor is abbreviated with TF.

HDACs, including SIRTs, are considered as promising drug targets, especially in cancer research. While four HDAC-targeting drugs have been approved by U.S. Food and Drug Administration, none of them target specifically SIRTs (Autin et al. 2019, Sanaei and Kavoosi 2019). Despite the great effort put into the development of small molecule SIRT deacetylase modulators, most of the modulators have targeted three SIRTs i.e. SIRT1, SIRT2, and SIRT3 while much fewer modulators for SIRT4, SIRT5, SIRT6, and SIRT7 have been published. Moreover, the number of small molecule SIRT deacetylase activators lags behind the inhibitors as the development of activators is more difficult due to the uncertainty related to both the binding site and the mechanism of enzyme activation (Dai et al. 2018). In addition to small molecule inhibitors and activators that alter the velocity of enzymatic reaction, cellular SIRT activity can be modulated by controlling the gene expression, cofactor levels and post-translational modifications of the SIRTs (Revollo and Li 2013, Zhao and Zhou 2020).

In this thesis, molecular modelling tools for binding site prediction and evaluation have been used to investigate the putative binding sites and interactions of small molecules inhibiting and activating SIRT6. Additionally, inhibition of BRD-containing proteins was investigated exprermintally as an alternative approach to modulating SIRT activity.

2 REVIEW OF THE LITERATURE

2.1 THE MODELS OF LIGAND-PROTEIN BINDING

The drug-binding sites are usually located in protein cavities that are quite commonly referred to as pockets (Stank et al. 2017). The size of drug-binding pockets varies; the average volume of a pocket has been estimated to be 930 $Å^3$, but it can vary from 100 to up to 1000 $Å^3$ (Liang et al. 1998, Nayal and Honig 2006). Besides the volume, also the shape, flexibility, and physicochemical properties of the pocket affect the binding of a drug or a DLM and thus not all proper-sized pockets are druggable (Ehrt et al. 2019). Different models describing the binding of ligands, including DLMs, to a protein pocket consider the size and shape of the pocket (Figure 2). In addition, some of them also consider the flexibility or physicochemical properties.

In 1894, Emil Fischer introduced the first theory describing the binding of a ligand to a protein (Fischer 1894). He stated that a ligand should fit into its binding pocket as a key fits into a lock (Figure 2). In other words, the shape of a ligand should be complementary to the shape of its pocket. However, the ligand and the protein pocket should not be considered as a static and rigid structure as usually molecules tend to be flexible. In fact, a ligand that approaches a protein binding pocket can induce some conformational changes in the structure of the pocket (Koshland 1958, Stank et al. 2016). Considering this dynamic nature of both protein and ligand, Daniel Koshland Jr. proposed an induced-fit model in 1958 (Figure 2).

Another model considering the pocket flexibility is the conformational selection model (aka population shift or selected fit model) (Figure 2) (Weikl and von Deuster 2009, Csermely et al. 2010, Kar et al. 2010, Paul and Weikl 2016). Instead of suggesting that a ligand induces changes in the conformation of the binding pocket, this theory proposes that the ligand selects one of the many possible pocket conformations. The zipper model is the third flexibility-considering method; it considers the ligand's flexibility rather than the flexibility of the pocket (Figure 2) (Burgen et al. 1975). It suggests that the ligand binds with one part to a subsite of the pocket which changes the ligand conformation. After the conformational change, the ligand can bind with another part to another subsite of the pocket.

Tripathi and Bankaitis (2017) have introduced the combination lock model that differs from the other models: it also considers the physicochemical environment of the pocket and the interactions in describing ligand-protein recognition (Figure 2). This model proposes that the physicochemical environment of a pocket should be compatible with a ligand, and that the pocket should form favourable interactions with the ligand.
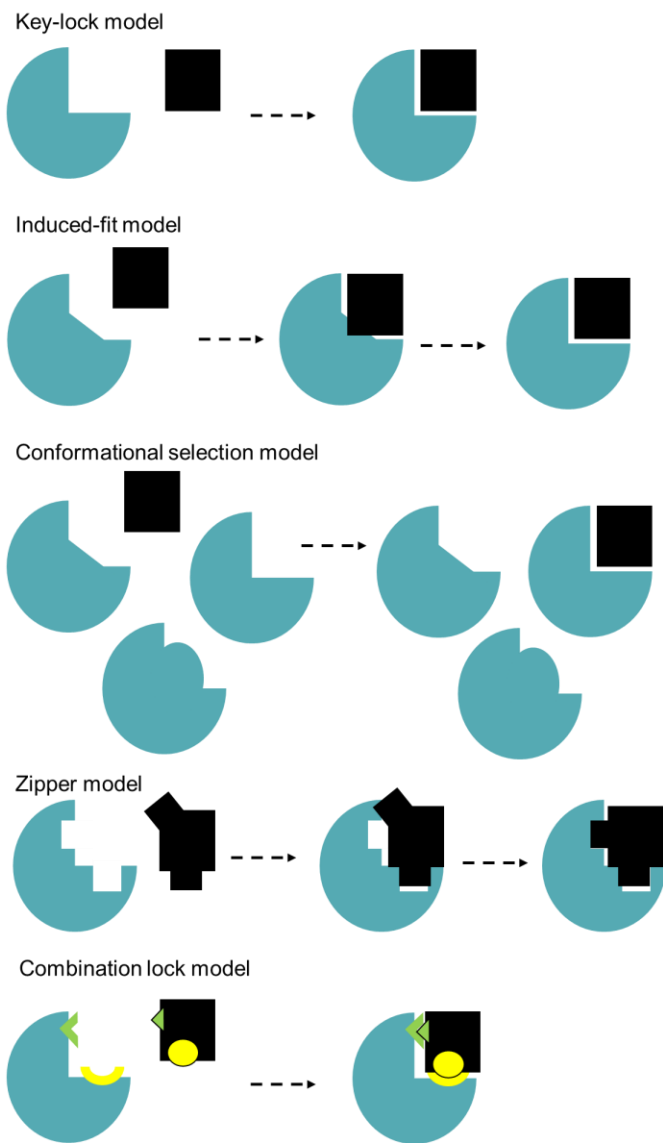
Figure 2. Schematic figure of different models of protein-drug binding. The turquoise shape represents the protein pocket, and the black shape represents the drug. In the combination lock model, the green and yellow shapes represent the features that should match.

All together, the different binding models consider the shape (geometry), conformation, and interactions of binding. The reason why they are important for ligand binding can be explained by thermodynamics (O'Brien et al. 2017). A thorough discussion of the thermodynamics of binding is outwith the scope of this thesis; the issue has been discussed broadly, for example by Velazquez-Campoy et al. (2001), Geschwindner et al. (2015), Du et al. (2016), and O'Brien et al. (2017). However, the principal idea is that a ligand can bind to a protein pocket only if the

energy of the system decreases (Du et al. 2016). This means that the drug-protein complex needs to have lower energy than the system where they are separated and interact with the solvent. Thus, the interactions between the protein and drug should be stronger than those that they have with the solvent when the drug is unbound (Du et al. 2016, O'Brien et al. 2017). However, also other factors, such as conformational freedom, affect the energy difference between the two systems. This energy difference is commonly described with Gibbs free energy, ΔG (Velazquez-Campoy et al. 2001, Du et al. 2016, O'Brien et al. 2017).

2.2 BINDING POCKET PREDICTION AND DETECTION

The lack of knowledge about the location and properties of a DLM binding pocket in the target protein can be a limiting factor in designing compounds that would alter the target's activity. Sometimes the structure of the target in a complex with a similar DLM or another ligand might be available, and the binding site can be estimated based on the co-crystallised ligand. However, estimating the site can be challenging if there are conflicts between different crystal structures. For example, the crystal structures of human sirtuins (SIRTs) in complex with their activators suggest that the activators might have diverse binding sites (Dai et al. 2018). Additionally, the binding site shown in a crystal structure might disagree with the *in vitro* results, as in case of a SIRT6 inhibitor (Wood et al. 2018, You and Steegborn 2018). If no ligands have been crystallised with the target, the binding pockets and sites can be predicted with computational methods or they can be determined with different experimental methods.

2.2.1 Computational applications for binding site prediction

Numerous computational algorithms and programs for predicting DLM binding sites have been developed during the past decades (Table 1) and they have been discussed in several reviews (Dukka 2013, Roche et al. 2015, Zhao et al. 2020). Here, the methods are divided into five main groups: geometric approaches, energetic approaches, sequence and structure comparison methods, machine learning methods, and molecular dynamics (MD) approaches. The predicted binding sites can be evaluated and ranked with druggability-assessing methods. Methods that are developed only for visualizing of predetermined cavities are not considered here as binding site prediction methods.

Geometric approaches
In general, the geometric approaches analyse protein 3D structure to find cavities that would be optimal in size and/or shape for DLM binding. Geometric approaches can be classified into different groups; in the current work they are divided into grid-based, and sphere-based methods. In grid-based methods, the protein is placed onto a 3D grid and the grid is scanned step-by-step to identify those grid points that would form the pocket (Simões et al. 2017). For example, the decision of whether a grid point

is a part of the pocket or not, can be made based on the distance of the grid point from the surrounding protein atoms or surfaces.

Table 1. Examples of different pocket detection methods.

APPROACH	ALGORITHM / PROGRAM	REFERENCE
GEOMETRIC APPROACHES		
Grid scanning	POCKET	Levitt and Banaszak 1992
	VOIDOO	Kleywegt and Jones 1994
	LIGSITE, LIGSITE[CSC]	Hendlich et al. 1997, Huang and Schroeder 2006
Grid scanning combined to energetic approach	SiteMap	Halgren 2007, Halgren 2009
Sphere-based	SURFNET	Laskowski 1995
	PASS	Brady and Stouten 2000
	SCREEN	Nayal and Honig 2006
	Roll/POCASA	Yu et al. 2010
	APROPOS	Peters et al.1996
	CAST	Liang et al. 1998
	Fpocket	Le Guilloux et al. 2009
	AlphaSpace	Rooklin et al. 2015
ENERGETIC APPROACHES		
Probe-based	GRID	Goodford 1985
	Q-SiteFinder	Laurie and Jackson 2005
	FTMap	Brenke et al. 2009
Potential map evaluation	PocketFinder	An et al. 2005
SEQUENCE AND STRUCTURE COMPARISON METHODS		
Evolution rate calculation	ConSurf	Armon et al. 2001, Glaser et al. 2003
	Rate4Site	Pupko et al. 2002
Sequence identity, alignment	FINDSITE	Brylinski and Sklonick 2008
Alignment	COFACTOR	Roy and Zhang 2012
	G-LoSA	Lee and Im 2012
MACHINE LEARNING METHODS		
Geometry- and sequence-based	ConCavity	Capra et al. 2009
Atom property considering	P2Rank	Krivák and Hoksza 2018
MD APPROACHES		
Probe based MD simulation	Isopropyl probe method	Seco et al. 2009
PCA tool	PocketAnalyzer[PCA]	Craig et al. 2011
Fpocket utilizing tool	MDPocket	Schmidtke et al. 2011
Multiple probe MD	MixMD	Ung et al. 2016

One of the first grid-based methods was POCKET that utilizes a density map in determining the binding pocket (Levitt and Banaszak 1992). Two years after POCKET's release, Kleywegt and Jones (1994) published a method called *VOIDOO*,

which can also be used in calculating the volume of the pockets. *VOIDOO* and another grid-based method, LIGSITE, use a smaller grid point spacing and sphere radius than POCKET, which makes them more accurate methods (Kleywegt and Jones 1994, Hendlich et al. 1997).

SiteMap is another grid-based binding site detection method (Halgren 2007, Halgren 2009). It determines binding sites by including the grid points (or site points) that are close enough to the protein and each other, and where a probe molecule displays good enough van der Waals interaction energies with protein atoms (Halgren 2009). Thus, SiteMap is a method that uses both geometric and energetic approaches in determining the location of a pocket. It uses the probe-based energetic approach also to characterise the hydrophilic and hydrophobic parts of the detected pockets.

Sphere-based geometric methods locate cavities by placing sphere probes on the different surfaces of protein without generating a grid. The probes can be placed between two, three or four atoms. SURFNET is an example of a sphere-based method that places the spheres between two atoms, and PASS is one of the programs that places spheres between three atoms (Laskowski 1995, Brady and Stouten 2000). The algorithms and programs that place the sphere between four atoms are based on the Alpha sphere algorithm (Edelsbrunner and Mücke 1994). Peters and co-workers were the first to introduce a shape-evaluating alpha sphere-based algorithm, APROPOS (Peters et al. 1996). Combinations of sphere- and grid-based approaches have been also introduced; for example, there is an algorithm called Roll that is implemented in POCASA (Yu et al. 2010).

Energetic approaches

In energetic pocket detection approaches, the protein can be probed with small chemical moieties such as a methyl group (Henrich et al. 2010). The interaction energies between the small molecule probe(s) and protein are then calculated in different interaction sites. The pockets are determined to be at the sites, where the probes have the strongest interaction energies with the protein. These types of methods are based on the assumption that the probe molecules are drug-like enough to describe the binding of DLMs.

The foundation of energetic pocket detection approaches was the method called GRID devised by Goodford (1985). Goodford used amino, oxygen, hydroxyl, methyl, and water probes. Other probe-using methods are Q-SiteFinder, that uses methyl as a probe, and FTMap that uses 16 different small organic molecules in probing (Laurie and Jackson 2005, Brenke et al. 2009). In FTMap, the sites where the clusters of different probes overlap are more likely to be drug binding sites, and the largest of overlapping site areas are usually the most important ones. FTMap has been improved in several ways to serve different purposes from binding site prediction to druggability evaluation (Ngan et al. 2012a, Ngan et al. 2012b, Grove et al. 2013, Bohnuud et al. 2014, Kozakov et al. 2015).

PocketFinder also uses a probe-in-pocket prediction, but in a different way than the above-mentioned methods (An et al. 2005). The probe is an aliphatic carbon atom which is used in determining potential map of the protein. The pockets are then determined based on the potential and volume.

Sequence and structure comparison methods
The principle idea behind sequence comparison methods, aka evolutionary methods, is that functionally important regions such as enzyme active sites are rather well conserved among evolutionary related homologous proteins (Lichtarge et al. 1996, Valdar 2002). The binding site location of a protein can be predicted by utilizing the information of binding sites in structurally related proteins. The Evolutionary Trace method by Lichtarge et al. (1996) was one of the first of these types of methods. It uses sequence comparison in determining functionally important residues. There are other sequence comparing algorithms e.g. ConSurf algorithm and Rat4Site (Armon et al. 2001, Pupko et al. 2002).

Structure comparison methods such as FINDSITE, COFACTOR, and G-LoSA all use structural alignment in the binding site prediction (Brylinski and Skolnick 2008, Lee and Im 2012, Roy and Zhang 2012). In general, structure comparison methods differ from sequence prediction methods in that the reference proteins do not need to be homologous to the target protein if they have similar folding characteristics.

Machine learning methods
The increasing amount of information about drug binding sites has led to the development of several machine learning methods (Zhao et al. 2020). Machine learning enables the combination of information concerning several properties of previously detected binding sites. For example, these properties can describe interactions, the solvent accessible surface area, or an amino acid sequence.

Capra et al. (2009) have introduced a machine learning-based algorithm called ConCavity that relies on geometry and sequence comparison methods. Another machine-learning tool called P2Rank uses the properties of surface exposed atoms in predicting the binding site (Krivák and Hoksza 2018). Other examples are SFCscore, MetaPocket, NNSCORE, and eFindSite (Sotriffer et al. 2008, Huang 2009, Durrant and McCammon 2010, Brylinski and Feinstein 2013).

MD approaches
While machine learning methods represent a powerful tool to combine large amounts of information about binding site properties, they still might fail to detect all possible binding sites (Zhao et al. 2020). Proteins and their pockets exist in different conformations, and a crystallised protein structure captures only one of these conformations. Several studies have reported pockets and sites that at are absent when the protein is not bound within a ligand (Gee et al. 2007, Hudson et al. 2018, Hollingsworth et al. 2019). These pockets and sites are called cryptic and many

studies have aimed to predict their locations in different proteins (Bowman and Geissler 2012, Kimura et al. 2017, Comitani and Gervasio 2018).

In addition to cryptic pockets and sites, the pockets might have different conformations and sometimes ligand binding can induce conformational changes in the pocket and even in the entire protein (Stank et al. 2016). For example, these changes can involve the formation of a new subpocket or an adjacent pocket, contractive or expansive movement of the pocket, the formation of a channel or tunnel at the opening of the pocket, and conformational changes induced by the binding of an allosteric modulator to an adjacent site.

Molecular dynamics (MD) simulations can be applied to search for the conformational changes of pockets and cryptic binding sites. MD simulations for detecting binding sites can be probe-based, in which the protein is simulated with a solvent mixture containing small drug-like probe molecule(s) (Seco et al. 2009, Ung et al. 2016). The affinity of the probe(s) for different interaction sites during the simulation is calculated, and the highest affinity sites are the most probable drug-binding sites. Thus, the basic principle is similar to the probe-based energetic pocket detection methods. Seco et al. (2009) introduced a probe-based MD method that uses isopropyl alcohol probes for predicting hot spots of protein-protein interactions (PPIs). Mixed-Solvent MD (MixMD) is another probe-based MD method where acetonitrile, isopropanol, and pyrimidine, are used as probes (Ung et al. 2016).

Alternatively, the target protein can be simulated without probe molecules with the binding sites being predicted based on the motions of the protein. Principal Component Analysis (PCA) can be used to detect the major motions in the protein structure during the simulations. The sites of the largest movements have been speculated to serve as possible drug binding sites (Ho and Agard 2009, Ha and Loh 2013, David and Jacobs 2014). Automated tools for analysing the MD trajectory to detect possible binding pockets have also been developed. For example, PocketAnalyzer[PCA] and MDPocket detect the pockets from MD ensembles with a grid-based geometrical algorithm (Craig et al. 2011, Schmidtke et al. 2011). Cimermancic et al. (2016) have also introduced a computational tool called CryptoSite that in combination MD simulations, uses sequence analysis, and docking for prediction of cryptic binding sites.

Pocket ranking

The process of evaluating which of the predicted sites is the best or most probable DLM binding site is referred as the binding site assessment or pocket ranking (Huang and Jacobson 2010, Krivák and Hoksza 2015, Yang et al. 2016, Choudhary et al. 2017). Here, the term pocket ranking is used for describing the process where pockets are ranked for example based on descriptors, amino acid composition, or free energy prediction.

The descriptor-based methods aim to predict the druggability of the detected pockets. The descriptors are related to the physicochemical properties as well as the size and geometry of the pocket, which are the main aspects in different ligand

binding models. Hajduk et al. (2005) were among the first investigators to introduce a druggability evaluation method; it used pocket compactness, total surface area, polarity, and residue charges as descriptors. SCREEN, that used 408 different descriptors, was developed later by Nayal and Honig (2006). They suggested that the most relevant descriptors for druggability would be related to the pocket geometry and size. SiteMap, a method used also for pocket detection, can also evaluate the druggability of the predicted site (Halgren 2007, Halgren 2009). Binding site size, pocket enclosure, and hydrophilicity are the main druggability descriptors utilized by SiteMap. Pocket druggability can be evaluated also based on the amino acid composition. The PLB Index and its improved version, MF-PLB, are examples of ranking methods that evaluate the druggability of the detected pockets based on their amino acid composition (Soga et al. 2007, Cao and Xu 2016).

Another way to rank the pockets is to try to predict the binding free energy of the active and inactive ligands. One way to assess the energy is to dock the ligands to the predicted site, as scoring functions of different docking protocols can predict the free energy of binding (Huang and Jacobson 2010, Patschull et al. 2012, Michel et al. 2019, Thornton et al. 2019). The docking methods can be divided roughly into **1)** rigid docking methods, where both receptor and ligand are treated as rigid structures (rarely used nowadays), **2)** flexible docking, such as Glide (Friesner et al. 2004) and FlexX (Rarey et al. 1996), where the conformation of the ligand is sampled, and into **3)** induced fit protocols, such as Induced Fit (Sherman et al. 2006) and FiberDock (Mashiach et al. 2010), where both ligand and pocket are treated as flexible structures. However, the accuracy of the scoring functions of the docking programs varies and might depend on the target being investigated or how the components of the scoring function, e.g. interactions and solvent effects, are weighted (Cross et al. 2009, Xu et al. 2015a, Wang et al. 2016a, Pagadala et al. 2017). For example, the highest scoring pose might be complementary with the pocket but have only a few or no interactions (Lionta et al. 2014). Thus, a visual inspection of the docking results should also be carried out to evaluate the ranking of the pockets.

Methods for evaluating the binding free energy from MD simulations are also used in pocket ranking. These methods include molecular mechanics with Poisson-Boltzmann or generalized Born and surface area continuum solvation (MM-PBSA/GBSA) (Broomhead and Soliman 2017). In those methods, free energy is determined for all the possible drug-protein interaction sites present in the simulations and then compared to the free energy of the system where the drug is unbound. (Kollman et al. 2000). In order to obtain statistically relevant results from MM-PBSA/GBSA, it is suggested to run several short simulations rather than a few long simulations (Genheden and Ryde 2010, Wright et al. 2014). Methods that assess the binding energies from MD simulations are linear interaction energy and free energy perturbation (FEP) (Neubauer de Amorim et al. 2008, Cournia et al. 2017). FEP simulations might be more accurate if the protein conformation does not change significantly (Fratev and Sirimulla 2019).

2.2.2 Binding site identification with experimental methods

Structure-based methods

One way to locate the DLM binding pockets in the target is to solve the structure of the target-ligand complex, for example with X-ray crystallography (Renaud et al. 2016). However, the quality of the crystal structure must be evaluated. For example, the resolution should be preferably under 2.5 Å, as higher resolution values might mean that there are inaccuracies in the structure (Djinovic-Carugo and Carugo 2015, Maveyraud and Mourey 2020). The crystal structure might also have missing residues especially in loops and in the N- and C-terminal tails, which are more flexible and thus, their accurate positions are more difficult to capture (Djinovic-Carugo and Carugo 2015). Additionally, the components of the crystallization solution, such as polyethylene glycol or acetate ions, should not occupy possible binding site as they could prevent the ligand-binding to the site (Yamanaka et al. 2011, Maveyraud and Mourey 2020). Moreover, co-crystallizing a ligand with a protein might show conformational changes in the pocket that are not shown with a soaking method where the protein structure has been crystallised prior to the introduction of ligand (Ehrmann et al. 2017). The binding mode of the ligand might also be slightly different.

Nuclear magnetic resonance (NMR) spectroscopy is another method for solving the structures of ligand-protein complexes (Yee et al. 2002, Ziarek et al. 2011, Maity et al. 2019). However, the NMR technique is limited by the target size; it has been proposed that it can be best utilized for proteins containing under 250 amino acids or proteins with molecular weights under 40 kDa (Yee et al. 2002, Maveyraud and Mourey 2020). NMR and X-ray crystallography can be used as complementary tools (Savchenko et al. 2003, Yee et al. 2005, Doerr 2006, Feng et al. 2011)

Affinity-based methods

Photo affinity labelling (PAL) is one direct *in vitro* approach for validating binding sites. The labelling reagent use in PAL contains two parts: one part binds to the predicted protein binding site reversibly, and the other part is a photoreactive group that is activated by light and forms a reactive intermediate that binds covalently to the protein (Ruoho et al. 1973, Gronemeyer and Govindan 1986, Smith and Collins 2015). Several studies identifying binding sites with PAL have been published (Seifert et al. 2016, Cheng et al. 2019, Hsieh et al. 2019).

Ligand-footprinting mass spectrometry (LiF-MS) is another direct method for detecting binding sites for active DLMs. The method's idea is to apply modifications (such as hydrogen to deuterium exchange) in the protein-ligand complex (Sirtori et al. 2018). After ligand dissociation, the binding site can be detected based on the assumption that the binding site is less modified as the ligand has decreased the rate of modifications of the binding site. The different approaches of LiF-MS have been described in more detail in several reviews and reports (Sirtori et al. 2018, Li et al. 2019, Guo et al. 2020, Lu et al. 2020b).

Site-directed mutagenesis (SDM), where a mutation is introduced into the proposed binding site, can be also used in confirming indirectly the DLM binding site (Geissler et al. 2007, Syson et al. 2016, Ricatti et al. 2019). After the mutation has been introduced, one can compare the activity or affinity data of the DLM between the mutated and the wild type protein. If the mutation is at the binding site of the DLM, one can assume that the affinity or efficacy of the DLM will decrease. The differences in the binding to wild type and mutated protein can be detected also with labelling methods such as PAL (Kim et al. 1997, Al-Mawsawi et al. 2006).

2.3   SIRTUINS

Sirtuins are class III subfamily of HDACs, and unlike other HDACs they require a nicotinamide adenine dinucleotide (NAD$^+$) cofactor in the enzymatic reaction (Tanny and Moazed 2001, Smith and Denu 2007, Seto and Yoshida 2014). The sirtuin-mediated lysine deacetylation starts with the cleavage of the nicotinamide (NAM) moiety of NAD$^+$. The remaining, adenosine diphosphate ribose (ADPr), forms an O-alkylamidate intermediate with the acetylated substrate (Figure 3) (Chen et al. 2015). The intermediate is transformed further to a 1'2'-cyclic intermediate with the help of the catalytically active histidine (Zhao et al. 2004, Smith and Denu 2006). Finally, the cyclic intermediate is decomposed into deacetylated lysine and O-acetylated adenosine diphosphate ribose (OAADPr). A more detailed description of each step of the reaction is reviewed by Chen et al. (2015).
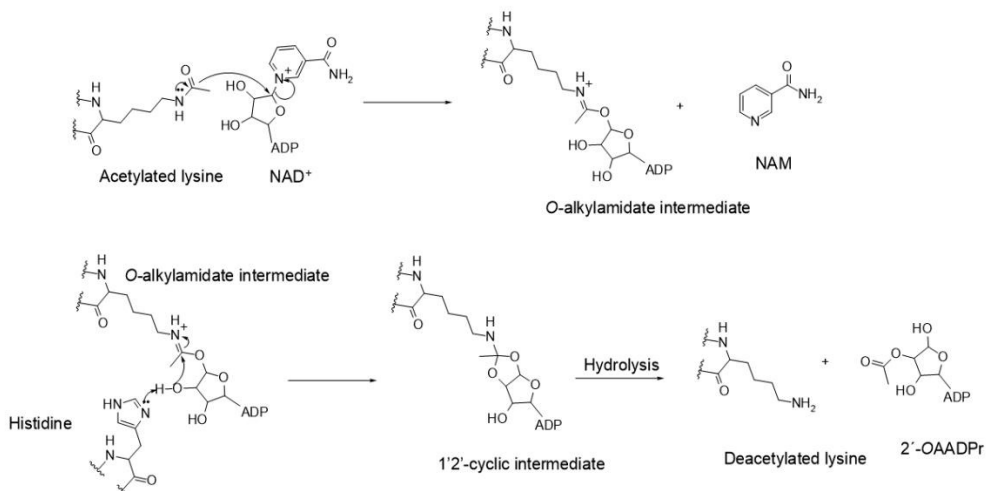

Figure 3. The deacetylation reaction mechanism of sirtuins.

The human sirtuin family (SIRTs) consists of seven sirtuins (SIRT1-7) that vary in their length (Table 2) and amino acid composition (Parenti et al. 2015). However, they have rather well conserved catalytical core that contains approximately 250 amino acids. The similarity is highest at the binding region of NAD$^+$. SIRTs are expressed

ubiquitously although the expression levels in different tissues can vary (Frye 1999, Michishita et al. 2005). SIRTs differ from each other in their main subcellular locations (Table 2) and their location can also vary depending on their mutational status or for example on the stress status of the cells (Tanno et al. 2007, Aquilano et al. 2010, Jedrusik-Bode et al. 2013, Yang et al. 2019a).

Table 2. Human sirtuins

Sirtuin	Amino acids	Primary subcellular location	Reference
SIRT1	747	Nucleoplasm	Vaziri et al. 2001, Michishita et al. 2005, UniProt 2020
SIRT2	389	Cytoplasm	Afshar and Murnane 1999, Perrod et al. 2001, Michishita et al. 2005, UniProt 2020
SIRT3	399	Mitochondria	Michishita et al. 2005, UniProt 2020
SIRT4	314	Mitochondria	Michishita et al. 2005, UniProt 2020
SIRT5	310	Mitochondria	Michishita et al. 2005, UniProt 2020
SIRT6	355	Nucleoplasm	Michishita et al. 2005, Ardestani and Liang 2012, UniProt 2020
SIRT7	400	Nucleolus	Michishita et al. 2005, UniProt 2020

SIRTs control gene expression directly through deacetylation of histone lysines, and indirectly by deacetylating non-histone targets (Gallinari et al. 2007, Feige and Auwerx 2008, Jing and Lin 2015, O'Callaghan and Vassilopoulos 2017). Moreover, SIRTs have also other lysine deacylase activities, such as demyristolyation, that have been suggested to affect multiple cellular pathways (Feldman et al. 2013, Du et al. 2015, Thinon and Hang 2015, Tong et al. 2017). SIRTs have also been proposed to ADP-ribosylate different proteins that control DNA repair (Haigis et al. 2006, Mao et al. 2011, Van Meter et al. 2014a). Due to these functions, SIRTs have attracted interest as possible targets in various diseases (Chalkiadaki and Guarente 2015, Matsushima and Sadoshima 2015, Jęśko et al. 2017, Kane and Sinclair 2018). Here we focus on SIRT6 that is one of the nuclear sirtuins. It has been less studied than SIRT1 and SIRT2, but recently it has been a focus of interest after the discovery of the first natural activators (Feldman et al. 2013).

2.3.1 The role of SIRT6 in health and disease

SIRT6 affects many cellular processes by deacetylating histones and a variety of other proteins (Table 3). In addition to deacetylation, SIRT6 catalyses other deacylation reactions and ADP-ribosylation (Mao et al. 2011, Feldman et al. 2013, Van Meter et

al. 2014a, Wang et al. 2016b). Due to these versatile functions, SIRT6 has been postulated to have protective roles in cardiovascular diseases, inflammatory diseases, Alzheimer's disease, and type 2 diabetes (Lee et al. 2013, Tian et al. 2015, Griñán-Ferré et al. 2016, Hou et al. 2017, Sociali et al. 2017, Arsiwala et al. 2020). In cancer, the role of SIRT6 is controversial and depends on the cancer type and stage (Table 4) (Garcia-Peterson et al. 2017, Desantis et al. 2018, Geng et al. 2018, He et al. 2020).

Table 3. The targets of SIRT6-catalyzed reactions.

Histone targets	Reaction	Affected process	References
H3K9	Deacetylation	Cancer, inflammation metabolism	Michishita et al. 2008, Kawahara et al. 2009, Zhong et al. 2010
H3K18	Deacetylation	DNA repair, senescence	Tasselli et al. 2016 Wang et al. 2016a, Wang et al. 2016b, Lavarone et al. 2019
H3K27	Deacetylation	Cell identity control	
H3K56	Deacetylation	DNA repair	Michishita et al. 2009, Toiber et al. 2013
Non-histone targets	**Reaction**	**Affected process**	**References**
Forkhead box protein O1 (FOXO1)	Deacetylation	Glucose and lipid metabolism	Zhang et al. 2014
General control non-repressed (GCN5)	Deacetylation	Hepatic glucose production	Dominy et al. 2012
Nicotinamide phosphoribosyltransferase (NAMPT)	Deacetylation	NAD^+ biosynthesis	Sociali et al. 2019
p53	Deacetylation	Apoptosis, cancer development	Wood et al. 2018
Pyruvate kinase M2 (PKM2)	Deacetylation	Cancer development	Bhardwaj and Das 2016
Tumor necrosis factor alpha (TNF-α)	Deacylation of long-chain fatty acyls	Immune responses	Jiang et al. 2013
KRAB-associated protein-1 (KAP1)	ADP-ribosylation	DNA repair	Van Meter et al. 2014a
Poly [ADP-ribose] polymerase 1 (PARP1)	ADP-ribosylation	DNA repair	Mao et al. 2011

Table 4. Examples of SIRT6-related cancers.

Cancer	Change in SIRT6 expression	Role of SIRT6	References
Breast cancer (paclitaxel and epirubicin resistant)	↑	Tumour promoter	Khongkow et al. 2013
Colon cancer	↑↓	Dual role	Geng et al. 2018 Li et al. 2018a Liu et al. 2018a Tian and Yuan 2018
Endometrial carcinoma	↑	Dual role	Colas et al. 2011 Fukuda et al. 2015
Gastric cancer	↓	Tumour suppressor	Zhou et al. 2017
Glioma	Unknown	Tumour suppressor	Feng et al. 2016 Zhu et al. 2019
Head and neck squamous cell carcinoma	↓	Tumour suppressor	Lai et al. 2013
Hepatic cancer	↓	Dual role	Tao et al. 2017 Xia et al. 2018 Han et al. 2019 Zhang et al. 2019a
Melanoma	↑↓	Dual role	Garcia-Peterson et al. 2017 Wang et al. 2018a
Non-small cell lung cancer	↑↓	Dual role	Li et al. 2018b Wang et al. 2018b Zhu et al. 2018 Krishnamoorthy and Vilwanathan 2020
Osteosarcoma	↓	Tumour suppressor	Gao et al. 2019
Ovarian cancer	Unknown	Dual role	Zhang et al. 2015 Bae et al. 2018 He et al. 2020
Papillary thyroid cancer	↑	Tumour promoter	Qu et al. 2017, Yang et al. 2019b, Yu et al. 2019
Renal cancer	↓	Dual role	Jeh et al. 2017 Ding et al. 2019

SIRT6 acts through multiple mechanisms in preventing cancer, for example by repressing the function of the oncogenic transcription factor c-Myc (Sebastián et al. 2012). SIRT6 also improves genomic stability via telomere maintenance and DNA damage repair (Xu et al. 2015b, Chen et al. 2017, Tian et al. 2019). Cancer cell metabolism is also controlled by SIRT6. Sebastián et al. (2012) demonstrated that the knock-out of the SIRT6 gene increased anaerobic glycolysis, that is a typical change in cancer cell metabolism (Zhong et al. 2010, Sebastián et al. 2012, Van Meter et al. 2014b). However, in papillary thyroid cancer cells, the activity of SIRT6 was speculated to increase anaerobic glycolysis through the production of reactive oxygen species (Yu et al. 2019). Thus, the role of SIRT6 in cancer cell metabolism

seems to be rather complex. SIRT6 has also been thought to play a role in inflammation, apoptosis, proliferation, and other cancer-related processes.

2.3.2 SIRT6 protein structure

The protein structure of SIRT6 was first published by Pan et al. (2011), and today a total of 15 SIRT6 structures are available (Table 5) (RCSB PDB 2020). All structures include at least ADPr and some of them include a ligand such as an inhibitor, an activator, or a myristoylated substrate. However, complete structure of SIRT6 remains still unknown, as the structures published today lack approximately the 50 C-terminal amino acids. In addition, most of the structures lack several N-terminal residues and none of them includes an acetylated substrate or NAD^+.

Table 5. SIRT6 structures published in RCSB PDB.

PDB ID (resolution)	Crystallised sequence	Ligands	Reference
3K35 (2.00 Å)	K15–K296 missing residues: A169–A176	ADPr	Pan et al. 2011
3PKI (2.04 Å)	A13–L297	ADPr	Pan et al. 2011
3PKJ (2.12 Å)	A13–K296 missing residues: A169–R175	2'N-Acetyl ADPr	Pan et al. 2011
3ZG6 (2.20 Å)	N4–K296	ADPr, myristoylated peptide	Jiang et al. 2013
5MF6 (1.87 Å)	A13–E298 missing residues: K170–A176	ADPr, UBCS039	You et al. 2017
5MFZ (2.10 Å)	A13–E298 missing residues: K170–A176	ADPr, UBCS40	You et al. 2017
5MFP (1.98 Å)	A13–E298 missing residues: K170–A176	ADPr, UBCS58	You et al. 2017
5MGN (2.07 Å)	A13–E298 missing residues: K170–A176	ADPr, UBCS38	You et al. 2017
5X16 (1.97 Å)	A7–P299	ADPr	RCSB PDB 2020
5Y2F (2.53 Å)	V3–P299	ADPr, myristoylated H3K9 peptide, MDL-801	Huang et al. 2018
6HOY (1.70 Å)	A13–L297 missing residues: K170–A176	ADPr, Trichostatin A	You and Steegborn 2018
6QCD (1.84 Å)	A13–E298 missing residues: K170–A176	ADPr, quercetin	You et al. 2019
6QCE (1.90 Å)	A13–E298 missing residues: K170–A176	ADPr, isoquercetin	You et al. 2019
6QCH (2.10 Å)	A13–L297 missing residues: K170–A176	ADPr, cyanidin	You et al. 2019
6QCJ (2.01 Å)	A13–E298 missing residues: K170–A176	ADPr, catechin gallate	You et al. 2019

Nevertheless, the crystal structures reveal that like other sirtuins, SIRT6 also has a large NAD+-binding Rossmann fold domain and a smaller zinc-binding domain (Figure 4). There is a tunnel-like binding pocket for the different substrates of SIRT6 between the two domains. The acylated part of the substrate enters into the binding site from the cleft between β6/α6 and β7/α7 loops which undergoes interactions with the peptide part of the substrate (Jiang et al. 2013, Huang et al. 2018). The other larger opening of the tunnel-like site is next to the α3 helix. Next to the substrate binding site is also the binding site of the NAM-moiety of NAD+ (Min et al. 2001, Gertz et al. 2013).
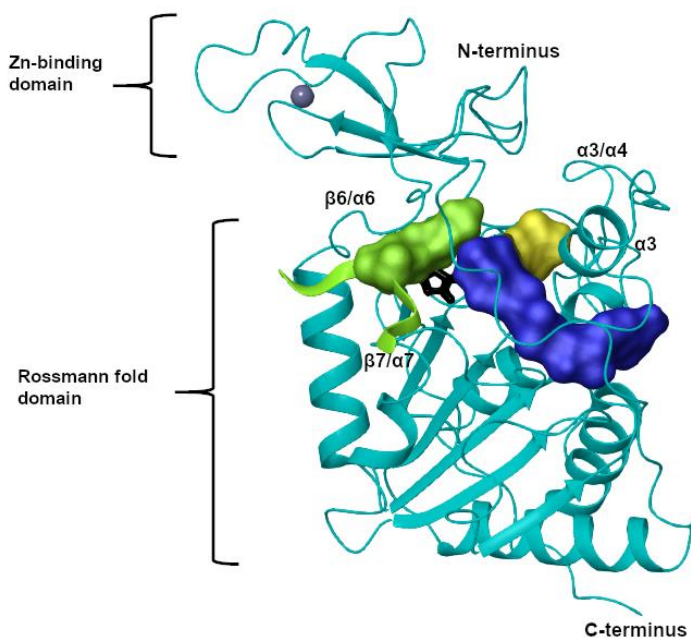
Figure 4. The structure of SIRT6 (PDB ID 5Y2F) (Huang et al. 2018). Zn ion is presented as a grey ball, acetylated substrate as a green surface and ribbon, and catalytically active histidine as black sticks. Blue surface represents the binding site for the ADPr moiety of NAD+, and the yellow surface indicates the NAM-moiety binding site.

2.3.3 SIRT6 deacetylase inhibitors

SIRT deacetylase inhibitors are compounds that decrease the velocity of SIRT-mediated deacetylation reaction. The SIRT6 inhibitors so far discovered are micromolar inhibitors that compete with the substrate-binding or disturb NAD+-binding (Table 6). Most of the inhibitors are unselective and inhibit also other SIRTs. The inhibitors include compounds that mimic the structure of peptide substrates and bind to the substrate area. Most of them are reported to be more potent against SIRT6 than for other SIRTs, except for the cyclic pentapeptide inhibitor. NAM and NAM-mimicking compounds, such as pyrazinamides (PZAs), bind to the NAM-binding

site and subsequently prevent NAD$^+$ from binding in the correct orientation to allow the reaction to proceed (Gertz et al. 2013, Zhao et al. 2013).

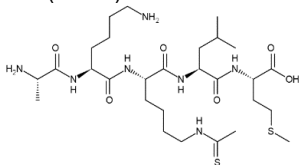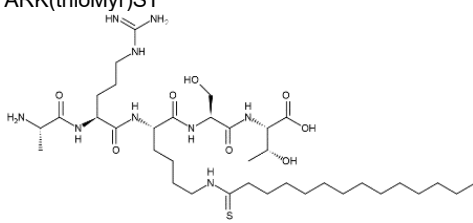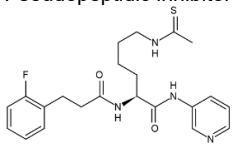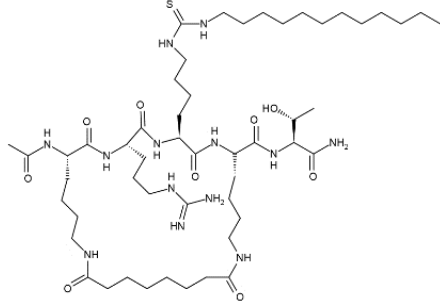Table 6. Examples of SIRT6 inhibitors and their activities against SIRT6 and other SIRTs.

COMPOUND	ACTIVITY DATA	REFERENCES
Substrate-based inhibitors		
AKK(thioAc)LM	IC_{50}(SIRT6) = 47 µM IC_{50}(SIRT1) = 380 nM IC_{50}(SIRT2) = 8.5 µM	Kokkonen et al. 2012
ARK(thioMyr)ST	IC_{50}(SIRT6) = 8.2 µM IC_{50}(SIRT1) = 4.4 µM IC_{50}(SIRT2) = 2.6 µM IC_{50}(SIRT3) = 5.6 µM	He et al. 2014
Pseudopeptidic inhibitor	At 200 µM compound concentration: Inhibition % (I%) (SIRT6) = 58 At 50 µM compound concentration: I% (SIRT1) = 94 I% (SIRT2) = 74 I% (SIRT3) = 72	Mellini et al. 2013 Kokkonen et al. 2014
Cyclic pentapeptide	IC_{50}(SIRT6) = 319 nM IC_{50}(SIRT1) = 730 nM IC_{50}(SIRT2) = 6.4 µM IC_{50}(SIRT3) = 3.5 µM IC_{50}(SIRT5) = >300 µM	Liu and Zheng 2016

Table 6 continues.
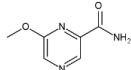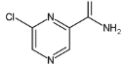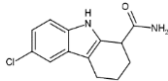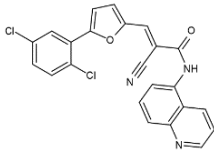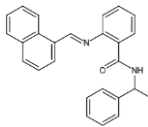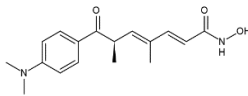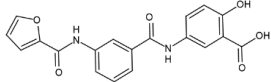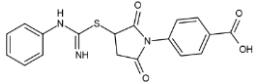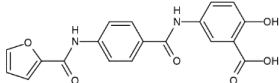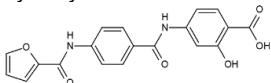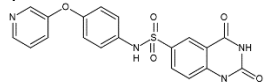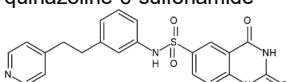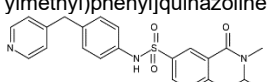
COMPOUND	ACTIVITY DATA	REFERENCES
NAM and NAM-mimicking inhibitors		
NAM	IC_{50}(SIRT6) = 184 µM – 3.5 mM IC_{50}(SIRT1) = 68–77 µM IC_{50}(SIRT2) = 10 µM IC_{50}(SIRT3) = 31–37 µM	Rye et al. 2011 Hu et al. 2013, Guan et al. 2014, Kokkonen et al. 2014, Bolivar and Welch 2017, Huang et al. 2018
5-MeO-PZA	IC_{50}(SIRT6) = 40 µM	Bolivar and Welch 2017
5-Cl-PZA	IC_{50}(SIRT6) = 33 µM	Bolivar and Welch 2017
Common SIRT and HDAC inhibitors with SIRT6 inhibitory activity		
EX527	IC_{50}(SIRT6) = 107 µM IC_{50}(SIRT1) = 100 nM IC_{50}(SIRT2) = 3 µM IC_{50}(SIRT3) = 165 µM	Ekblad and Schüler 2016
AGK2	At 300 µM compound concentration: I% (SIRT6) = 27 I% (SIRT2) = 22 IC_{50}(SIRT2) = 3–66 µM	Outeiro et al. 2007 He et al. 2014
Sirtinol	At 200 µM compound concentration: I% (SIRT6) < 50 At 300 µM compound concentration: I% (SIRT1) = 21 IC_{50}(SIRT2) = 65 µM IC_{50}(SIRT3) = 150 µM	Hu et al. 2013, He et al. 2014
Trichostatin A	K_{i}(SIRT6) = 2–4.6 µM (for different acetylated substrates)	Wood et al. 2018

Table 6 continues.

COMPOUND	ACTIVITY DATA	REFERENCES
Benzoic acid and quinazoline sulfonamides		
5-[[3-(furan-2-carbonylamino)benzoyl]amino]-2-hydroxybenzoic acid	IC_{50}(SIRT6) = 89 µM IC_{50}(SIRT1) = 1.6 mM IC_{50}(SIRT2) = 751 µM	Parenti et al. 2014
4-[2,5-dioxo-3-(N'-phenylcarbamimidoyl)sulfanylpyrrolidin-1-yl]benzoic acid	IC_{50}(SIRT6) = 181 µM IC_{50}(SIRT1) = 3.5 mM IC_{50}(SIRT2) = 1.7 mM	Parenti et al. 2014
5-[[4-(furan-2-carbonylamino)benzoyl]amino]-2-hydroxybenzoic acid	IC_{50}(SIRT6) = 34 µM IC_{50}(SIRT1) = 783 µM IC_{50}(SIRT2) = 453 µM	Damonte et al. 2017
4-[[4-(furan-2-carbonylamino)benzoyl]amino]-2-hydroxybenzoic acid	IC_{50}(SIRT6) = 22 µM IC_{50}(SIRT1) = 599 µM IC_{50}(SIRT2) = 482 µM	Damonte et al. 2017
2,4-dioxo-N-(4-pyridin-3-yloxyphenyl)-1H-quinazoline-6-sulfonamide	IC_{50}(SIRT6) = 106 µM IC_{50}(SIRT1) = 314 µM IC_{50}(SIRT2) = 114 µM	Parenti et al. 2014
2,4-dioxo-N-[3-(2-pyridin-4-ylethyl)phenyl]-1H-quinazoline-6-sulfonamide	IC_{50}(SIRT6) = 37 µM IC_{50}(SIRT1) = 424 µM IC_{50}(SIRT2) = 85 µM	Sociali et al. 2015
1,3-dimethyl-2,4-dioxo-N-[4-(pyridin-4-ylmethyl)phenyl]quinazoline-6-sulfonamide	IC_{50}(SIRT6) = 49 µM IC_{50}(SIRT1) = 6.5 mM IC_{50}(SIRT2) = 242 µM	Sociali et al. 2015

Compounds that have been previously reported to inhibit other sirtuins such as EX527, AGK2, and Sirtinol have also been shown to inhibit SIRT6 (Table 6) (Outeiro et al. 2007, Hu et al. 2013, He et al. 2014, Ekblad and Schüler 2016). From these, EX527 and AGK2 are suggested to bind to the NAM-binding site (Outeiro et al. 2007, Gertz et al. 2013). Trichostatin A, an HDAC inhibitor, has also been reported to inhibit SIRT6 but no other SIRTs (Wood et al. 2018). Although the kinetic studies hinted that

it was a substrate competitive inhibitor, the crystal structure of SIRT6 complexed with Trichostatin A indicated that it binds to the NAM-binding site (Wood et al. 2018, You and Steegborn 2018).
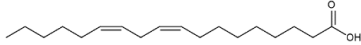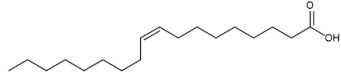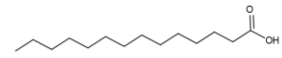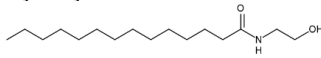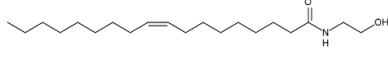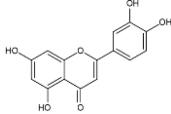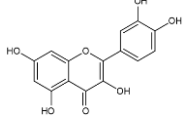
SIRT6-inhibiting benzoic acid and quinazoline sulfonamide derivatives were developed by Parenti et al. (2014), Sociali et al. (2015), and Damonte et al. (2017). Some of these compounds have been reported to be better inhibitors for SIRT6 than for SIRT1 and SIRT2 (Table 6). These inhibitors have been suggested to bind partly to the SIRT6 NAM-binding site and also to occupy the substrate-binding area (Parenti et al. 2014, Sociali et al. 2015, Damonte et al. 2017). In cellular studies, these inhibitors reduced Tumor necrosis factor alpha (TNF-α) secretion and increased glucose uptake by enhancing the expression of Glucose transporter type 1 (GLUT-1). Some of these inhibitors also sensitize pancreatic cancer cells to chemotherapeutics, improve glucose tolerance in type 2 diabetes mouse models, and are effective against hepatitis B virus (Sociali et al. 2015, Damonte et al. 2017).

2.3.4 SIRT6 deacetylase activators

SIRT deacetylase activators increase the velocity of SIRT-mediated deacetylation reaction. The first SIRT6 activators that were published were natural fatty acids: linoleic and oleic acid (Feldman et al. 2013). Later, other fatty acid-like activators were developed (Table 7) (Rahnasto-Rilla et al. 2016, Klein et al. 2020). Other natural compounds and their derivatives have also been shown to increase SIRT6 deacetylase activity (Yasuda et al. 2011, Rahnasto-Rilla et al. 2016, Rahnasto-Rilla et al. 2017, You et al. 2019). However, some non-fatty acid compounds such as luteolin and quercetin were found to have also SIRT6 inhibition potential (Rahnasto-Rilla et al. 2016). The reason for their ability to activate and inhibit SIRT6 is still unclear but it depends on the compound's concentration. The inhibition at higher concentration might be due to the formation of colloidal aggregates that can function as unspecific inhibitors (Pohjala and Tammela 2012, Reker et al. 2019). A few synthetic activators have also been developed (Table 7) of which UBCS039 has been shown to induce lethal autophagy in epithelial cervix carcinoma and non-small cell lung cancer cells (You et al. 2017, Huang et al. 2018, Klein et al. 2020). One of the most efficient activators is lysophosphatidic acid.

Two different activator-binding sites for SIRT6 have been proposed. The fatty acids, fatty acid-like compounds, and some synthetic activators have been suggested to bind to the same site where the long acyl chain of some substrates bind (Feldman et al. 2013, You et al. 2017, Klein et al. 2020). Another binding site was suggested for the activator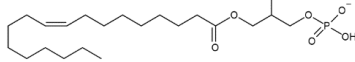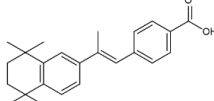 MDL-801 that was shown to bind between the Zn-binding domain and $\alpha 3$-$\alpha 4$ loop in a crystal structure (Figure 5) (Huang et al. 2018). Moreover, MDL-801 does not inhibit the binding of long-chain acyl substrates which supports the theory that there is another activator-binding site in addition to the long acyl chain binding site.
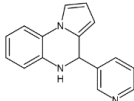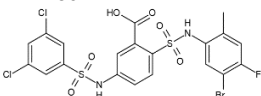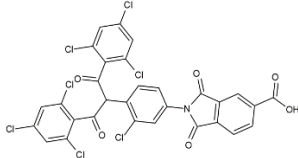
Table 7. Examples of SIRT6 activators and compounds with dual activity.

COMPOUND	SIRT6 ACTIVITY DATA	REFERENCES
Fatty acids and fatty acid-like activators		
Linoleic acid	[1]$FA_{max} \approx 7$ $EC_{50} = 90\ \mu M$	Feldman et al. 2013
Oleic acid	$FA_{max} \approx 6$ $EC_{50} = 100\ \mu M$	Feldman et al. 2013
Myristic acid	$FA_{max} \approx 11$ $EC_{50} = 246\ \mu M$	Feldman et al. 2013
Myristoylethanolamide	$FA_{max} \approx 2$ $EC_{50} = 7.5\ \mu M$	Rahnasto-Rilla et al. 2016
Oleoylethanolamide	$FA_{max} \approx 2$ $EC_{50} = 3.1\ \mu M$	Rahnasto-Rilla et al. 2016
Lysophosphatidic acid	$FA_{max} = 30$ $EC_{50} = 25\ \mu M$	Klein et al. 2020
Other SIRT6-activating natural compounds or their derivatives		
Fucoidan extract from brown seaweed *Fucus distichus*, exact structure unknown	At 100 µg/ml extract concentration [2]$FA = 140–355$	Rahnasto-Rilla et al. 2017
Arotinoid acid	$FA_{max} = 15$ $EC_{50} = 53\ \mu M$	Klein et al. 2020
Luteolin	$FA_{max} \approx 6$ At 100 µM compound concentration: $I\% = 30$	Rahnasto-Rilla et al. 2016, You et al. 2019
Quercetin	$FA_{max} = 6$ At 100 µM compound concentration: $I\% = 38$	Rahnasto-Rilla et al. 2016, You et al. 2019

[1] FA_{max} = Maximal increase in enzymatic activity that can be achieved with the compound
[2] FA = Fold of inrease in enzymatic activity at certain concentration

Table 7 continues

COMPOUND	ACTIVITY DATA	REFERENCES
Synthetic activators		
UBCS039	$FA_{max} \approx 2$ $EC_{50} = 38 \mu M$	You et al. 2017
MDL-801	At 100 µM compound concentration: FA > 22 $EC_{50} = 5.7 \mu M$	Huang et al. 2018
CL5D	At 3 µM compound concentration: FA = 4 $EC_{50} = 16 \mu M$	Klein et al. 2020
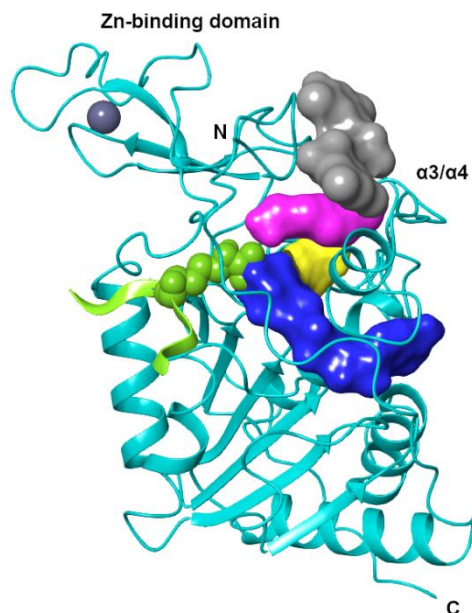
Figure 5. Suggested allosteric activator binding site (grey surface), and the binding site proposed for SIRT6 activating natural fatty acids and some synthetic compounds (magenta surface). Acetylated substrate is marked with light green, ADPr-binding site with blue, and NAM-binding site with yellow.

2.4 BROMODOMAIN AND EXTRATERMINAL MOTIF PROTEINS

In addition to molecular activators and inhibitors, HDAC and SIRT activity can possibly be altered by affecting the expression of these proteins. One approach might be the inhibition of bromodomain and extraterminal motif proteins (BETs) as the most extensively studied BET inhibitor, (+)-JQ1, has been shown to induce HDAC6 and SIRT1 expression in various cell lines including T-cell, multiple myeloma, and breast cancer cell lines (Banerjee et al. 2012, Kokkola et al. 2015, Carew et al. 2019).

BETs, in common with all bromodomain-containing proteins, can bind to histone lysine acetylation marks and anchor simultaneously transcription factors near DNA (Yang et al. 2005, Peng et al. 2007, Filippakopoulos et al. 2012). BET inhibitors are designed to block the interaction between BETs and acetylated lysine by occupying the binding pocket of acetylated lysine in the BETs. This pocket is highly conserved between all BETs: BRD2, BRD3, BRD4, and BRDT (Pervaiz et al. 2018). For that reason, the BET inhibitors developed up until now lack selectivity within the BET family.

The first BET inhibitors were diazepine derivatives such as (+)-JQ1 and OTX015 (Birabresib) (Figure 6) (Filippakopoulos et al. 2010, Noel et al. 2013). There were also some dimethylisoxazole-containing compounds among the first inhibitors, e.g. I-BET151 and GS-5829 (Alobresib) (Figure 6) (Dawson et al. 2011, Bonazzoli et al. 2018). Quinazolinone compounds, such as Pfi-1 and RVX2135, and several pyrrolopyridinone compounds, including ABBV-075 (Mivebresib) have also shown potency in inhibiting BETs (Figure 6) (Fish et al. 2012, Faivre et al. 2016, Fidanze et al. 2018). Several other scaffolds have also been introduced for BET inhibitors and they have been discussed in the reviews by Zhang and Ma 2018, Cochran et al. 2019, Yang et al. 2019c, and Lu et al. 2020c.

BET inhibitors have been shown to exert tumour suppressive effects; for example, they downregulate the transcription c-Myc-related transcription of different oncogenes (Delmore et al. 2011). They can also potentiate the effects of other compounds that have anticancer activity (Karakashev et al. 2017, Echevarría-Vargas et al. 2018, Hupe et al. 2019, Miller et al. 2019). Interestingly, HDAC inhibitors are one group of the compounds which have shown synergistic effects with BET inhibitors against cancer (Table 8). The synergy between BET inhibitors and SIRT modulators has not been investigated. However, BETs and SIRTs have been shown to regulate the same cellular processes and they target the same histone lysine acetylation sites (Filippakopoulos et al. 2012, Mellers et al. 2018, Guo et al. 2019).
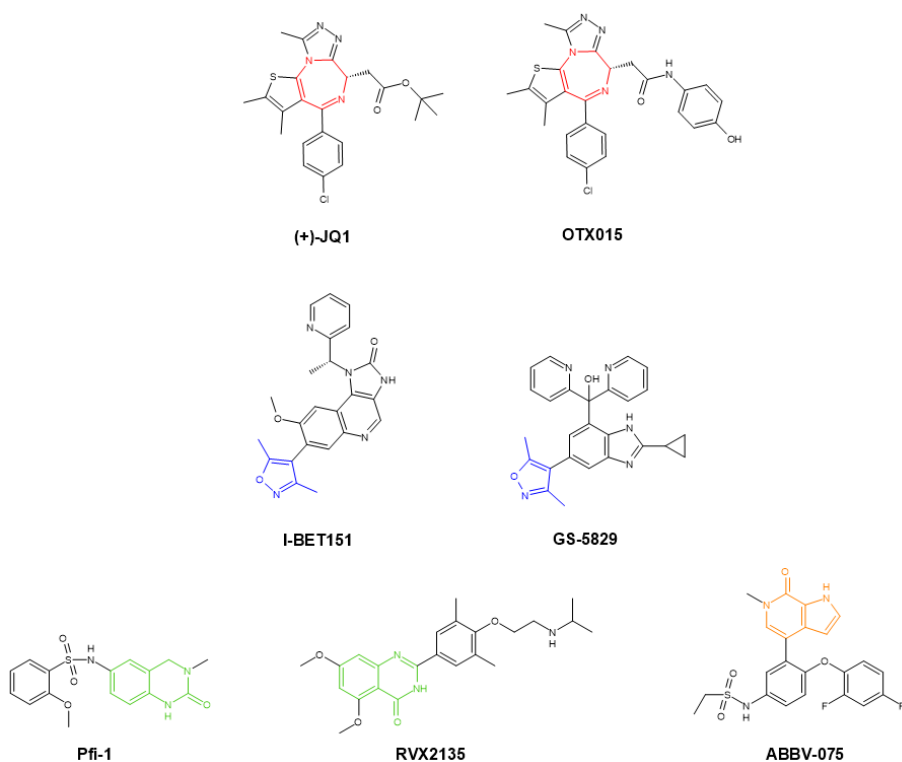
Figure 6. Examples of BET inhibitors containing diazepine (red), dimethylisoxazole (blue), quinazolinone (green), or pyrrolopyridinone moiety (orange).

Table 8. The synergy between different BET inhibitors and HDAC inhibitors in cancers.

BET inhibitor	HDAC inhibitor	Cancer	Reference
(+)-JQ1	Romidepsin	Urothelial carcinoma Lymphomas	Hölscher et al. 2018 Kim et al. 2018 Cortiguera et al. 2019
	Vorinostat	Pancreatic ductal adenocarcinoma Cutaneous T-cell lymphoma	Mazur et al. 2015 Kim et al. 2018
	Panobinostat	Neuroblastoma Globlastoma Myelogenous leukaemia	Fiskus et al. 2014 Meng et al. 2018 Cortiguera et al. 2019
	Sulforaphane	Colon cancer	Rajendran et al. 2019
OTX015	Panobionstat	Glioblastoma	Meng et al. 2018
I-BET151	LBH589	Melanoma	Heinemann et al. 2015
ABBV-075	Vorinostat, romidepsin	T-cell lymphoma	Kim et al. 2018

3   AIMS OF THE STUDY

The overall aim was to discover new SIRT6 modulators and to investigate how SIRT activity could be modulated indirectly through regulation of their expression.
The specific aims of the studies were
- To discover novel SIRT6 inhibitors and activators
- To explore possible binding sites for the identified SIRT6 modulators and to study their possible binding modes and with computational modelling methods
- To explore the functional link between BET inhibition and SIRT1 protein expression

4 METHODS

4.1 *IN VITRO* METHODS FOR DETERMINING INHIBITION AND ACTIVATION OF SIRT DEACETYLASE ACTIVITY (STUDIES I–III)

4.1.1 Compounds

Several natural flavonoids, including catechins, flavanols, flavanones, and anthocyanidins, as well as quercetin, flavone and dihydropyridine derivatives (Figure 7) were tested *in vitro* for their ability to modulate SIRT6 deacetylation activity. The previously reported quercetin (Table 7) was used as a reference compound in studies I–III. The compounds were ordered from Sigma Aldrich (USA) or MolPort, or they were provided by our collaborators.
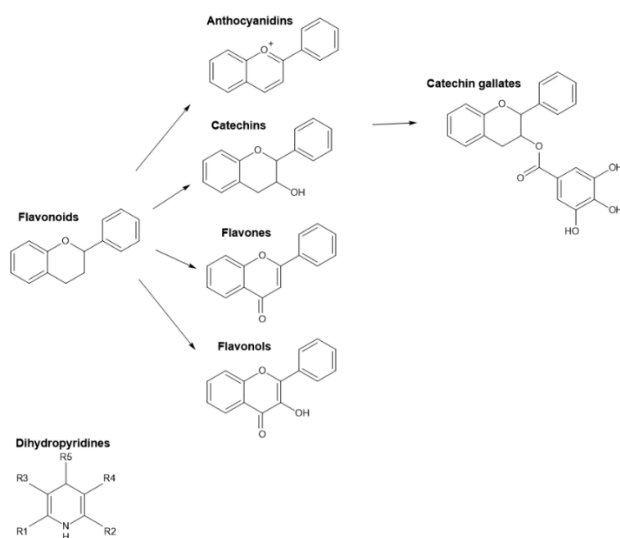
Figure 7. Examples of the core structures of the compounds screened in studies I-III.

4.1.2 Deacetylation assays

SIRT6 HPLC assay

In studies I and III, a high-performance liquid chromatography (HPLC) assay was used to determine the effect of the compounds on SIRT6 activity. The compounds were tested at 10 and/or 100 µM concentrations in both studies. A dose response curve was determined for the most potent inhibitors and activators with compound concentrations of 10–1000 µM. In study III, a steady state kinetical analysis

(Michaelis-Menten kinetics) was performed for the most potent activator (50 µM) to determine if it improved substrate or NAD$^+$ binding.

The HPLC assay is described in more detail in the publication of Rahnasto-Rilla et al. (2017). Briefly, compounds were incubated in the reaction mixture (pH 8) with recombinant SIRT6, acetylated substrate, and NAD$^+$ (Table 9). The deacetylation reaction was stopped with cold 10% formic acid. In kinetic analyses, the concentration of either NAD$^+$ or acetylated substrate was increased while the concentration of the other compound was kept at a saturating concentration (2.5 mM for NAD$^+$ and 2 mM for H3K9Ac). Control samples were prepared without NAD$^+$ or SIRT6. Samples were analysed with reversed-phase HPLC. Peaks for H3K9Ac and for the deacetylated product (H3K9) were detected. The percent of inhibition was calculated based on the peak size.

Table 9. The concentrations of the substrates and NAD$^+$ in SIRT deacetylation assays.

	SIRT6 HPLC assay	SIRT6 fluorescence assay	SIRT1 inhibition %	SIRT2 inhibition %	SIRT3 inhibition %
Substrate and its concentration	H3K9Ac peptide (residues 1–21) Activation assay 40 or 70 µM Inhibition assay 200 µM Kinetic analyses: 2 mM or increasing	Ac-RYQK(Ac)-AMC, 320 µM Kinetic analyses: 600 µM or 100 µM – 1.2 mM	BioMol KI117, 58 µM	BioMol KI179, 198 µM	BioMol KI79, 32 µM
NAD$^+$ concentration	500 µM Kinetic analyses: 3 mM or increasing	3 mM Kinetic analyses: 3 mM or 300 µM – 2.4 mM	558 µM	547 µM	2 mM

SIRT6 and SIRT1–3 fluorescence assays

In study II, a fluorescence-based assay was applied to determine the SIRT6 and SIRT1–3 inhibition percentage for the compounds. The concentrations of the compounds used in the SIRT6 assay were 50 µM and 200 µM and in SIRT1–3 assays 10–200 µM. Dose response curves for SIRT2 and SIRT6 inhibition were determined for the most potent compounds at 12–1000 µM concentrations. Additionally, the SIRT6 inhibition mechanism of the selected compounds was investigated with kinetic analysis (Lineweaver-Burk assay) where the concentration of either NAD$^+$ or substrate was changed while the concentration of the compound was held constant (3 mM for NAD$^+$ and 600 µM for substrate).

The detailed description of the SIRT6 assay can be found in publication of Kokkonen et al. 2014, and the SIRT1–3 assay was performed according to the instructions of the assay kit's product sheet (BioMol, Enzo Life Sciences). Briefly, compounds were incubated in a reaction mixture (pH 8.0) containing recombinant

SIRT, acetylated substrate, and NAD$^+$ (Table 9). After incubation, the reaction was stopped with NAM, and trypsin was added to free the fluorophore from deacetylated substrates.

Western blotting assay

As the results concerning certain compounds in the SIRT6 HPLC-assay and Fluorescence assay were ambiguous, the effect of those compounds on SIRT6 activity was confirmed with Western blotting using full length H3 histone substrates. The detailed description of the method can be found in publications I and II. Briefly, the compounds (50 μM, 100 μM, or 200 μM) were incubated with recombinant human purified chicken core histones (H3), and NAD$^+$. The deacetylation reaction was stopped with Laemmli buffer, and the sample proteins were separated with sodium dodecyl sulphate-polyacrylamide gel electrophoresis (SDS-PAGE). Separated proteins were transferred to polyvinylidene difluoride (PVDF) membranes. H3 and acetylated H3K9 (H3K9Ac) protein bands were detected with chemiluminescence method by using specific antibodies. Densitometric analyses of protein bands were carried out to determine the H3K9 acetylation level in relation to total H3 amount.

4.2 CELL-BASED EXPERIMENTS WITH SIRT6 DEACETYLASE ACTIVATORS

Western blotting

The most potent SIRT6 deacetylase activator discovered in study I was examined with human epithelial colorectal adenocarcinoma cells and its effects on the protein expression of SIRT6 and SIRT6-associated proteins was determined. The proteins from the cell samples were separated on SDS-PAGE and transferred to PVDF membranes. The bands of the proteins were detected with specific antibodies using a chemiluminescence method. H3 and α-tubulin were utilized as controls.

qPCR

In study III, the effect of the most potent activator of that study was investigated with various types of breast cancer cells with differing hormone receptor profiles. The effect of that activator (1 μM and 10 μM) on SIRT6 gene expression was determined with quantitative polymerase chain reaction (qPCR). The total RNA from treated cells was extracted and purified and the RNA was reverse transcribed to cDNA using random priming. SIRT6 specific primer was used in determining SIRT6 from the cDNA and B-actin was determined as an endogenous control.

PI-digitonin assay

The effect of the activator (1–100 μM) of study III on cell viability and proliferation in the selected breast cancer cell lines was determined with the propidium iodide (PI) digitonin assay as described in Huovinen et al. (2011). In order to study cell viability, the activator-treated cells were exposed to fluorescent PI that binds to the DNA of

dead cells with damaged membranes. The fluorescence was then measured to determine the dead cell number that describes cell viability. Subsequently, the cells were exposed to digitonin to degrade the cell membranes and thus to allow PI to enter all cells. The fluorescence was then measured to determine the total cell number that was used in determining the effect of the activator on proliferation.

Cell cycle analysis
The effect of the most potent activator (10 μM and 50 μM) on cell cycle progression was determined with a flow cytometry method. After treatment with activator, the cells were made permeable to PI and DNA content of the cells was analysed by measuring the fluorescence signal. The amount of DNA within cells varies depending on the cell cycle phase, and thus cells in different phases display different fluorescence signal strengths.

4.3 MOLECULAR MODELLING METHODS

Molecular modelling methods were used to study the possible binding sites, poses, and interactions of the SIRT6 modulators discovered in studies I–III to obtain information for future SIRT6 modulator development. Different versions of Schrödinger Maestro software and force fields were used (Table 11) (Schrödinger 2016, Schrödinger 2017, Schrödinger 2019). The 3D structures for SIRT6 (studies I-III) and for SIRT2 (study II) were downloaded from RCSB PDB (Table 11). The SIRT6 structure 3ZG6 (resolution 2.2 Å) was selected for studies I and II as it contained N-terminal residues that were lacking from the other SIRT6 structures (Jiang et al. 2013). The SIRT6 structure 6QCD (resolution 1.84 Å), that was published after the studies I and II, was selected for study III as the structure contained a co-crystallised quercetin that is structurally related to the activator discovered in the study (You et al. 2019). In study II, the SIRT2 structure 4RMG (resolution 1.88 Å) was selected as it contained a co-crystallised inhibitor, SirReal2.

The protein structures were prepared with Maestro's Protein Preparation Wizard (Sastry et al. 2013). The default preparation protocol included adding hydrogens, assigning bond orders, creating zero-order bonds to metals, and creating disulphide bonds. Possible missing loops and side chains were added with Prime (Jacobson et al. 2004). All unnecessary small molecules, such as the reagents used in the crystallization, were removed. Ionization states for retained small molecules (Table 11) were generated with Epik at a target pH of 7.4 (Greenwood et al. 2010). Hydrogen bonds were assigned with PROPKA and waters having less than 3 hydrogen bonds to non-waters were removed. Final minimization was executed with OPLS3 (studies I and II) or OPLS3e (study III) with root mean squared deviation (RMSD) limit for heavy atom converging at 0.3 Å (Harder et al. 2016). The structure quality was confirmed with the Ramachandran plot.

The structures of SIRT6 deacetylase modulators in studies I–III were sketched with Maestro's 2D sketcher and prepared and minimized with Maestro's LigPrep

tool using OPLS3 (studies I and II) or OPLS3e force field (study III) (Harder et al. 2016). Ionization states were generated with Epik at target pH of 7.4 (Greenwood et al. 2010). In study I, the chirality of the compounds was known and thus, no stereoisomers were generated. In studies II and III, all possible stereoisomers were generated for the compounds.

Table 11. Summary of software, protein structures, and docking settings used in different studies of this work.

| | **STUDY** | | |
	I	**II**	**III**
Schrödinger release	2016-4	2017-4	2019-4
Maestro version	11.0	11.4	12.2
Force field	OPLS3	OPLS3	OPLS3e
Protein PDB ID	3ZG6 (SIRT6)	3ZG6 (SIRT6) 4RMG (SIRT2)	6QCD (SIRT6)
Retained ligands	ADPr, Zn^{2+}	ADPr, Zn^{2+} (3ZG6) NAD^+, Zn^{2+}, SirReal2 (4RMG)	ADPr, Zn^{2+}, quercetin
Grid center	Inhibitor docking: According to prior knowledge of EX527 in SIRT1 Activator docking: according to SiteMap results	SIRT6: NAM-binding site and Substrate-binding site SIRT2: according to the co-crystallised SirReal2	Inhibitor-docking: NAM-binding site Activator docking: according to the co-crystallised quercetin
Docking method	Induced Fit	Induced Fit	Glide docking with SP (for activator) and with XP (for inhibitors)

Binding site prediction and molecular docking

In study I, Schrödinger SiteMap with default settings was used for searching the possible drug-like molecule (DLM) binding sites from the SIRT6 structure 3ZG6 (Halgren et al. 2009). Default settings were applied: at least 10 site points were required for each site, a more restrictive definition of hydrophobicity was used, and site maps were cropped at 4 Å from the nearest site point. In addition to visualizing the predicted binding sites, SiteMap reports two values for evaluating the sites: SiteScore and Dscore (Halgren 2009). SiteScore is used to distinguish the sites that could serve as small ligand binding sites: scores over 0.8 are indicative of a good binding site. Dscore, that uses the same properties as SiteScore but with different weightings, can be used to evaluate if the site is undruggable, difficult, or druggable. Dscores under 0.83 indicate an undruggable site, Dscores between 0.83 and 0.98

indicate difficult binding sites, and sites having Dscore larger than 0.98 are considered as druggable.

In study I, the grid for the activator docking was assigned based on the SiteMap results. The grid for inhibitor docking was determined by selecting the residues in SIRT6 that corresponded to the residues of EX527 binding site in SIRT1. In study II, two grid centres for SIRT6 were applied: one at the substrate-binding site and one at the NAM-binding site. The grid centre for SIRT2 in study II was assigned based on the co-crystallised SirReal2. In study III, the grid for activator docking was set based on the co-crystallised quercetin, and the grid centre for inhibitor docking was at the binding site of NAM.

Induced Fit docking that considers the flexibility of the binding pocket was used in studies I and II (Table 11) (Farid et al. 2006). Default settings for Induced Fit docking were used. Compound ring conformations were sampled with an energy limit of 2.6 kcal/mol and nonpolar amide bond conformations were penalized. Receptor and ligand van der Waals scaling was 0.5 Å. Amino acid residues within 5.0 Å of ligand poses were refined. Ligands were redocked in structures within 30.0 kcal/mol of the best structure with standard precision (SP).

In study III, the compounds were docked with Glide docking, where the receptor structure is rigid (Table 11) (Friesner et al. 2006). SP docking was used in activator docking and extra precision (XP) was used in inhibitor docking. The docking position of activator was restricted to the position of the co-crystallised quercetin with. For inhibitor docking, extra precision (XP) with accurate scoring function was used. Default settings were applied in the dockings: van der Waals radii scaling for the ligand nonpolar parts was applied with scaling factor of 0.8 and partial charge cut-off of 0.15. Compounds were docked flexibly by sampling nitrogen inversions and ring conformations, and sampling of torsions was biased only for amides.

4.4 BET INHIBITOR EXPERIMENTS

The effect of BET inhibition on SIRT1 cellular levels and activity was investigated in study IV. Three BET inhibitors (+)-JQ1, I-BET151, and Pfi-1 that have differing structures and inhibition potential against BETs were selected for this study (Figure 8). All of them have IC_{50} values in the nanomolar range with (+)-JQ1 being the most potent: it is twice as potent as Pfi-1 and ten times more potent than I-BET151. Previously the effect of (+)-JQ1 on SIRT1 levels has been examined in estrogen and progesterone receptor positive MCF-7 cells (Kokkola et al. 2015). Therefore, the same cell line was selected also for study IV. The other cell line selected for this experiment was a triple-negative MDA-MB-231 breast cancer cell line. The cells were treated with the BET inhibitors at various concentrations.

After the treatments, the protein contents of the cell samples were analysed with Western blotting. Briefly, the proteins were separated with SDS-PAGE and transferred to a PVDF membrane. The amounts of SIRT1, acetylated p53 (at K382), total p53, and total α-tubulin (loading control) were detected with specific antibodies

from the membranes. Detection was carried out with chemiluminescence method. One-way ANOVA with Bonferroni post-hoc test was used in the statistical analysis.

(+)-JQ1   I-BET151   Pfi-1
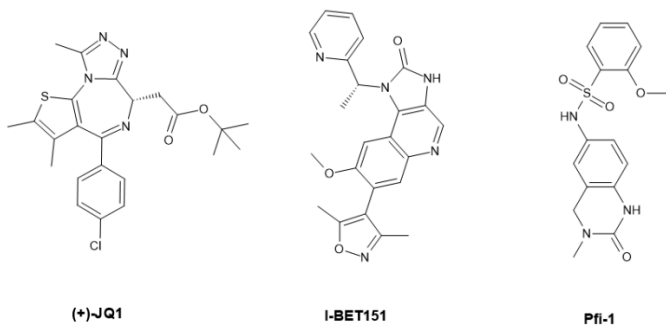
Figure 8. Structures of the BET inhibitors used in study IV.

5 RESULTS

5.1 NATURAL FLAVONOIDS MODULATE SIRT6 DEACETYLATION ACTIVITY (STUDY I)

Several flavonoids were discovered to inhibit or activate SIRT6 deacetylation activity *in vitro* (Figure 9). The possible binding sites and poses of these flavonoids were studied with docking methods.
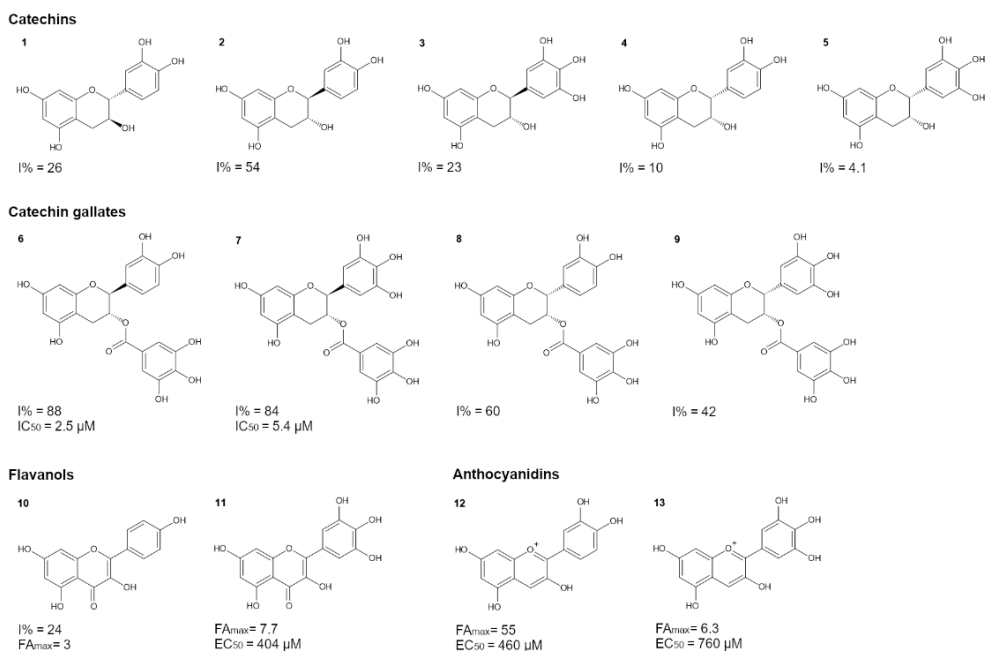
Figure 9. The structures of SIRT6 inhibitors and activators and their activities. The compound concentration for reported inhibition % (I%) and maximal-fold of activation (FA_{max}) is 100 µM.

The binding mode of inhibitors

The most potent inhibitors were discovered in the catechins (compounds **1**–**9**). Catechin compounds **1**–**5** were in general less potent than their larger derivatives catechin gallates (compounds **6**–**9**) (Figure 9). The inhibitory compounds were docked close to the NAM-binding site that includes residues N114, V115, and D116. The docking results suggested that the compounds **1**–**5** could find multiple poses in the binding pocket: they could either be located near to the NAM-binding site or (Figure 10A) more towards the substrate-binding site (Figure 10B).
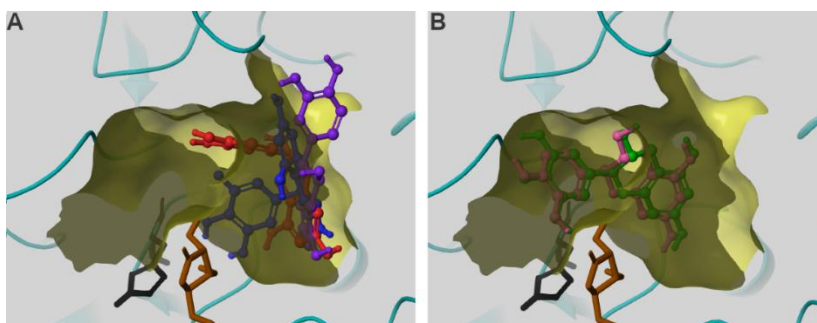
Figure 10. Representative docking poses of catechins at NAM-binding site (A) and closer to the substrate-binding site (B). Yellow surface represents the shape of the pocket. Catalytically active histidine is marked with black, and co-crystallised ADPr with brown. Compounds in figure A are **1** (blue), **2** (purple), and **4** (red), and in figure B **3** (green) and **5** (pink).

The most potent inhibitors, compounds **6**, **7**, and **8** had the most complementary shape with the pocket structure (Figure 11A–C). Overall, these compounds filled the pocket better than the less potent catechins (compounds **1–5**) (Figure 11). Compounds **6** and **7** were more potent than their stereoisomers, compounds **8** and **9**. The docking results suggested that compounds **6** and **7** were directing the gallate moiety towards the substrate-binding area whereas compound **8** directed it to the NAM-binding site. The least potent catechin gallate, compound **9,** could not fit completely inside the pocket (Figure 11D). Thus, the change in the stereochemistry of the catechin structures can cause differences in their binding modes and interactions of the compounds and subsequently in their inhibition potencies.
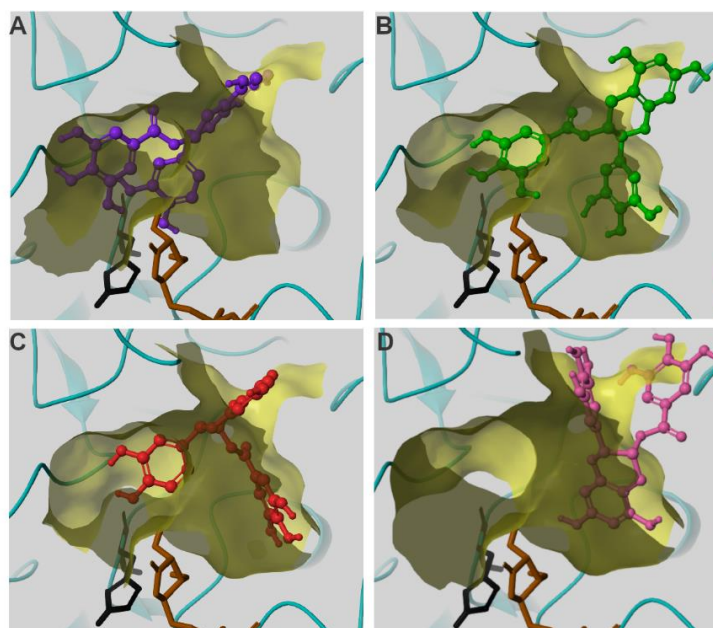
Figure 11. Representative docking poses of catechin gallate compounds **6** (A), **7** (B), **8** (C), and **9** (D). Yellow surface represents the shape of the binding pocket, catalytically active histidine is marked with black, and co-crystallised ADPr is with brown colour.

The docking results of the most potent inhibitors, compounds **6** and **7**, suggest that they form interactions with N4 at N-terminus, P62 and F64 in the ADPr-binding site, W71 at α3 helix, F82, T84, F86 at α3/α4-loop, Q113 at NAM-binding site, and L186 and D187 at substrate-binding site (Figure 12). Previously other SIRT6 inhibitors, trichostatin A and some of the benzoic acid and quinazoline sulfonamide derivatives (Table 5), have been suggested to form interactions also to P62, F64, W71, and D187 (Parenti et al. 2014, You and Steegborn 2018).
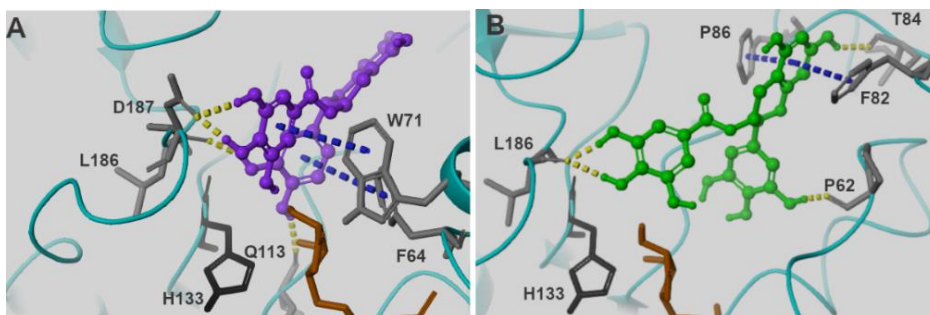
Figure 12. Representative docking poses and interactions of the most potent inhibitors of study I: compounds **6** (A) and **7** (B). H133 is the active histidine and co-crystallised ADPr is marked with brown. Hydrogen bonds are presented with yellow and π-π-stacking with blue dashes.

Compound **10** showed inhibition at a lower compound concentration but activation at a higher compound concentration. The reference compound quercetin had been previously shown to be a dual modulator that can inhibit or activate SIRT6 (Rahnasto-Rilla et al. 2016). These dual modulators were also docked to SIRT6, but the reason for their dual effect is still unclear.

The binding mode of activators

To determine a possible activator binding site, DLM binding sites in SIRT6 structure were predicted with SiteMap. SiteMap reported five sites for SIRT6, but only two of these sites were predicted to be druggable (Dscore > 0.98), with the others being undruggable and unlikely to bind small molecules (SiteScore < 0.8). The best scored site covered the substrate-binding site and the NAM-binding pocket at the cleft between the Rossmann fold and Zn-binding domain (SiteScore 1.077, Dscore 1.097, volume 482 Å^3) (Figure 13). The second-best site was predicted to be next to the substrate-binding site between the substrate-binding β6/α6-loop and Zn-binding domain. It did not overlap with the best scored site, and it had a SiteScore of 1.003, Dscore of 1.022, and volume of 342 Å^3. This second-best site was selected as the activator docking site.
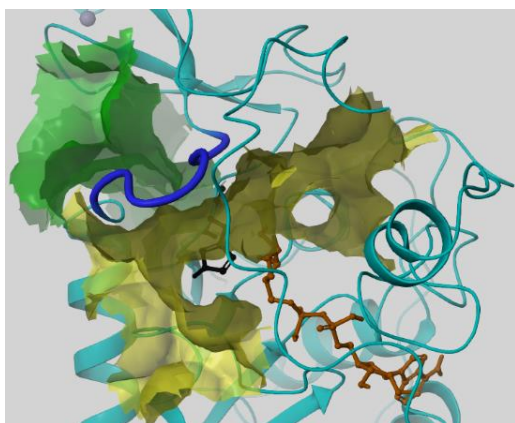
Figure 13. The druggable sites predicted by SiteMap on SIRT6 structure (PDB ID: 3ZG6) (Pan et al. 2011). The best scoring site is marked with yellow and the second-best site is marked with green. The grey ball is Zn^{2+}, blue loop is the substrate-binding β6/α6, active histidine is coloured with black, and co-crystallised ADPr with brown.

The most potent activators, compounds **11–13**, had docking poses outside the substrate-binding cleft. They formed π-π interactions with W188, salt bridges with D187, and hydrogen bonds with substrate-binding β6/α6-loop residues and Zn-binding domain residue G158 (Figure 14). The interactions of the activators with the substrate-binding loop might have an influence on the conformation or orientation of the loop residues. These effects can further influence the binding ability of the substrate.
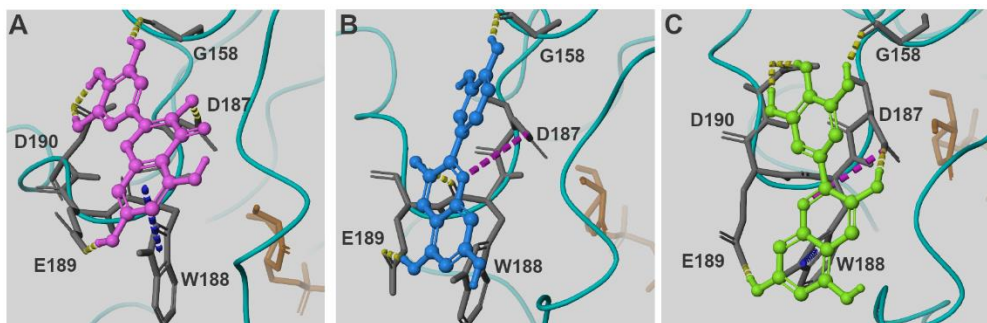
Figure 14. Representative docking poses and interactions of the activators: compounds **11** (A), **12** (B), and **13** (C). Yellow dashed indicate hydrogen bonding, magenta dashes salt bridges, and blue dashes π-π-stacking. Co-crystallised ADPr is marked with brown.

5.2 SYNTHETIC QUERCETIN DERIVATIVES INHIBIT SIRT6 (STUDY II)

Two SIRT6 inhibitors were discovered in study II. These compounds were synthetic quercetin derivatives compounds **14** and **15** (Figure 15) that were previously shown to have antioxidative effects (Veverka et al. 2013). They inhibited also SIRT1–3, and compound **15** was shown to be an especially potent inhibitor of SIRT2 (Figure 15). The dual modulators quercetin and compound **10** from study I were used as reference compounds. The results indicated that all the tested compounds would act only as inhibitors. As the results of the fluorescence assay for compound **10** and

quercetin were ambiguous and disagreed with the results of the HPLC assay in study I, the effect of the compounds on SIRT6 deacetylation activity was confirmed with Western blotting. In the Western blotting method, a full length H3 histone was used as a substrate, whereas in the other methods, the substrate was a H3 peptide (residues 1–21). The results of Western blotting indicated that compound **10** was an activator whereas quercetin and compounds **14** and **15** were inhibitors. The kinetic studies showed that compound **14** was NAD⁺ competitive inhibitor whereas compound **15** competed with the peptide substrate.

I% (SIRT6) ≈ 20
IC₅₀ (SIRT6) = 130 μM
I% (SIRT2) = 29

I% (SIRT6) ≈ 20
IC₅₀ (SIRT6) = 55 μM
I% (SIRT2) = 85
IC₅₀ (SIRT2) = 14 μM
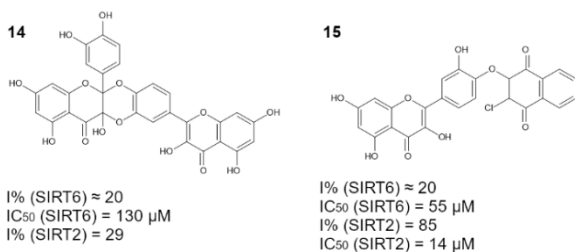
Figure 15. SIRT6 inhibitors discovered in study II. The compound concentration for reported inhibition % (I%) of SIRT6 and SIRT2 is 50 μM.

The binding modes of quercetin derivatives in SIRT6

Before docking, compound **14** and **15** were prepared, and possible ionization stages and isomers were generated as the isomer composition of the substance applied in *in vitro* studies was unknown. Compound **15** did not have any stereoisomers but compound **14** had four unionized stereoisomers (Figure 16). Compounds **14** and **15** were docked to the substrate-binding site and also close to the NAM-binding site in order to explore the possible reasons why compound **14** was NAD⁺-competitive whereas compound **15** competed with the substrate.
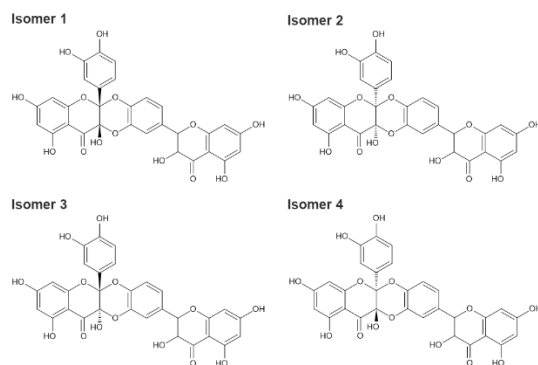
Figure 16. The isomers of compound **14**.

All compound **14** isomers found poses in the hydrophobic pocket that includes the NAM-binding site, but isomers 1 and 2 had poses with more interactions than the other isomers (Figure 17). Isomer 3 was the only compound that had poses also at the substrate binding site. These results suggest that the isomers 1 and 2 are unlikely to bind to the substrate-binding site. The isomers of compound **14** underwent π-π

interactions and h-bonds with the N-terminus (N4), ADPr-binding site (P62 and F64), α3/α4 loop (P80, F82, W84, T85, and F86), NAM-binding site (V115 and D116), active histidine (H133), Zn-binding domain (G155), and substrate-binding site (L186). The SIRT 6 inhibiting trichostatin A and benzoic acid and quinazoline sulfonamide derivatives have also been suggested to interact with P62, F64, V115, and D116 (Parenti et al. 2014, You and Steegborn 2018).
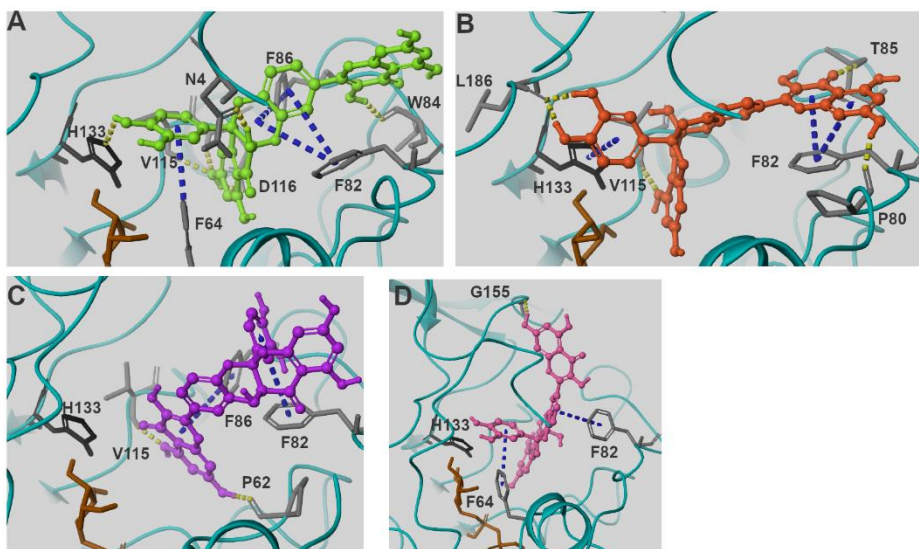
Figure 17. Representative docking poses of the isomers 1 (A), 2 (B), 3 (C), and 4(D) of compound **14**. H133 is the catalytically active histidine and ADPr is presented with brown colour. Hydrogen bonds are presented with yellow dashes, and π-π-stacking with blue dashing.

Compound **15** fitted better into the substrate binding site than into the site near NAM-binding site where the lipophilic chloronaphthoquinone-moiety of compound **15** was positioned outside the pocket and was exposed to solvent (Figure 18). The docking pose of compound **15** at substrate-binding site revealed that it formed π-π interactions with W188 and F64 and hydrogen bonds with E189 and D190. F64 is located in the ADPr-binding site while the rest of the residues were located in the substrate-binding β6/α6 loop.
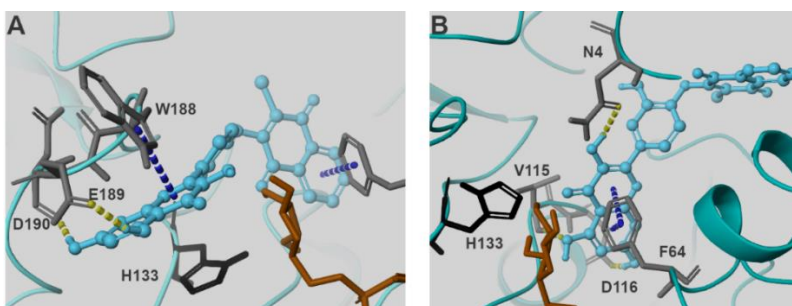
Figure 18. Representative docking poses of compound **15** at substrate-binding site (A), and at the site that includes the NAM-binding site (B). H133 is the catalytically active histidine and ADPr is presented with brown colour. Hydrogen bonds are presented with yellow dashes, and π-π-stacking with blue dashes.

The binding mode of quercetin derivatives in SIRT2

As compounds **14** and **15** were also potent SIRT2 inhibitors, they were docked to theSIRT2 structure at the binding site of SirReal2 that is approximately the same size as the compounds **14** and **15**. Based on the results, both of these compounds might position slightly differently than SirReal2 within the cleft between the Zn-binding domain and Rossmann-fold domain (Figure 19).
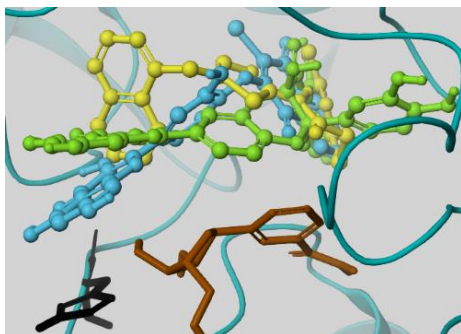
Figure 19. Representative docking poses of compound **14** (isomer 1) (green) and compound **15** (light blue) aligned with co-crystallised SirReal2 (yellow) at SIRT2 inhibitor binding site. Co-crystallised SirReal2 is represented with, compound **14** with light green, and compound **15** with light blue colour. Black residue is the catalytically active histidine and brown compound is NAD⁺.

5.3 NOVEL FLAVONE DERIVATIVE IS A POTENT SIRT6 DEACETYLASE ACTIVATOR (STUDY III)

In study III, one potent SIRT6 activator and two SIRT6 inhibitors were discovered (Figure 20). The activator was a synthetic flavone derivative (compound **16**) and the results of the kinetic studies suggested that it improved the binding of the substrate considerably but had no effect on the binding of NAD⁺. The inhibitors discovered in study III were novel dihydropyridine derivatives synthetized by a collaborating research group (compounds **17** and **18**) and they were approximately as potent as compound **8** discovered in study I (Figure 9).

16

FA_max = 30–40
EC50 = 80 μM

15

I% ≈ 60

17

I% ≈ 60
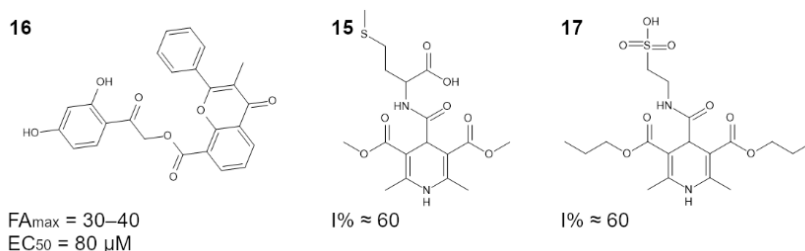
Figure 20. SIRT6 modulators discovered in study III.

The binding mode of the potent SIRT6 activating flavone derivative

Compound **16** was predicted to have a total charge of -1 at pH 7.4 (Figure 21A). The docking revealed that compound **16** has a pose where the flavone moiety places according to the quercetin and the rest of the compound positioned next to α3 helix (Figure 21B). The activator formed a hydrogen bond with E74 locating in α3 helix. This pose was compared with known SIRT6 activators. The flavone moiety of compound **16** places to the binding site of activator UBCS039, and the rest of the compound occupies a part of the binding site of MDL-801 (Figure 21C) (You et al. 2017, Huang et al. 2018).
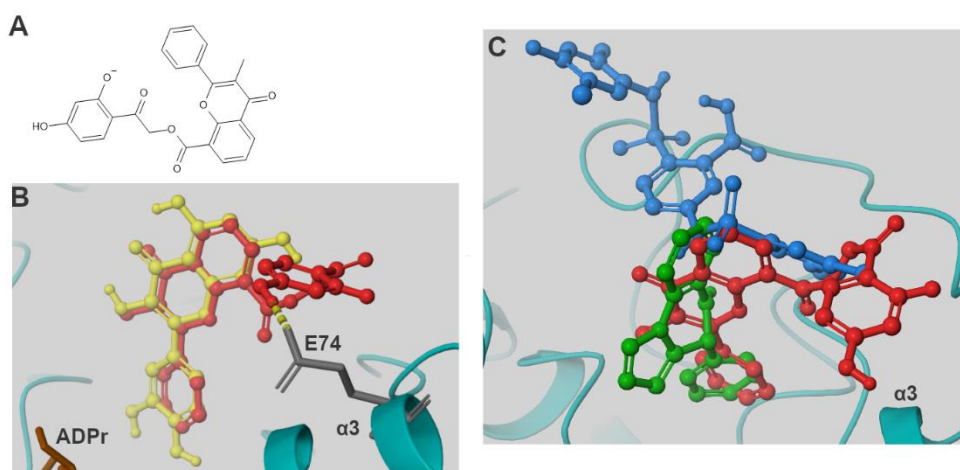
Figure 21. (A) The ionised form of compound **16**. (B) The docking pose of compound **16** (red) aligned with co-crystallised quercetin (yellow). Yellow dashes indicate hydrogen bonding. (C) The docking pose of compound **16** (red) aligned with the crystallised poses of SIRT6 activators UBCS039 (green) and MDL-801 (blue).

The binding modes of SIRT6 inhibiting dihydropyridine derivatives

Compounds **17** and **18** were predicted to have a net charge of -1 at pH 7.4 (Figure 22). Additionally, compound **17** was predicted to have two stereoisomers (Figure 22) that were both docked. The grid centre for the inhibitors was assigned to be at the NAM-binding site. Both compound **17** isomers could occupy a part of the NAM-binding site but neither of them could be placed near to the substrate-binding site

(Figure 23A). Interestingly, compound **18** found two alternative poses: one reaching deeper into NAM-binding pocket and one reaching deeper into the substrate binding site (Figure 23B). The inhibitors formed interactions with F82 in the $\alpha3/\alpha4$ loop and with L186 and W188 in the $\beta6/\alpha6$ loop. Interestingly, compound **18** had no electrostatic interactions when occupying the NAM-binding site.
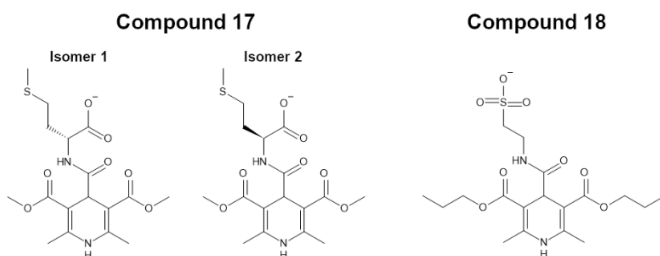
Figure 22. The deprotonated structures of compound **17** isomers and compound **18**.
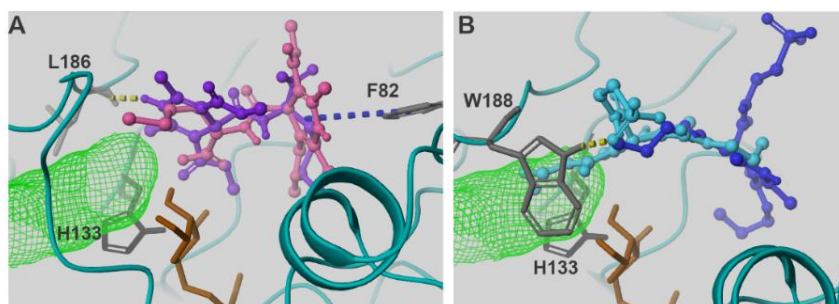
Figure 23. Representative docking poses of compound **17** isomers 1 (pink) and 2 (purple) (A). Two different docking poses of compound **18** (blue and light blue) (B). Substrate-binding site is marked with green mesh and ADPr with brown colour. Blue dashes indicate π-π-stacking and yellow dashes hydrogen bonds.

5.4 CELLULAR EFFECTS OF SIRT6 DEACETYLASE ACTIVATORS (STUDIES I AND III)

The effects of the SIRT6 activating compound **12** on cellular SIRT6 protein levels were investigated in Caco-2 cells. Compound **12** upregulated the protein levels of SIRT6. It also downregulated the protein levels of Twist-related protein 1 (Twist1) and GLUT-1 and upregulated the levels of forkhead box O3 (FoxO3α). These proteins are all associated with SIRT6 and have been claimed to be involved in cancer (Zhong et al. 2010, Han et al. 2014, Zhao et al. 2017, Liu et al. 2018b, Zhang et al. 2019b).

In study III, the SIRT6 activating compound **16** was administered to a variety of breast cancer cell lines and the effect on SIRT6 mRNA levels was examined. The results showed that compound **16** has no significant effect on the expression of SIRT6. The effect of compound **16** on cell viability of non-tumorigenic immortalized MCF10A breast cells and variety of breast cancer cells was investigated at concentrations of 1–100 μM. At 100 μM concentration, the activator decreased the viability of the MCF10A cells and triple negative (Hs578T) cancer cells. No effect was

detected on the viability of the other breast cancer cells. However, compound **16** decreased the cell number of all cancer cell lines investigated, and thus inhibited their proliferation. As the compound **16** affected the proliferation, its effect on cell cycle was investigated. The compound arrested the cell cycle in cell lines but in different cell cycle phases depending on the cell type.

5.5 BET INHIBITION CAN ALTER SIRTUIN LEVELS IN BREAST CANCER CELLS (STUDY IV)

In study IV, an alternative approach to modulate SIRT activity was investigated. BET proteins, that bind to acetylated lysines of histones and serve a binding platform for different transcription factors, were inhibited and the effect on SIRT1 was measured. The effect of BET inhibition was investigated in two breast cancer cell lines: estrogen and progesterone receptor positive MCF-7 and triple negative MDA-MB-231 cells. Previously (+)-JQ1 was reported to increase the levels of SIRT1 in MCF-7 cells as well as in two other human cell lines (Kokkola et al. 2015). In study IV, in addition to (+)-JQ1, two structurally diverse inhibitors were used: I-BET151 and Pfi-1. Interestingly, the effects of the inhibitors were different.

The impacts of BET inhibition on SIRT1 protein levels and acetylation of p53(K382) in MCF-7 cells
I-BET151 exerted increasing effects on SIRT1 protein levels in MCF-7 cells while Pfi-1 was inactive (Figure 24A&B). To examine if the changes in SIRT1 levels correlated to the SIRT1 mediated deacetylation, the levels of acetylated p53 (acp53) lysine 382 (K382) were determined. Even though I-BET151 increased SIRT1 levels, the acetylation level of SIRT1 target acp53(K382) did not decrease accordingly (Figure 24C). In addition, Pfi-1 had no statistically significant effect on the levels of acp53(K382) (Figure 24D). The levels of total p53 were constant (Figure 24E&F).

Figure 24. Western blotting results of I-BET151 and Pfi-1 treated MCF-7 cells. Data are presented as mean ±SEM (n=3). Statistical significance is presented with *(p < 0.05 vs. control).

The impacts of BET inhibition on SIRT1 levels levels and acetylation of p53(K382) in MDA-MB-231 cells

(+)-JQ1 decreased SIRT1 levels in MDA-MB-231 cells (Figure 25A) and thus, the effect was opposite than that reported in MCF-7 cells (Kokkola et al. 2015). However, I-BET151 and Pfi-1 displayed similar effects in MDA-MB-231 cells on SIRT1 as in MCF-7 cells: I-BET151 increased SIRT1 levels, and Pfi-1 had no effect (Figure 25B&C). Despite the opposite effects on SIRT1 protein levels, both (+)-JQ1 and I-BET151

increased p53(K382) acetylation (Figure 25D&E). This indicates that the change in SIRT1 levels might not correlate with the acetylation level of its target, p53(K382). Pfi-1 had no significant effect on the acetylation level of p53(K382) (Figure 25F). Interestingly, (+)-JQ1 and I-BET151 decreased total p53 levels at all concentrations, and the effect of I-BET151 was significant (Figure 25G&H). Pfi-1 decreased total p53 levels only at the concentration of 350 nM (Figure 25L). The results for Pfi-1 at the 700 nM concentration were omitted since it caused a decrease in α-tubulin levels.
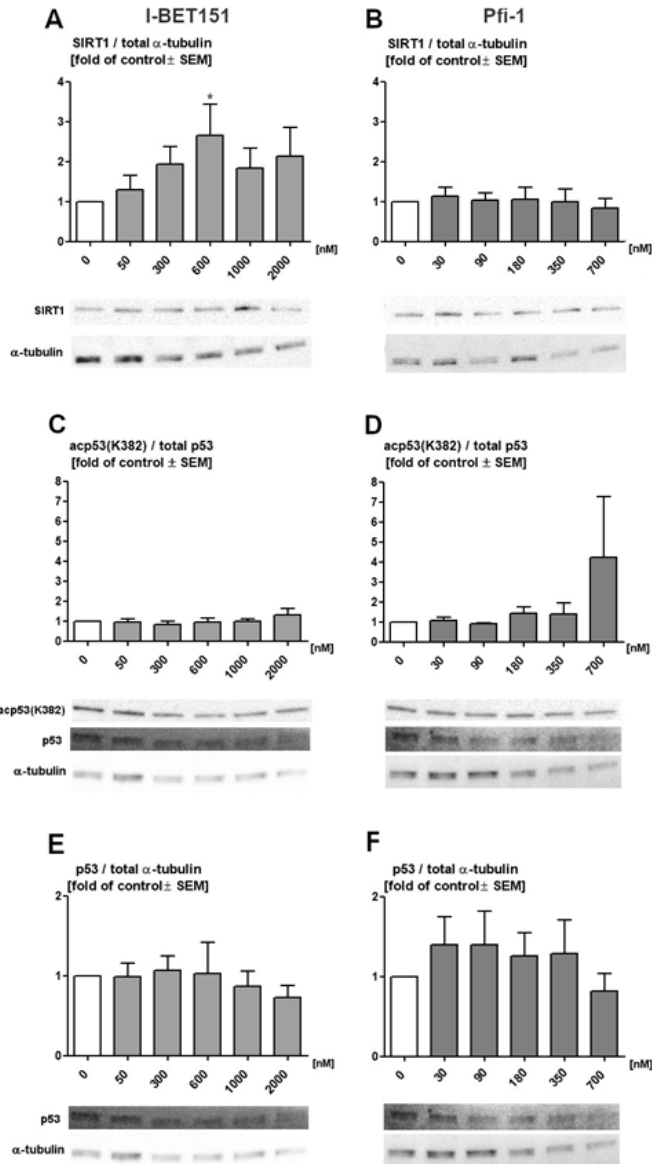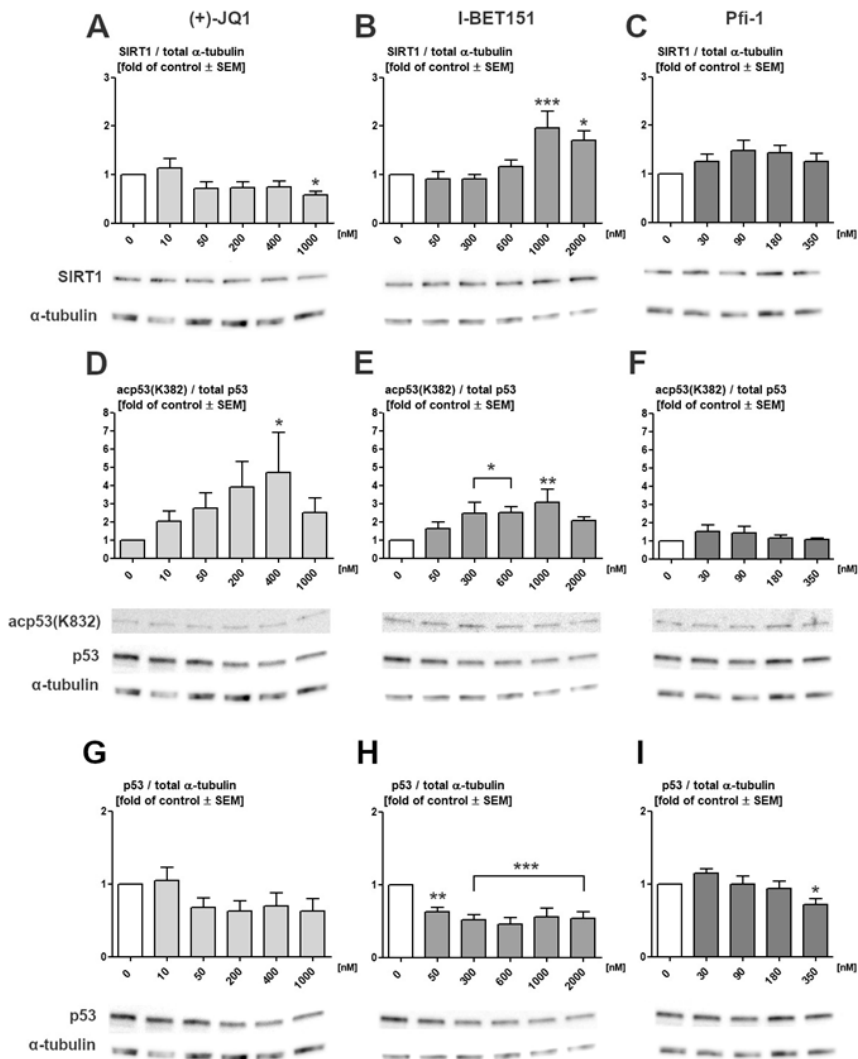

Figure 25. Western blotting results BET inhibitor treated MDA-MB-231 cells. Data are presented as mean ±SEM (n=3). Statistical significance is presented with * (p < 0.05 vs. control), ** (p < 0.01 vs. control), and *** (p < 0.001 vs. control).

6 DISCUSSION

6.1 SIRT6 DEACETYLASE MODULATORS

Fewer modulators for SIRT6 have been developed than for SIRT1–3. When starting this thesis work, only a few non-peptide SIRT6 inhibitors had been published, and the most potent of them had an IC_{50} value of 37 µM (Table 5) (Sociali et al. 2015). Moreover, the only compounds known to activate SIRT6 deacetylation reaction were certain natural fatty acids and their derivatives as well as quercetin and luteolin (Feldman et al. 2013, Rahnasto-Rilla et al. 2016).

In this work, several potent SIRT6 deacetylase modulators with novel scaffolds were discovered. The majority of the compounds were natural polyphenols that affect multiple disease-related processes (Li et al. 2014). The most potent inhibitors were catechin gallate compounds **6** and **7** that were discovered in study I (Figure 9). These compounds were more potent than the previously published SIRT6 inhibitors except for the cyclic pentapeptide inhibitor described by Liu and Zheng (2016). Moreover, two very potent SIRT6 activators were discovered: compound **12** in study I and compound **16** in study III that had FA_{max} values of 55 and 30–40, respectively. Only the lysophosphatidic acid that was reported recently has a comparable FA_{max} value (Table 6) (Klein et al. 2020). Synthetic quercetin derivatives were also shown to inhibit SIRT6 and have IC_{50} values similar to those of benzoic acid and quinazoline sulfonamide compounds (Table 5). In addition, dihydropyridine derivatives were shown for the first time to inhibit SIRT6.

However, it is challenging to compare the potency of the modulators discovered in this work to those compounds examined in other studies due to the differences in assay conditions. Different studies have shown that the effect of SIRT deacetylase modulators, especially in the case of activators, can vary between substrates, as the reaction rate and affinity for different substrates can differ (Dai et al. 2010, Wood et al. 2018). This work also revealed that the substrate affects the results of deacetylation assays: Compound **10** and quercetin, that were designated as being concentration dependent dual modulators in the peptide-based HPLC assay, showed only activation (compound **10**) or inhibition (quercetin) with the full-length H3 substrate. In addition to the differences in the substrates, also variations in the concentrations of the substrate or NAD^+ can affect the results.

However, quercetin and some other polyphenolic compounds have been demonstrated to form aggregates at higher concentrations at certain assay concentrations (Pohjala and Tammela 2012, Reker et al. 2019). The aggregates on the other hand can cause unspesific inhibition through denaturation or conformational changes. Thus, some of the polyphenolic compounds can show inhibition because they form aggregates.

6.2 THE BINDING SITES OF SIRT6 MODULATORS

At the beginning of this work, no inhibitors or activators had been crystallised with SIRT6: the first SIRT6 structure with an activator was published on 2017, and the first structure with an inhibitor was released on 2018 (Table 5) (You et al. 2017, You and Steegborn 2018). The binding sites of SIRT6 inhibitors for docking were assigned to be at the substrate-binding site or closer to the NAM-binding site as they are the most common SIRT inhibitor binding sites. The results of inhibitor docking implied that the shape complementarity with the pocket affects to the inhibition potency. Additionally, simultaneous interactions with NAM- and substrate-binding sites, N-terminus, $\alpha 3$ helix, and $\alpha 3/\alpha 4$ loop might also be important for inhibition. Some of the interactions suggested by docking in this work have previously been reported for other SIRT6 inhibitors and thus, they might be critical for the inhibitory effects of these compounds. (Parenti et al. 2014, You and Steegborn 2018). In summary, the results of all SIRT6 docking studies indicated that the SIRT6 inhibitors can bind either to the substrate-binding site or to the NAM-binding site, or they can occupy both sites simultaneously.

At the time of study I, no activators had been crystallised with SIRT6 and there was conflicting knowledge about the binding sites of other SIRT activators (Dai et al. 2018). Thus, SiteMap was used to predict possible DLM binding sites. As the most druggable binding site covered the inhibitor binding site, the other druggable site was chosen for activator docking. The activators formed interactions with the substrate-binding loop from the outside of the substrate-binding cleft. Since they might undergo interactions with the substrate-binding loop, they might subsequently affect the substrate binding properties. However, as the SIRT6 crystal structure lacks approximately the 50 C-terminal amino acids, the possible C-terminal binding site(s) were undetected with SiteMap that predicts the pockets based on the protein's 3D structure. Thus, the C-terminal domain might include a better binding site for the activators.

Before study III was started, a crystal structure of SIRT6 in a complex with the dual modulator quercetin was published (PDB ID 6QCD); it showed that quercetin would bind to the cleft between the Zn-binding domain and the Rossmann-fold domain (You et al. 2019). The docking results of the most potent activator, compound **16**, showed that while the flavonoid moiety positioned according to the quercetin, the rest of the molecule placed next to $\alpha 3/\alpha 4$ loop. The pose had similarities with previously published activator UBCS039 that has been suggested to bind to the propsed binding site of SIRT6 activating fatty acids (You et al. 2017, Klein et al. 2020). Moreover, compound **16** occupied partly the binding site of allosteric SIRT6 activator MDL-801. Overall, it seems that SIRT6 might have more than only one activator binding site.

After study I, SIRT6 crystal structures containing compounds **6** and **12** were reported (PDB ID 6QCJ and 6QCH) (You et al. 2019). The binding pose of compound **6** differed from the onr suggested by docking. As the molecular modelling results are

predictions, the differences between the crystallisation and docking can originate from errors in the docking. However, also the crystallization process might have resulted in inaccuracies in the binding mode since the compounds have been soaked after crystallizing SIRT6 with ADPr. Additionally, the crystal structure lacks several N-terminal residues that participate in forming at least the myristoyl binding site in the cleft between the Rossmann-fold and the Zn-binding domain (Jiang et al. 2013, Huang et al. 2018). Thus, they are likely to form also parts of the other binding pockets located in that cleft.

Moreover, the N-terminal domain might be important for SIRT6 activator-binding similarly to the situation with SIRT1 as the polyphenolic SIRT1 activator, resveratrol, has been shown to bind between the N-terminal domain and substrate (Cao et al. 2015). Additionally, none of the SIRT6 crystal structures have included co-crystallised NAD^+ nor acetylated substrate. Thus, their exact interactions and binding modes at SIRT6 are unknown and it is difficult to compare the interactions and poses of inhibitors with substrate or the NAM-moiety of NAD^+.

In addition to the problems in SIRT6 crystal structures, modelling the ionisation states and subsequent enolates of the activating compounds **11**, **12**, and **13** are possible sources of errors. Those activators have been predicted to have pKa values close to physiological values or assay pH (~8) (Álvarez-Diduk et al. 2013, León-Carmona et al. 2016). Thus, they might exist in more than one ionisation form in those conditions, and thus it seems that the modelling methods used in this work are imprecise in predicting the exact form of the compounds.

6.3   THE IMPLICATIONS OF SIRT6 MODULATORS

SIRT6 can be a possible drug target in a variety of diseases including cancer, metabolic diseases, and inflammation (Khan et al. 2018). However, SIRT6 possesses diverse roles in cancer e.g. depending on the cancer type (Garcia-Peterson et al. 2017, Desantis et al. 2018). In this work, the two most potent activators, compounds **12** and **16** were investigated in different cancer cell lines. In Caco-2 cells, compound **12** increased the protein levels of SIRT6 and subsequently decreased the protein levels of Twist1 and GLUT-1, i.e. two proteins that are tumour promotors (Zhong et al. 2010, Zhao et al. 2017). Compound **12** also increased the protein levels of the tumour suppressor FoxO3α, a protein known to induce the expression of SIRT6 (Liu et al. 2018b, Zhang et al. 2019b). Thus, compound **12** could potentially exert several anti-cancer effects.

Compound **16** was investigated in breast cancer cell lines. The results imply that it inhibited the proliferation and arrested the cell cycle in either the G1 or G2 phase. However, the magnitude of the proliferation effect and the effect on cell cycle varied between the cell lines.

The natural flavonoids that modulated SIRT6 activity have been reported also to affect other targets and disease pathways (Pan et al. 2010, Abotaleb et al. 2019, Neri-Numa et al. 2020). Thus, some of the cellular effects observed for the activators might

be caused by the modulation of some other protein and not SIRT6. In fact, some of the drug candidates in clinical trials actually might induce tumour suppressive effects through their off-targets (Lin et al. 2019).

Examples of the other targets for the SIRT6 modulators of this work are inflammation-related interleukin 17A, inhibited by compound **12**, and various kinases that interact at least with compounds **8**, **10**, and **11** (Kim et al. 2015, Fechtner et al. 2017, Liu et al. 2017, Stoll et al. 2019). Additionally, the quercetin derivatives (study II) and dihydropyridine derivatives (study III) modulate other SIRTs (Mai et al. 2009). Nonetheless, since these off-targets affect the same processes as SIRT6, modulating them together with SIRT6 might represent a good strategy in the treatment of different diseases. In cancer, for example, targeting multiple proteins has been suggested to be one approach to overcomimg possible drug resistance (Apaya et al. 2016, Rao et al. 2019). Moreover, targeting multiple SIRTs might have synergistic effects in cancer, as both activators and inhibitors of SIRT1 potentiate the anti-tumour effects of HDAC inhibitors (Cea et al. 2011, Kala et al. 2015).

6.4 THE INTERPLAY BETWEEN BET INHIBITION AND SIRT EXPRESSION

Due to the difficulties in the development SIRT activators, an alternative way to affect SIRT activity was explored. BET inhibition was shown to affect the SIRT1 protein levels, with the effect varying both between the inhibitors and the cell lines. The change in SIRT1 levels did not correlate with the acetylation level of its target, p53(K382). Thus, the cellular activity of SIRT1 might not increase accordingly with SIRT1 levels, or the BET inhibitors can cause an opposite effect on p53(K382) acetylation by acting on other pathways.

The results from this work and previous studies imply that the effects of BET inhibitors on SIRT1 can be cell type-dependent (Banerjee et al. 2012, Kokkola et al. 2015, Hytti et al. 2016). Thus, BET inhibitors should be investigated with different types of cells when developing BET inhibition-based treatments. Moreover, conclusions made based on only one type of BET inhibitors should be avoided, as these compounds might exert individual effects. For example, their unexpected effects on the expression of other epigenetic proteins or possible off-targets might cause unwanted side-effects that could lead to a failure in clinical trials (Andrieu et al. 2016).

In addition to SIRT1, BET inhibition has been demonstrated to upregulate the expression of HDAC6 (Carew et al. 2019). Moreover, different BET inhibitors have exerted synergistic effects with HDAC inhibitors (Table 8). Thus, similar synergy might exist also between BET inhibitors and SIRTs. As SIRT1 modulators and HDAC inhibitors have also shown synergistic effects in cancer, the idea of aiming at a triple target of BETs, SIRTs, and other HDACs might represent an interesting approach in the therapy of cancer.

7   CONCLUSIONS AND FUTURE PROSPECTS

In this work, several previously unreported SIRT6 deacetylase modulators were discovered; these represent interesting new starting points for developing more SIRT6 modulators and investigating SIRT6-related diseases. Two of the inhibitors, compounds **6** and **7**, were more potent than the previously reported non-peptide inhibitors with IC_{50} values of 2.5 μM and 5.4 μM, respectively. Moreover, two highly potent activators, compounds **12** and **16**, were discovered. They were determined to activate SIRT6 catalysed deacetylation reaction up to 55- and 30–40-fold, respectively. They also displayed anticancer effects in different cell lines. Thus, SIRT6 activation can serve as a novel approach to develop treatments against cancer. The anticancer effects of SIRT6 inhibitors should also be investigated as the role of SIRT6 in cancer seems to depends on both the cancer type and its stage.

The SIRT6 modulating flavonoids discovered in this work are unselective. In the future studies, selective SIRT6 modulators will be needed to clarify the SIRT6-specific effects in cells. Nevertheless their target proteins are related to the same processes influenced by SIRT6 and thus, co-targeting these other proteins and SIRT6 could be investigated as a future strategy for cancer treatment.

In the future molecular modelling tools can help in developing selective and more efficient SIRT6 modulators that could enter into clinical trials. However, a full length SIRT6 is needed if one wishes to investigate all the possible sites and interactions. Moreover, the structure should include NAD^+ and acetylated substrate since that would demonstrate the exact catalytical interactions and conformations.

Despite the incomplete SIRT6 structures, this work provided insights into the possible interactions and binding modes of SIRT6 modulators. As the site for activators remained unconfirmed, the possible binding sites should be still examined with other computational tools, for example with MD-based methods. Alternatively, an experimental method, such as PAL could be used in detecting the binding site.

BET inhibition was shown to be an alternative approach to modulate SIRTs. This approach could be considered in developing future treatments intended to modulate SIRT activity. However, the effect seems to be cell line-dependent and should be investigated further and confirmed for other SIRTs. Nevertheless, as BET inhibitors and SIRT modulators can both exert synergistic effects with HDAC inhibitors, exploiting this epigenetic triplet might be a future approach in targeting serious diseases, such as cancer.

REFERENCES

Abotaleb M, Samuel SM, Varghese E, Varghese S, Kubatka P, Liskova A, et al. Flavonoids in cancer and apoptosis. Cancers (Basel) 11: 28, 2019

Afshar G, Murnane JP. Characterization of a human gene with sequence homology to *Saccharomyces cerevisiae SIR2*. Gene 234: 161–8, 1999

Al-Mawsawi LQ, Fikkert V, Dayam R, Witvrouw M, Burke TR Jr, Borchers CH, et al. Discovery of a small-molecule HIV-1 integrase inhibitor-binding site. Proc Natl Acad Sci U S A 103: 10080–5, 2006

Álvarez-Diduk R, Ramírez-Silva MT, Galano A, Merkoçi A. Deprotonation mechanism and acidity constants in aqueous solution of flavonols: a combined experimental and theoretical study. J Phys Chem B 117: 12347–59, 2013

An J, Totrov M, Abagyan R. Pocketome via comprehensive identification and classification of ligand binding envelopes. Mol Cell Proteomics 4: 752–61, 2005

Andrieu G, Belkina AC, Denis GV. Clinical trials for BET inhibitors run ahead of the science. Drug Discov Today Technol 19: 45–50, 2016

Apaya MK, Chang M-T, Shyur L-F. Phytomedicine polypharmacology: cancer therapy through modulating the tumor microenvironment and oxylipin dynamics. Pharmacol Ther 162: 58–68, 2016

Aquilano K, Vigilanza P, Baldelli S, Pagliei B, Rotilio G, Ciriolo MR. Peroxisome proliferator-activated receptor γ co-activator 1α (PGC-1α) and Sirtuin 1 (SIRT1) reside in mitochondria. J Biol Chem 285: 21590–9, 2010

Ardestani PM, Liang F. Sub-cellular localization, expression and functions of Sirt6 during the cell cycle in HeLa cells. Nucleus 3: 442–51, 2012

Armon A, Graur D, Ben-Tal N. ConSurf: an algorithmic tool for the identification of functional regions in proteins by surface mapping of phylogenetic information. J Mol Biol 307: 447–63, 2001

Arsiwala T, Pahla J, van Tits LJ, Bisceglie L, Gaul DS, Costantino S, et al. *Sirt6* deletion in bone marrow-derived cells increases atherosclerosis – central role of macrophage scavenger receptor 1. J Mol Cell Cardiol 139: 24–32, 2020

Autin P, Blanquart C, Fradin D. Epigenetic drugs for cancer and microRNAs: A focus on histone deacetylase inhibitors. Cancers (Basel) 11: 1530, 2019

Bae JS, Noh SJ, Kim KM, Park S-H, Hussein UK, Park HS, et al. SIRT6 is involved in the progression of ovarian carcinomas via β-catenin-mediated epithelial to mesenchymal transition. Front Oncol 8: 538, 2018

Banerjee C, Archin N, Michaels D, Belkina AC, Denis GV, Bradner J, et al. BET bromodomain inhibition as a novel strategy for reactivation of HIV-1. J Leukoc Biol 92: 1147–54, 2012

Berman HM, Westbrook J, Feng Z, Gilliland G, Bhat TN, Weissig H, et al. The Protein Data Bank. Nucleic Acid Res 28: 235–42, 2000

Bhardwaj A, Das S. SIRT6 deacetylates PKM2 to suppress its nuclear localization and oncogenic functions. Proc Natl Acad Sci U S A 113: E538–47, 2016

Bohnuud T, Kozakov D, Vajda S. Evidence of conformational selection driving the fromation of ligand binding sites in protein-protein interfaces. PLoS Comput Biol 10: e1003872, 2014

Bolivar BE, Welch JT. Studies of the binding of modest modulators of the human enzyme, Sirtuin 6, by STD NMR. ChemBioChem 18: 931–40, 2017

Bonazzoli E, Predolini F, Cocco E, Bellone S, Altwerger G, Menderes G, et al. Inhibition of BET bromodomain proteins with GS-5829 and GS-626510 in uterine serous carcinoma, a biologically aggressive variant of endometrial cancer. Clin Cancer Res 24: 4845–53, 2018

Bowman GR, Geissler PL. Equilibrium fluctuations of a single folded protein reveal a multitude of potential cryptic allosteric sites. Proc Natl Acad Sci U S A 109: 11681–6, 2012

Brady GP Jr, Stouten PFW. Fast prediction and visualization of protein binding pockets with PASS. J Comput Aided Mol Des 14: 383–401, 2000

Brenke R, Kozakov D, Chuang G-Y, Beglov D, Hall D, Landon MR, et al. Fragment-based identification of druggable 'hot spots' of proteins using Fourier domain correlation techniques. Bioinformatics 25: 621–7, 2009

Broomhead NK, Soliman ME. Can we rely on computational predictions to correctly identify ligand binding sites on novel protein drug targets? Assessment of binding site prediction methods and a protocol for validation of predicted binding sites. Cell Biochem Biophys 75: 15–23, 2017

Brylinski M, Feinstein WP. eFindSite: improved prediction of ligand binding sites in protein models using meta-threading, machine learning and auxiliary ligands. J Comput Aided Mol Des 27: 551–67, 2013

Brylinski M, Skolnick J. A threading-based method (FINDSITE) for ligand-binding site prediction and functional annotation. Proc Natl Acad Sci U S A 105: 129– 34, 2008

Burgen ASV, Roberts GCK, Feeney J. Binding of flexible ligands to macromolecules. Nature 253: 753–5, 1975

Cao C, Xu S. Improving the performance of the PLB index for ligand-binding site prediction using dihedral angles and the solvent-accessible surface area. Sci Rep 6: 33232, 2016

Cao D, Wang M, Qiu X, Liu D, Jiang H, Yang N, et al. Structural basis for allosteric, substrate-dependent stimulation of SIRT1 activity by resveratrol. Genes Dev 29: 1316–25, 2015

Capra JA, Laskowski RA, Thornton JM, Singh M, Funkhouser TA. Predicting protein ligand binding sites by combining evolutionary sequence conservation and 3D structure. PLoS Comput Biol 5: e1000585, 2009

Carew JS, Espitia CM, Zhao W, Visconte V, Anwer F, Kelly KR, et al. Rational cotargeting of HDAC6 and BET proteins yields synergistic antimyeloma activity. Blood Adv 3: 1318–29, 2019

Cea M, Soncini D, Fruscione F, Raffaghello L, Garuti A, Emionite L, et al. Synergistic interactions between HDAC and sirtuin inhibitors in human leukemia cells. PLoS One 6: e22739, 2011

Chalkiadaki A, Guarente L. The multifaceted functions of sirtuins in cancer. Nat Rev Cancer 15: 608–24, 2015

Chen B, Zang W, Wang J, Huang Y, He Y, Yan L, et al. The chemical biology of sirtuins. Chem Soc Rev 44: 5246–64, 2015

Chen W, Liu N, Zhang H, Zhang H, Qiao J, Jia W, et al. Sirt6 promotes DNA end joining in iPSCs derived from old mice. Cell Rep 18: 2880–92, 2017

Cheng WWL, Budelier MM, Sugasawa Y, Bergdoll L, Queralt-Martín M, Rosencrans W, et al. Multiple neurosteroid and cholesterol binding sites in voltage-dependent anion channel-1 determined by photo-affinity labeling. Biochim Biophys Acta Mol Cell Biol Lipids 1864: 1269–79, 2019

Choudhary P, Kumar S, Bachhawat AK, Pandit SB. CSmetaPred: A consensus method for prediction of catalytic residues. BMC Bioinformatics 18: 583, 2017

Cimermancic P, Weinkam P, Rettenmaier TJ, Bichmann L, Keedy DA, Woldeyes RA, et al. CryptoSite: Expanding the druggable proteome by characterization and prediction of cryptic binding sites. J Mol Biol 428: 709–19, 2016

Cochran AG, Conery AR, Sims 3rd RJ. Bromodomains: a new target class for drug development. Nat Rev Drug Discov 18: 609–28, 2019

Colas E, Perez C, Cabrera S, Pedrola N, Monge M, Castellvi J, et al. Molecular markers of endometrial carcinoma detected in uterine aspirates. Int J Cancer 129: 2435–44, 2011

Comitani F, Gervasio FL. Exploring cryptic pockets formation in targets of pharmaceutical interest with SWISH. J Chem Theory Comput 14: 3321–31, 2018

Cortiguera MG, García-Gaipo L, Wagner SD, León J, Battle-López A, Delgado MD. Suppression of BCL6 function by HDAC inhibitor mediated acetylation and chromatin modification enhances BET inhibitor effects in B-cell lymphoma cells. Sci Rep 9: 16495, 2019

Cournia Z, Allen B, Sherman W. Relative binding free energy calculations in drug discovery: recent advances and practical considerations. J Chem Inf Model 57: 2911-37, 2017

Craig IR, Pfleger C, Gohlke H, Essex JW, Spiegel K. Pocket-space maps to identify novel binding-site conformations in proteins. J Chem Inf Model 51: 2666–79, 2011

Cross JB, Thompson DC, Rai BK, Baber JC, Fan KY, Hu Y, et al. Comparison of several molecular docking programs: pose prediction and virtual screening accuracy. J Chem Inf Model 49: 1455–74, 2009

Csermely P, Palotai R, Nussinov R. Induced fit, conformational selection and independent dynamic segments: an extended view of binding events. Trends Biochem Sci 35: 539–46, 2010

Dai H, Kustigian L, Carney D, Case A, Considine T, Hubbard BP, et al. SIRT1 activation by small molecules: kinetic and biophysical evidence for direct interaction of enzyme and activator. J Biol Chem 285: 32695–703, 2010

Dai H, Sinclair DA, Ellis JL, Steegborn C. Sirtuin activators and inhibitors: Promises, achievements, and challenges. Pharmacol Ther 188: 140–54, 2018

Damonte P, Sociali G, Parenti MD, Soncini D, Bauer I, Boero S, et al. SIRT6 inhibitors with salicylate-like structure show immunosuppressive and chemosensitizing effects. Bioorg Med Chem 25: 5849–58, 2017

David CC, Jacobs DJ. Principal component analysis: a method for determining the essential dynamics of proteins. Methods Mol Biol 1084: 193–226, 2014

Dawson MA, Prinjha RK, Dittmann A, Giotopoulos G, Bantscheff M, Chan W-I, et al. Inhibition of BET recruitment to chromatin as an effective treatment for MLL-fusion leukaemia. Nature 478: 529–33, 2011

Delmore JE, Issa GC, Lemieux ME, Rahl PB, Shi J, Jacobs HM, et al. BET bromodomain inhibition as a therapeutic strategy to target c-Myc. Cell 146: 904–17, 2011

Desantis V, Lamanuzzi A, Vacca A. The role of SIRT6 in tumors. Haematologica 103: 1–4, 2018

Ding Y, Wu S, Huo Y, Chen X, Chai L, Wang Y, et al. Inhibition of Sirt6 suppresses tumor growth by inducing G1/S phase arrest in renal cancer cells. Int J Clin Exp Pathol 12: 2526–35, 2019

Djinovic-Carugo K, Carugo O. Missing strings of residues in protein crystal structures. Intrinsically Disord Proteins 3: e1095697, 2015

Doerr A. Together at last: crystallography and NMR. Nature Methods 3: 6, 2006

Dominy JE Jr, Lee Y, Jedrychowski MP, Chim H, Jurczak MJ, Camporez JP, et al. The deacetylase Sirt6 activates the acetyltransferase GCN5 and suppresses hepatic gluconeogenesis. Mol Cell 48: 900–13, 2012

Du X, Li Y, Xia Y-L, Ai S-M, Liang J, Sang P, et al. Insights into protein-ligand interactions: mechanisms, models, and methods. Int J Mol Sci 17: 144, 2016

Du Y, Cai T, Li T, Xue P, Zhou B, He X, et al. Lysine malonylation is elevated in type 2 diabetic mouse models and enriched in metabolic associated proteins. Mol Cell Proteomics 14: 227–36, 2015

Dukka BKC. Structure-based methods for computational protein functional site prediction. Comp Struct Biotechnol J 8: e201308005, 2013

Durrant JD, McCammon JA. NNScore: a neural-network-based scoring function for the characterization of protein–ligand complexes. J Chem Inf Model 50: 1865–71, 2010

Echevarría-Vargas IM, Reyes-Uribe PI, Guterres AN, Yin X, Kossenkov AV, Liu Q, et al. Co-targeting BET and MEK as salvage therapy for MAPK and checkpoint inhibitor-resistant melanoma. EMBO Mol Med 10: e8446, 2018

Edelsbrunner H, Mücke EP. Three-dimensional alpha shapes. ACM Trans Graph 13: 43–72, 1994

Edfeldt FNB, Folmer RHA, Breeze AL. Fragment screening to predict druggability (ligandability) and lead discovery success. Drug Discov Today 16: 284–7, 2011

Ehrmann FR, Stojko J, Metz A, Debaene F, Barandun LJ, Heine A, et al. Soaking suggests "alternative facts": Only co-crystallization discloses major ligand-induced interface rearrangements of a homodimeric tRNA-binding protein indicating a novel mode-of-inhibition. PLoS ONE 12: e0175723, 2017

Ehrt C, Brinkjost T, Koch O. Binding site characterization – similarity, promiscuity, and druggability. Medchemcomm 10: 1145–59, 2019

Ekblad T, Schüler H. Sirtuins are unaffected by PARP inhibitors containing planar nicotinamide bioisosteres. Chem Biol Drug Design 87: 478–82, 2016

Faivre EJ, Wilcox DM, Hessler P, Uziel T, Tapang P, Magoc T, et al. Abstract 4694: ABBV-075, a novel BET family inhibitor, disrupts critical transcription programs that drive prostate cancer growth to induce potent anti-tumor activity *in vitro* and *in vivo*. Cancer Res 76: 4694, 2016

Farid R, Day T, Friesner RA, Pearlstein RA. New insights about HERG blockade obtained from protein modeling, potential energy mapping, and docking studies. Bioorg Med Chem 14: 3160–73, 2006

Fechtner S, Singh A, Chourasia M, Ahmed S. Molecular insights into the differences in anti-inflammatory activities of green tea catechins on IL-1β signaling in rheumatoid arthritis synovial fibroblasts. Toxicol Appl Pharmacol 329: 112–20, 2017

Feige JN, Auwrex J. Transcriptional targets of sirtuins in the coordination of mammalian physiology. Curr Opin Cell Biol 20: 303–9, 2008

Feldman JL, Baeza J, Denu JM. Activation of the protein deacetylase SIRT6 by long-chain fatty acids and widespread deacylation by mammalian sirtuins. J Biol Chem 288: 31350–6, 2013

Feng J, Yan P-F, Zhao H-Y, Zhang F-C, Zhao W-H, Feng M. SIRT6 suppresses glioma cell growth via induction of apoptosis, inhibition of oxidative stress and suppression of JAK2/STAT3 signaling pathway activation. Oncol Rep 35: 1395–402, 2016

Feng W, Pan LF, Zhang MJ. Combination of NMR spectroscopy and X-ray crystallography offers unique advantages for elucidation of the structural basis of protein complex assembly. Sci China Life Sci 54: 101–11, 2011

Fidanze SD, Liu D, Mantei RA, Hasvold LA, Pratt JK, Sheppard GS, et al. Discovery and optimization of novel constrained pyrrolopyridone BET family inhibitors. Bioorg Med Chem Lett 28: 1804–10, 2018

Filippakopoulos P, Picaud S, Mangos M, Keates T, Lambert J-P, Barsyte-Lovejoy D, et al. Histone recognition and large-scale structural analysis of the human bromodomain family. Cell 149: 214–31, 2012

Filippakopoulos P, Qi J, Picaud S, Shen Y, Smith WB, Fedorov O, et al. Selective inhibition of BET bromodomains. Nature 468: 1067–73, 2010

Fischer E. Einfluss der Configuration auf die Wirkung der Enzyme. Ber Dtsch Chem Ges 27: 2985–93, 1894

Fish PV, Filippakopoulos P, Bish G, Brennan PE, Bunnage ME, Cook AS, et al. Identification of a chemical probe for bromo and extra C-terminal bromodomain inhibition through optimization of a fragment-derived hit. J Med Chem 55: 9831–7, 2012

Fiskus W, Sharma S, Qi J, Valenta JA, Schaub LJ, Shah B, et al. Highly active combination of BRD4 antagonist and histone deacetylase inhibitor against human acute myelogenous leukemia cells. Mol Cancer Ther 13: 1142–54, 2014

Fratev F, Sirimulla S. An improved free energy perturbation FEP+ sampling protocol for flexible ligand-binding domains. Sci Rep 9: 16829, 2019

Friesner RA, Banks JL, Murphy RB, Halgren TA, Klicic JJ, Mainz DT, et al. Glide: a new approach for rapid, accurate docking and scoring. 1. Method and assessment of docking accuracy. J Med Chem 47: 1739–49, 2004

Friesner RA, Murphy RB, Repasky MP, Frye LL, Greenwood JR, Halgren TA, et al. Extra precision glide: docking and scoring incorporating a model of hydrophobic enclosure for protein-ligand complexes. J Med Chem 49: 6177–96, 2006

Frye RA. Characterization of five human cDNAs with homology to the yeast SIR2 gene: Sir2-like proteins (sirtuins) metabolize NAD and may have protein ADP-ribosyltransferase activity. Biochem Biophys Res Commun 260: 273–9, 1999

Fukuda T, Wada-Hiraike O, Oda K, Tanikawa M, Makii C, Inaba K, et al. Putative tumor suppression function of SIRT6 in endometrial cancer. FEBS Lett 589: 2274–81, 2015

Gallinari P, Di Marco S, Jones P, Pallaoro M, Steinkühler C. HDACs, histone deacetylation and gene transcription: from molecular biology to cancer therapeutics. Cell Res 17: 195–211, 2007

Gao Y, Qu Y, Zhou Q, Ma Y. SIRT6 inhibits proliferation and invasion in osteosarcoma cells by targeting N-cadherin. Oncol Lett 17: 1237–44, 2019

Garcia-Peterson LM, Ndiaye MA, Singh CK, Chhabra G, Huang W, Ahmad N. SIRT6 histone deacetylase functions as a potential oncogene in human melanoma. Genes Cancer 8: 701–12, 2017

Gee CL, Drinkwater N, Tyndall JDA, Grunewald GL, Wu Q, McLeish MJ, et al. Enzyme adaptation to inhibitor binding: a cryptic binding site in phenylethanolamine N-methyltransferase. J Med Chem 50: 4845–53, 2007

Geissler R, Brandt W, Ziegler J. Molecular modeling and site-directed mutagenesis reveal the benzylisoquinoline binding site of the short-chain dehydrogenase/reductase salutaridine reductase. Plant Physiol 143: 1493–503, 2007

Geng C-H, Zhang C-L, Zhang J-Y, Gao P, He M, Li Y-L. Overexpression of Sirt6 is a novel biomarker of malignant human colon carcinoma. J Cell Biochem 119: 3957–67, 2018

Genheden S, Ryde U. How to obtain statistically converged MM/GBSA results. J Comput Chem 31: 837–46, 2010

Gertz M, Fischer F, Nguyen GTT, Lakshminarasimhan M, Schutkowski M, Weynad M, et al. Ex-527 inhibits Sirtuins by exploiting their unique NAD^+-dependent deacetylation mechanism. Proc Natl Acad Sci U S A 110: E2772–81, 2013

Geschwindner S, Ulander J, Johansson P. Ligand binding thermodynamics in drug discovery: still a hot tip? J Med Chem 58: 6321–35, 2015

Glaser F, Pupko T, Paz I, Bell RE, Bechor-Shental D, Martz E, et al. ConSurf: identification of functional regions in proteins by surface-mapping of phylogenetic information. Bioinformatics 19: 163–4, 2003

Goodford PJ. A computational procedure for determining energetically favorable binding sites on biologically important macromolecules. J Med Chem 28: 849–57, 1985

Greenwood JR, Calkins D, Sullivan AP, Shelley JC. Towards the comprehensive, rapid, and accurate prediction of the favorable tautomeric states of drug-like molecules in aqueous solution. J Comput Aided Mol Des 24: 591–604, 2010

Griñán-Ferré C, Sarroca S, Ivanova A, Puigoriol-Illamola D, Aguado F, Camins A, et al. Epigenetic mechanisms underlying cognitive impairment and Alzheimer disease hallmarks in 5XFAD mice. Aging (Albany NY) 8: 664–84, 2016

Gronemeyer H, Govindan MV. Affinity labelling of steroid hormone receptors. Mol Cell Endocrinol 46: 1–19, 1986

Grove LE, Hall DR, Beglov D, Vajda S, Kozakov D. FTFlex: accounting for binding site flexibility to improve fragment-based identification of druggable hot spots. Bioinformatics 29: 1218–9, 2013

Guan X, Lin P, Knoll E, Chakrabarti R. Mechanism of inhibition of the human sirtuin enzyme SIRT3 by nicotinamide: computational and experimental studies. PLoS One 9: e107729, 2014

Guo C, Steinberg LK, Cheng M, Song JH, Henderson JP, Gross ML. Site-specific siderocalin binding to ferric and ferric-free enterobactin as revealed by mass spectrometry. ACS Chem Biol 15: 1154–60, 2020

Guo N-H, Zheng J-F, Zi F-M, Cheng J. I-BET151 suppresses osteoclast formation and inflammatory cytokines secretion by targetting BRD4 in multiple myeloma. Biosci Rep 39: BSR20181245, 2019

Ha J-H, Loh SN. Protein conformational switches: from nature to design. Chemistry 18: 7984–99, 2013

Haigis MC, Mostoslavsky R, Haigis KM, Fahie K, Christodoulou DC, Murphy AJ, et al. SIRT4 inhibits glutamate dehydrogenase and opposes the effects of calorie restriction in pancreatic β cells. Cell 126: 941–54, 2006

Hajduk PJ, Huth JR, Fesik SW. Druggability indices for protein targets derived from NMR-based screening data. J Med Chem 48: 25518–25, 2005

Halgren T. New method for fast and accurate binding-site identification and analysis. Chem Biol Drug Des 69: 146–8, 2007

Halgren TA. Identifying and characterizing binding sites and assessing druggability. J Chem Inf Model 49: 377–89, 2009

Han LL, Jia L, Wu F, Huang C. Sirtuin6 (SIRT6) promotes the EMT of hepatocellular carcinoma by stimulating autophagic degradation of E-cadherin. Mol Cancer Res 17: 2267–80, 2019

Han Z, Liu L, Liu Y, Li S. Sirtuin SIRT6 suppresses cell proliferation through inhibition of Twist1 expression in non-small cell lung cancer. Int J Clin Exp Pathol 7: 4774–81, 2014

Harder E, Damm W, Maple J, Wu C, Reboul M, Xiang JY, et al. OPLS3: a force field providing broad coverage of drug-like small molecules and proteins. J Chem Theory Comput 12: 281–96, 2016

He B, Hu J, Zhang X, Lin H. Thiomyristoyl peptides as cell-permeable Sirt6 inhibitors. Org Biomol Chem 12: 7498–502, 2014

He Q, Chen K, Ye R, Dai N, Guo P, Wang L. Associations of sirtuins with clinicopathological variables and prognosis in human ovarian cancer. Oncol Lett 19: 3278–88, 2020

Heinemann A, Cullinane C, De Paoli-Iseppi R, Wilmott JS, Gunatilake D, Madore J, et al. Combining BET and HDAC inhibitors synergistically induces apoptosis of melanoma and suppresses AKT and YAP signaling. Oncotarget 6: 21507–21, 2015

Hendlich M, Rippmann F, Barnickel G. LIGSITE: automatic and efficient detection of potential small molecule-binding sites in proteins. J Mol Graph Model 15: 359–63, 1997

Henrich S, Salo-Ahen OMH, Huang B, Rippmann FF, Cruciani G, Wade RC. Computational approaches to identifying and characterizing protein binding sites for ligand design. J Mol Recognit 23: 209–19, 2010

Hingorani AD, Kuan V, Finan C, Kruger FA, Gaulton A, Chopade S, et al. Improving the odds of drug development success through human genomics: modelling study. Sci Rep 9: 18911, 2019

Ho BK, Agard DA. Probing the flexibility of large conformational changes in protein structures through local perturbations. PLoS Comput Biol 5: e1000343, 2009

Hollingsworth SA, Kelly B, Valant C, Michaelis JA, Mastromihalis O, Thompson G, et al. Cryptic pocket formation underlies allosteric modulator selectivity at muscarinic GPCRs. Nat Commun 10: 3289, 2019

Hopkins AL, Groom CR. The druggable genome. Nat Rev Drug Discov 1: 727–30, 2002

Hou K-L, Lin S-K, Chao L-H, Lai EH-H, Chang C-C, Shun C-T, et al. Sirtuin 6 suppresses hypoxia-induced inflammatory response in human osteoblasts via inhibition of reactive oxygen species production and glycolysis–A therapeutic implication in inflammatory bone resorption. Biofactors 43: 170–80, 2017

Hsieh C-J, Ferrie JJ, Xu K, Lee I, Graham TJA, Tu Z, et al. Alpha synuclein fibrils contain multiple binding sites for small molecules. ACS Chem Neurosci 9: 2521–27, 2019

Hu J, He B, Bhargava S, Lin H. A fluorogenic assay for screening Sirt6 modulators. Org Biomol Chem 11: 5213–6, 2013

Huang B. MetaPocket: a meta approach to improve protein ligand binding site prediction. OMICS 13: 325–30, 2009

Huang B, Schroeder M. LIGSITE^{CSC}: predicting ligand binding sites using the Connolly surface and degree of conservation. BMC Struct Biol 6: 19, 2006

Huang N, Jacobson MP. Binding-site assessment by virtual fragment screening. PLoS One 5: e10109, 2010

Huang Z, Zhao J, Deng W, Chen Y, Shang J, Song K, et al. Identification of cellularly active SIRT6 allosteric activator. Nat Chem Biol 14: 1118–1126, 2018

Hudson WH, de Vera IMS, Nwachukwu JC, Weikum ER, Herbst AG, Yang Q, et al. Cryptic glucocorticoid receptor-binding sites pervade genomic NF-κB response elements. Nat Commun 9: 1337, 2018

Huovinen M, Loikkanen J, Myllynen P, Vähäkangas KH. Characterization of human breast cancer cell lines for the studies on p53 in chemical carcinogenesis. Toxicol In Vitro 25: 1007–17, 2011

Hupe MC, Hoda MR, Zengerling F, Perner S, Merseburger AS, Cronauer MV. The BET-inhibitor PFI-1 diminishes AR/AR-V7 signaling in prostate cancer cells. World J Urol 37: 343–9, 2019

Hussein HA, Geneix C, Petitjean M, Borrel A, Flatters D, Camproux A-C. Global vision of druggability issues: applications and perspectives. Drug Discov Today 22: 404–15, 2017

Hytti M, Tokarz P, Määttä E, Piippo N, Korhonen E, Suuronen T, et al. Inhibition of BET bromodomains alleviates inflammation in human RPE Cells. Biochem Pharmacol 110–111: 71–9, 2016

Hölscher AS, Schulz WA, Pinkerneil M, Niegisch G, Hoffmann MJ. Combined inhibition of BET proteins and class I HDACs synergistically induces apoptosis in urothelial carcinoma cell lines. Clin Epigenetics 10: 1, 2018

Jacobson MP, Pincus DL, Rapp CS, Day TJF, Honig B, Shaw DE, et al. A hierarchical approach to all-atom protein loop prediction. Proteins 55: 351–67, 2004

Jedrusik-Bode M, Studencka M, Smolka C, Baumann T, Schmidt H, Kampf J, et al. The sirtuin SIRT6 regulates stress granule formation in *C. elegans* and mammals. J Cell Sci 126: 5166–77, 2013

Jeh SU, Park JJ, Lee JS, Kim DC, Do J, Lee SW, et al. Differential expression of the sirtuin family in renal cell carcinoma: Aspects of carcinogenesis and prognostic significance. Urol Oncol 35: 675.e9–675.e15, 2017

Jęśko H, Wencel P, Strosznajder RP, Strosznajder JB. Sirtuins and their roles in brain aging and neurodegenerative disorders. Neurochem Res 42: 876–890, 2017

Jiang H, Khan S Wang Y, Charron G, He B, Sebastian C, et al. SIRT6 regulates TNF-α secretion through hydrolysis of long-chain fatty acyl lysine. Nature 496: 110–3, 2013

Jin L, Wang W, Fang G. Targeting protein-protein interaction by small molecules. Annu Rev Pharmacol Toxicol 54: 435–56, 2014

Jing H, Lin H. Sirtuins in epigenetic regulation. Chem Rev 115: 2350–75, 2015

Kala R, Shah HN, Martin SL, Tollefsbol TO. Epigenetic-based combinatorial resveratrol and pterostilbene alters DNA damage response by affecting SIRT1 and DNMT enzyme expression, including SIRT1-dependent γ-H2AX and telomerase regulation in triple-negative breast cancer. BMC Cancer 15: 672, 2015

Kane AE, Sinclair DA. Sirtuins and NAD+ in the development and treatment of metabolic and cardiovascular diseases. Circ Res 123: 868–85, 2018

Kar G, Keskin O, Gursoy A, Nussinov R. Allostery and population shift in drug discovery. Curr Opin Pharmacol 10: 715–22, 2010

Karakashev S, Zhu H, Yokoyama Y, Zhao B, Fatkhutdinov N, Kossenkov AV, et al. BET bromodomain inhibition synergizes with PARP inhibitor in epithelial ovarian cancer. Cell Rep 21: 3398–405, 2017

Kawahara TLA, Michishita E, Adler AS, Damian M, Berber E, Lin M, et al. SIRT6 links histone H3 lysine 9 deacetylation to NF-κB-dependent gene expression and organismal life span. Cell 136: 62–74, 2009

Khan RI, Nirzhor SSR, Akter R. A review of the recent advances made with SIRT6 and its implications on aging related processes, major human diseases, and possible therapeutic targets. Biomolecules 8: 44, 2018

Khongkow M, Olmos Y, Gong C, Gomes AR, Monteiro LJ, Yagüe E, et al. SIRT6 modulates paclitaxel and epirubicin resistance and survival in breast cancer. Carcinogenesis 34: 1476–86, 2013

Kim H, Jacobson MK, Rolli V, Ménissier-de Murcia J, Reinbolt J, Simonin F, et al. Photoaffinity labelling of human poly(ADP-ribose) polymerase catalytic domain. Biochem J 322: 469–75, 1997

Kim SH, Park JG, Lee J, Yang WS, Park GW, Kim HG, et al. The dietary flavonoid kaempferol mediates anti-inflammatory responses via the Src, Syk, IRAK1, and IRAK4 molecular targets. Mediators Inflamm 2015: 904142, 2015

Kim SR, Lewis JM, Cyrenne BM, Monico PF, Mirza FN, Carlson KR, et al. BET inhibition in advanced cutaneous T cell lymphoma is synergistically potentiated by BCL2 inhibition or HDAC inhibition. Oncotarget 9: 29193–207, 2018

Kimura SR, Hu HP, Ruvinsky AM, Sherman W, Favia AD. Deciphering cryptic binding sites on proteins by mixed-solvent molecular dynamics. J Chem Inf Model 57: 1388–401, 2017

Klein MA, Liu C, Kuznetsov VI, Feltenberger JB, Tang W, Denu JM. Mechanism of activation for the sirtuin 6 protein deacylase. J Biol Chem 295: 1385–99, 2020

Kleywegt GJ, Jones TA. Detection, delineation, measurement and display of cavities in macromolecular structures. Acta Crystallogr D Biol Crystallogr 50: 178–85, 1994

Kokkola T, Suuronen T, Pesonen M, Filippakopoulos P, Salminen A, Jarho EM, et al. BET inhibition upregulates SIRT1 and alleviates inflammatory responses. Chembiochem 16: 1997–2001, 2015

Kokkonen P, Rahnasto-Rilla M, Kiviranta PH, Huhtiniemi T, Laitinen T, Poso A, et al. Peptides and pseudopeptides as SIRT6 deacetylation inhibitors. ACS Med Chem Lett 3: 969–74, 2012

Kokkonen P, Rahnasto-Rilla M, Mellini P, Jarho E, Lahtela-Kakkonen M, Kokkola T. Studying SIRT6 regulation using H3K56 based substrate and small molecules. Eur J Pharm Sci 63: 71–76, 2014

Kollman PA, Massova I, Reyes C, Kuhn B, Huo S, Chong L, et al. Calculating structures and free energies of complex molecules: combining molecular mechanics and continuum models. Acc Chem Res 33: 889–97, 2000

Koshland DE Jr. Application of a theory of enzyme specificity to protein synthesis. Proc Natl Acad Sci U S A 44: 98–104, 1958

Kozakov D, Hall DR, Napoleon RL, Yueh C, Whitty A, Vajda S. New frontiers in druggability. J Med Chem 58: 9063–88, 2015

Krishnamoorthy V, Vilwanathan R. Silencing Sirtuin 6 induces cell cycle arrest and apoptosis in non-small cell lung cancer cell lines. Genomics 112: 3703–12, 2020

Krivák R, Hoksza D. Improving protein-ligand binding site prediction accuracy by classification of inner pocket points using local features. J Cheminform 7: 12, 2015

Krivák R, Hoksza D. P2Rank: machine learning based tool for rapid and accurate prediction of ligand binding sites from protein structure. J Cheminform 10: 39, 2018

Lai C-C, Lin P-M, Lin S-F, Hsu C-H, Lin H-C, Hu M-L, et al. Altered expression of *SIRT* gene family in head and neck squamous cell carcinoma. Tumour Biol 34: 1847–54, 2013

Lanza M, Benincasa G, Costa D, Napoli C. Clinical role of epigenetics and network analysis in eye diseases: a translational science review. J Ophthalmol 2019: 2424956, 2019

Laskowski RA. SURFNET: a program for visualizing molecular surfaces, cavities, and intermolecular interactions. J Mol Graph 13: 323–30, 1995

Laurie ATR, Jackson RM. Q-SiteFinder: an energy-based method for the prediction of protein-ligand binding sites. Bioinformatics 21: 1908–16, 2005

Lavarone E, Barbieri CM, Pasini D. Dissecting the role of H3K27 acetylation and methylation in PRC2 mediated control of cellular identity. Nat Commun 10: 1679, 2019

Le Guilloux V, Schmidtke P, Tuffery P. Fpocket: An open source platform for ligand pocket detection. BMC Bioinformatics 10: 168, 2009

Lee HS, Im W. Identification of ligand templates using local structure alignment for structure-based drug design. J Chem Inf Model 52: 2784–95, 2012

Lee H-S, Ka S-O, Lee S-M, Lee S-I, Park J-W, Park B-H. Overexpression of sirtuin 6 suppresses inflammatory responses and bone destruction in mice with collagen-induced arthritis. Arthritis Rheum 65: 1776–85, 2013

León-Carmona JR, Galano A, Álvarez-Idaboy JR. Deprotonation routes of anthocyanidins in aqueous solution, pK_a values, and speciation under physiological conditions. RCS Adv 6: 53421–9, 2016

Levitt DG, Banaszak LJ. POCKET: A computer graphics method for identifying and displaying protein cavities and their surrounding amino acids. J Mol Graph 10: 229–34, 1992

Li A-N, Li S, Zhang Y-J, Xu X-R, Chen Y-M, Li H-B. Resources and biological activities of natural polyphenols. Nutrients 6: 6020–47, 2014

Li KS, Schaper Bergman ET, Beno BR, Huang RY-C, Deyanova E, Chen G, et al. Hydrogen-deuterium exchange and hydroxyl radical footprinting for mapping hydrophobic interactions of human bromodomain with a small molecule inhibitor. J Am Soc Mass Spectrom 30: 2795–804, 2019

Li N, Mao D, Cao Y, Li H, Ren F, Li K. Downregulation of SIRT6 by miR-34c-5p is associated with poor prognosis and promotes colon cancer proliferation through inhibiting apoptosis via the JAK2/STAT3 signaling pathway. Int J Oncol 52: 1515–27, 2018a

Li Z, Huang J, Shen S, Ding Z, Luo Q, Chen Z, et al. SIRT6 drives epithelial-to-mesenchymal transition and metastasis in non-small cell lung cancer via snail-dependent transrepression of KLF4. J Exp Clin Cancer Res 37: 323, 2018b

Liang J, Edelsbrunner H, Woodward C. Anatomy of protein pockets and cavities: measurement of binding site geometry and implications for ligand design. Protein Sci 7: 1884–97, 1998

Lichtarge O, Bourne HR, Cohen FE. An evolutionary trace method defines binding surfaces common to protein families. J Mol Biol 257: 342–58, 1996

Lin A, Giuliano CJ, Palladino A, John KM, Abramowicz C, Yuan ML, et al. Off-target toxicity is a common mechanism of action of cancer drugs undergoing clinical trials. Sci Transl Med 11: eaaw8412, 2019

Lionta E, Spyrou G, Vassilatis DK, Cournia Z. Structure-based virtual screening for drug discovery: principles, applications and recent advances. Curr Top Med Chem 14: 1923–38, 2014

Lisi GP, Loria JP. Allostery in enzyme catalysis. Curr Opin Struct Biol 47: 123–30, 2017

Liu C, Zhu L, Fukuda K, Ouyang S, Chen X, Wang C, et al. The flavonoid cyanidin blocks binding of the cytokine interleukin-17A to the IL-17RA subunit to alleviate inflammation in vivo. Sci Signal 10: eaaf8823, 2017

Liu J, Zheng W. Cyclic peptide-based potent human SIRT6 inhibitors. Org Biomol Chem 14: 5928–35, 2016

Liu W, Wu M, Du H, Shi X, Zhang T, Li J. SIRT6 inhibits colorectal cancer stem cell proliferation by targeting CDC25A. Oncol Lett 15: 5368–74, 2018a

Liu Y, Ao X, Ding W, Ponnusamy M, Wu W, Hao X, et al. Critical role of FOXO3a in carcinogenesis. Mol Cancer 17: 104, 2018b

Lu G, Xu X, Li G, Sun H, Wang N, Zhu Y, et al. Subresidue-resolution footprinting of ligand-protein interactions by carbene chemistry and ion mobility-mass spectrometry. Anal Chem 92: 947–56, 2020b

Lu T, Lu W, Luo C. A patent review of BRD4 inhibitors (2013-2019). Expert Opin Ther Pat 30: 57–81, 2020c

Lu Y, Chan Y-T, Tan H-Y, Li S, Wang N, Feng Y. Epigenetic regulation in human cancer: the potential role of epi-drug in cancer therapy. Mol Cancer 19: 79, 2020a

Mai A, Valente S, Meade S, Carafa V, Tardugno M, Nebbioso A, et al. Study of 1,4-dihydropyridine structural scaffold: discovery of novel sirtuin activators and inhibitors. J Med Chem 52: 5496–504, 2009

Maity S, Gundampati RK, Kumar TKS. NMR methods to characterize protein-ligand interactions. Nat Prod Commun 14: 1934578X1984929, 2019

Mao Z, Hine C, Tian X, Van Meter M, Au M, Vaidya A, et al. SIRT6 promotes DNA repair under stress by activating PARP1. Science 332: 1443–6, 2011

Mashiach E, Nussinov R, Wolfson HJ. FiberDock: Flexible induced-fit backbone refinement in molecular docking. Proteins 78: 1503–19, 2010

Matsushima S, Sadoshima J. The role of sirtuins in cardiac disease. Am J Physiol Heart Circ Physiol 309: H1375–89, 2015

Maveyraud L, Mourey L. Protein X-ray crystallography and drug discovery. Molecules 25: 1030, 2020

Mazur PK, Herner A, Mello SS, Wirth M, Hausmann S, Sánchez-Rivera FJ, et al. Combined inhibition of BET family proteins and histone deacetylases as a potential epigenetics-based therapy for pancreatic ductal adenocarcinoma. Nat Med 21: 1163–71, 2015

Mellers KM, Yang C, Castro-Rivera CI, Candelario-Jalil E. Selective degradation of BET proteins with dBET1, a proteolysis-targeting chimera, potently reduces pro-inflammatory responses in lipopolysaccharide-activated microglia. Biochem Biophys Res Commun 497: 410–5, 2018

Mellini P, Kokkola T, Suuronen T, Salo HS, Tolvanen L, Mai A, et al. Screen of pseudopeptidic inhibitors of human sirtuins 1–3: two lead compounds with antiproliferative effects in cancer cells. J Med Chem 56: 6681–95, 2013

Meng W, Wang B, Mao W, Wang J, Zhao Y, Li Q, et al. Enhanced efficacy of histone deacetylase inhibitor combined with bromodomain inhibitor in glioblastoma. J Exp Clin Cancer Res 37: 241, 2018

Michel M, Visnes T, Homan EJ, Seashore-Ludlow B, Hedenström M, Wiita E, et al. Computational and experimental druggability assessment of human DNA glycosylases. ACS Omega 4: 11642–56, 2019

Michishita E, McCord RA, Berber E, Kioi M, Padilla-Nash H, Damian M, et al. SIRT6 is a histone H3 lysine 9 deacetylase that modulates telomeric chromatin. Nature 452: 492–6, 2008

Michishita E, McCord RA, Boxer LD, Barber MF, Hong T, Gozani O, et al. Cell cycle-dependent deacetylation of telomeric histone H3 lysine K56 by human SIRT6. Cell Cycle 8: 2664–6, 2009

Michishita E, Park JY, Burneskis JM, Barrett JC, Horikawa I. Evolutionarily conserved and nonconserved cellular localizations and functions of human SIRT proteins. Mol Biol Cell 16: 4623–35, 2005

Miller AL, Fehling SC, Garcia PL, Gamblin TL, Council LN, van Waardenburg RCAM, et al. The BET inhibitor JQ1 attenuates double-strand break repair and sensitizes models of pancreatic ductal adenocarcinoma to PARP inhibitors. EBioMedicine 44: 419–30, 2019

Min J, Landry J, Sternglaz R, Xu R-M. Crystal structure of a SIR2 homolog-NAD complex. Cell 105: 269–79, 2001

Nayal M, Honig B. On the nature of cavities on protein surfaces: application to the identification of drug-binding sites. Proteins 63: 892–906, 2006

Neri-Numa IA, Cazarin CBB, Ruiz ALTG, Paulino BN, Molina G, Pastore GM. Targeting flavonoids on modulation of metabolic syndrome. J Funct Foods 73: 104132, 2020

Neubauer de Amorim HL, Caceres RA, Netz PA. Linear interaction energy (LIE) method in lead discovery and optimization. Curr Drug Targets 9: 1100–5, 2008

Ngan CH, Bohnuud T, Mottarella SE, Beglov D, Villar EA, Hall DR, et al. FTMAP: extended protein mapping with user-selected probe molecules. Nucleic Acids Res 40: W271–5, 2012a

Ngan C-H, Hall DR, Zerbe B, Grove LE, Kozakov D, Vajda S. FTSite: high accuracy detection of ligand binding sites on unbound protein structures. Bioinformatics 28: 286–7, 2012b

Noel JK, Iwata K, Ooike S, Sugahara K, Nakamura H, Daibata M. Abstract C244: Development of the BET bromodomain inhibitor OTX015. Mol Cancer Ther 12: C244, 2013

O'Brien R, Markova N, Holdgate GA. Thermodynamics in drug discovery. In book: Applied biophysics for drug discovery. 1. edition, pp. 7–28. Edited by Huddler D, Zartler ER. John Wiley & Sons Ltd, Chichester, 2017

O'Callaghan C, Vassilopoulos A. Sirtuins at the crossroads of stemness, aging, and cancer. Aging Cell 16: 1208–18, 2017

Outeiro TF, Kontopoulos E, Altmann SM, Kufareva I, Starthearn KE, Amore AM, et al. Sirtuin 2 inhibitors rescue α-synuclein–mediated toxicity in models of Parkinson's disease. Science 317: 516–9, 2007

Overington JP, Al-Lazikani B, Hopkins AL. How many drug targets are there? Nat Rev Drug Discov 5: 993–6, 2006

Pagadala NS, Syed K, Tuszynski J. Software for molecular docking: a review. Biophys Rev 9: 91–102, 2017

Pan M-H, Lai C-S, Ho C-T. Anti-inflammatory activity of natural dietary flavonoids. Food Funct 1: 15–31, 2010

Pan PW, Feldman JL, Devries MK, Dong A, Edwards AM, Denu JM. Structure and biochemical functions of SIRT6. J Biol Chem 286: 14575–87, 2011

Parenti MD, Bruzzone S, Nencioni A, Del Rio A. Selectivity hot-spots of sirtuin catalytic cores. Mol BioSyst 11: 2263–72, 2015

Parenti MD, Grozio A, Bauer I, Galeno L, Damonte P, Millo E, et al. Discovery of novel and selective SIRT6 inhibitors. J Med Chem 57: 4796–804, 2014

Patschull AOM, Gooptu B, Ashford P, Daviter T, Nobeli I. *In Silico* assessment of potential druggable pockets on the surface of α1-antitrypsin conformers. PLoS ONE 7: e36612, 2012

Paul F, Weikl TR. How to distinguish conformational selection and induced fit based on chemical relaxation rates. PLoS Comput Biol 12: e1005067, 2016

Peng J, Dong W, Chen L, Zou T, Qi Y, Liu Y. Brd2 is a TBP-associated protein and recruits TBP into E2F-1 transcriptional complex in response to serum stimulation. Mol Cell Biochem 294: 45–54, 2007

Perrod S, Cockell MM, Laroche T, Renauld H, Ducrest A-L, Bonnard C, et al. A cytosolic NAD-dependent deacetylase Hst2p, can modulate nucleolar and telomeric silencing in yeast. EMBO J 20: 197–209, 2001

Pervaiz M, Mishra P, Günther S. Bromodomain drug discovery – the past, the present, and the future. Chem Rec 18: 1808–17, 2018

Peters KP, Fauck J, Frömmel C. The automatic search for ligand binding sites in proteins of known three-dimensional structure using only geometric criteria. J Mol Biol 256: 201–13, 1996

Pohjala L, Tammela P. Aggregating behavior of phenolic compounds – a source of false bioassay results? Molecules 17: 10774–90, 2012

Pupko T, Bell RE, Mayrose I, Glaser F, Ben-Tal N. Rate4Site: an algorithmic tool for the identification of functional regions in proteins by surface mapping of evolutionary determinants within their homologues. Bioinformatics 18 Suppl 1: S71–7, 2002

Qu N, Hu J-Q, Liu L, Zhang T-T, Sun G-H, Shi R-L, et al. SIRT6 is upregulated and associated with cancer aggressiveness in papillary thyroid cancer via BRAF/ERK/Mcl-1 pathway. Int J Oncol 50: 1683–92, 2017

Rahnasto-Rilla M, Kokkola T, Jarho E, Lahtela-Kakkonen M, Moaddel R. N-acylethanolamines bind to SIRT6. Chembiochem 17: 77–81, 2016

Rahnasto-Rilla MK, McLoughlin P, Kulikowicz T, Doyle M, Bohr VA, Lahtela-Kakkonen M, et al. The identification of a SIRT6 activator from brown algae *Fucus distichus*. Mar Drugs 15: 190, 2017

Rajendran P, Johnson G, Li L, Chen Y-S, Dashwood M, Nguyen N, et al. Acetylation of CCAR2 establishes a BET/BRD9 acetyl switch in response to combined deacetylase and bromodomain inhibition. Cancer Res 79: 918–27, 2019

Rao S, Du G, Hafner M, Subramanian K, Sorger PK, Gray NS. A multitargeted probe-based strategy to identify signaling vulnerabilities in cancers. J Biol Chem 294: 8664–73, 2019

Rarey M, Kramer B, Lengauer T, Klebe G. A fast flexible docking method using an incremental construction algorithm. J Mol Biol 261: 470–89, 1996

RCSB PDB. Searched from the Internet 9.11.2020. www.rcsb.org

Reker D, Bernardes GJL, Rodrigues T. Computational advances in combating colloidal aggregation in drug discovery. Nat Chem 11: 402–18, 2019

Renaud J-P, Chung C-W, Danielson UH, Egner U, Hennig M, Hubbard RE, et al. Biophysics in drug discovery: impact, challenges and opportunities. Nat Rev Drug Discov 15: 679–98, 2016

Revollo JR, Li X. The ways and means that fine tune Sirt1 activity. Trends Biochem Sci 38: 160–7, 2013

Ricatti J, Acquasaliente L, Ribaudo G, De Filippis V, Bellini M, Llovera RE, et al. Effects of point mutations in the binding pocket of the mouse major urinary protein MUP20 on ligand affinity and specificity. Sci Rep 9: 300, 2019

Roche DB, Brackenridge DA, McGuffin LJ. Proteins and their interacting partners: an introduction to protein-ligand binding site prediction methods. Int J Mol Sci 16: 29829–42, 2015

Rooklin D, Wang C, Katigbak J, Arora PS, Zhang Y. AlphaSpace: fragment-centric topographical mapping to target protein-protein interaction interfaces. J Chem Inf Model 55: 1585–99, 2015

Roy A, Zhang Y. Recognizing protein-ligand binding sites by global structural alignment and local geometry refinement. Structure 20: 987–97, 2012

Ruoho AE, Kiefer H, Roeder PE, Singer SJ. The mechanism of photoaffinity labeling. Proc Nat Acad Sci USA 70: 2567–71, 1973

Rye PT, Frick LE, Ozbal CC, Lamarr WA. Advances in label-free screening approaches for studying sirtuin-mediated deacetylation. J Biomol Screen 16: 1217–26, 2011

Sanaei M, Kavoosi F. Histone deacetylases and histone deacetylase inhibitors: molecular mechanisms of action in various cancers. Adv Biomed Res 8: 63, 2019

Santos R, Ursu O, Gaulton A, Bento AP, Donadi RS, Bologa CG, et al. A comprehensive map of molecular drug targets. Nat Rev Drug Discov 16: 19–34, 2017

Sastry GM, Adzhigirey M, Day T, Annabhimoju R, Sherman W. Protein and ligand preparation: parameters, protocols, and influence on virtual screening enrichments. J Comput Aided Mol Des 27: 221–34, 2013

Savchenko A, Yee A, Khachatryan A, Skarina T, Evdokimova E, Pavlova M, et al. Strategies for structural proteomics of prokaryotes: quantifying the advantages of studying orthologous proteins and of using both NMR and X-ray crystallography approaches. Proteins 50: 392–9, 2003

Schiano C, Benincasa G, Franzese M, Mura ND, Pane K, Salvatore M, et al. Epigenetic-sensitive pathways in personalized therapy of major cardiovascular diseases. Pharmacol Ther 210: 107514, 2020

Schmidtke P, Bidon-Chanal A, Luque FJ, Barril X. MDpocket: open-source cavity detection and characterization on molecular dynamics trajectories. Bioinformatics 27: 3276–85, 2011

Schrödinger Release 2016-4: Epik, Glide, Induced Fit Docking protocol, LigPrep, Maestro, Prime, Protein Preparation Wizard, SiteMap, Schrödinger, LLC, New York, NY, 2016

Schrödinger Release 2017-4: Epik, Glide, Induced Fit Docking protocol, LigPrep, Maestro, Prime, Protein Preparation Wizard, SiteMap, Schrödinger, LLC, New York, NY, 2017

Schrödinger Release 2019-4: Epik, Glide, LigPrep, Maestro, Prime, Protein Preparation Wizard, SiteMap, Schrödinger, LLC, New York, NY, 2019

Schwartz TW, Holst B. Allosteric enhancers, allosteric agonists and ago-allosteric modulators: where do they bind and how do they act? Trends Pharmacol Sci 28: 366–73, 2007

Sebastián C, Zwaans BMM, Silberman DM, Gymrek M, Goren A, Zhong L, et al. The histone deacetylase SIRT6 is a tumor suppressor that controls cancer metabolism. Cell 151: 1185–99, 2012

Seco J, Luque FJ, Barril X. Binding site detection and druggability index from first principles. J Med Chem 52: 2363–71, 2009

Seifert T, Malo M, Lengqvist J, Sihlbom C, Jarho EM, Luthman K. Identification of the binding site of chroman-4-one-based Sirtuin 2-selective inhibitors using photoaffinity labeling in combination with tandem mass spectrometry. J Med Chem 59: 10749–99, 2016

Seto E, Yoshida M. Erasers of histone acetylation: The histone deacetylase enzymes. Cold Spring Harb Perspect Biol 6: a018713, 2014

Sherman W, Day T, Jacobson MP, Friesner RA, Farid R. Novel procedure for modeling ligand/receptor induced fit effects. J Med Chem 49: 534–53, 2006

Simões T, Lopes D, Dias S, Fernandes F, Pereira J, Jorge J, et al. Geometric detection algorithms for cavities on protein surfaces in molecular graphics: a survey. Comput Garph Forum 36: 643–83, 2017

Sirtori FR, Altomare A, Carini M, Aldini G, Regazzoni L. MS methods to study macromolecule-ligand interaction: applications in drug discovery. Methods 144: 152–74, 2018

Smith BC, Denu JM. Sir2 deacetylases exhibit nucleophilic participation of acetyl-lysine in NAD^{+} cleavage. J Am Chem Soc 129: 5802–3, 2007

Smith BC, Denu JM. Sir2 protein deacetylases: evidence for chemical intermediates and functions of a conserved histidine. Biochemistry 45: 272–82, 2006

Smith E, Collins I. Photoaffinity labeling in target- and binding-site identification. Future Med Chem 7: 159–83, 2015

Sociali G, Galeno L, Parenti MD, Grozio A, Bauer I, Passalacqua M, et al. Quinazolinedione SIRT6 inhibitors sensitize cancer cells to chemotherapeutics. Eur J Med Chem 102: 530–9, 2015

Sociali G, Grozio A, Caffa I, Schuster S, Becherini P, Damonte P, et al. SIRT6 deacetylase activity regulates NAMPT activity and NAD(P)(H) pools in cancer cells. FASEB J 33: 3704–17, 2019

Sociali G, Magnone M, Ravera S, Damonte P, Vigliarolo T, Von Holtey M, et al. Pharmacological Sirt6 inhibition improves glucose tolerance in a type 2 diabetes mouse model. FASEB J 31: 3138–49, 2017

Soga S, Shirai H, Kobori M, Hirayama N. Use of amino acid composition to predict ligand-binding sites. J Chem Inf Model 47: 400–6, 2007

Sotriffer CA, Sanschagrin P, Matter H, Klebe G. SFCscore: scoring functions for affinity prediction of protein–ligand complexes. Proteins 73: 395–419, 2008

Stank A, Kokh DB, Fuller JC, Wade RC. Protein binding pocket dynamics. Acc Chem Res 49: 809–15, 2016

Stank A, Kokh DB, Horn M, Sizikova E, Neil R, Panecka J, et al. TRAPP webserver: predicting protein binding site flexibility and detecting transient binding pockets. Nucleic Acids Res 45: W325–30, 2017

Stoll S, Bitencourt S, Laufer S, Goettert MI. Myricetin inhibits panel of kinases implicated in tumorigenesis. Basic Clin Pharmacol Toxicol 125: 3–7, 2019

Syson K, Stevenson CEM, Miah F, Barclay JE, Tang M, Gorelik A, et al. Ligand-bound structures and site-directed mutagenesis identify the acceptor and secondary binding sites of *Streptomyces coelicolor* maltosyltransferase GlgE. J Biol Chem 291: 21531–40, 2016

Tanno M, Sakamoto J, Miura T, Shimamoto K, Horio Y. Nucleocytoplasmic shuttling of the NAD$^+$-dependent histone deacetylase SIRT1. J Biol Chem 282: 6823–32, 2007

Tanny JC, Moazed D. Coupling of histone deacetylation to NAD breakdown by the yeast silencing protein Sir2: evidence for acetyl transfer from substrate to an NAD breakdown product. Proc Natl Acad Sci U S A 98: 415–20, 2001

Tao N-N, Ren J-H, Tang H, Ran L-K, Zhou H-Z, Liu B, et al. Deacetylation of Ku70 by SIRT6 attenuates Bax-mediated apoptosis in hepatocellular carcinoma. Biochem Biophys Res Commun 485: 713–9, 2017

Tasselli L, Xi Y, Zheng W, Tennen RI, Odrowaz Z, Simeoni F, et al. SIRT6 deacetylates H3K18ac at pericentric chromatin to prevent mitotic errors and cellular senescence. Nat Struct Mol Biol 23: 434–40, 2016

Thinon E, Hang HC. Chemical reporters for exploring protein acylation. Biochem Soc Trans 43: 253–61, 2015

Thornton BP, Johns A, Al-Sidhani R, Álvarez-Carretero S, Storer ISR, Bromley MJ, et al. Identification of functional and druggable sites in *Aspergillus fumigatus* essential phosphatases by virtual screening. Int J Mol Sci 20: 4636, 2019

Tian J, Yuan L. Sirtuin 6 inhibits colon cancer progression by modulating PTEN/AKT signaling. Biomed Pharmacother 106: 109–16, 2018

Tian K, Liu Z, Wang J, Xu S, You T, Liu P. Sirtuin-6 inhibits cardiac fibroblasts differentiation into myofibroblasts via inactivation of nuclear factor κB signaling. Transl Res 165: 374–86, 2015

Tian X, Firsanov D, Zhang Z, Cheng Y, Luo L, Tombline G, et al. SIRT6 is responsible for more efficient DNA double-strand break repair in long-lived species. Cell 177: 622–638.e22, 2019

Tong Z, Wang M, Wang Y, Kim DD, Grenier JK, Cao J, et al. SIRT7 is an RNA-activated protein lysine deacylase. ACS Chem Biol 12: 300–10, 2017

Tripathi A, Bankaitis VA. Molecular docking: from lock and key to combination lock. J Mol Med Clin Appl 2: 10.16966/2575-0305.106, 2017

Ung PMU, Ghanakota P, Graham SE, Lexa KW, Carlson HA. Identifying binding hot spots on protein surfaces by mixed-solvent molecular dynamics: HIV-1 protease as a test case. Biopolymers 105: 21–34, 2016

UniProt Database. Searched from the Internet 9.4.2020. www.uniprot.org

Valdar WSJ. Scoring residue conservation. Proteins 48: 227–41, 2002

Van Meter M, Gorbunova V, Seluanov A. SIRT6: A promising target for cancer prevention and therapy. Adv Exp Med Biol 818: 181–96, 2014b

Van Meter M, Kashyap M, Rezazadeh S, Geneva AJ, Morello TD, Seluanov A, et al. SIRT6 represses LINE1 retrotransposons by ribosylating KAP1 but this repression fails with stress and age. Nat Commun 5: 5011, 2014a

Vaziri H, Dessain SK, Eaton EN, Imai S-I, Frye RA, Pandita TK, et al. *hSIR2*[SIRT1] functions as an NAD-dependent p53 deacetylase. Cell 107: 149–59, 2001

Velazquez-Campoy A, Luque I, Freire E. The application of thermodynamic methods in drug design. Thermochim Acta 380: 217–27, 2001

Veverka M, Gallovič J, Švajdlenka E, Veverková E, Prónayová N, Miláčková I, et al. Novel quercetin derivatives: synthesis and screening for anti-oxidant activity and aldose reductase inhibition. Chem Pap 67: 76–83, 2013

Wang J, Sheng Z, Cai Y. SIRT6 overexpression inhibits HIF1α expression and its impact on tumor angiogenesis in lung cancer. Int J Clin Exp Pathol 11: 2940–7, 2018b

Wang L, Guo W, Ma J, Dai W, Liu L, Guo S, et al. Aberrant SIRT6 expression contributes to melanoma growth: eole of the autophagy paradox and IGF-AKT signaling. Autophagy 14: 518–33, 2018a

Wang WW, Zeng Y, Wu B, Deiters A, Liu WR. A Chemical biology approach to reveal Sirt6-targeted histone H3 sites in nucleosomes. ACS Chem Biol 11: 1973–81, 2016b

Wang Z, Sun H, Yao X, Li D, Xu L, Li Y, et al. Comprehensive evaluation of ten docking programs on a diverse set of protein–ligand complexes: the prediction accuracy of sampling power and scoring power. Phys Chem Chem Phys 18: 12964–75, 2016a

Weikl TR, von Deuster C. Selected-fit versus induced-fit protein binding: kinetic differences and mutational analysis. Proteins 75: 104–10, 2009

Wenthur CJ, Gentry PR, Mathews TP, Lindsley CW. Drugs for allosteric sites on receptors. Annu Rev Pharmacol Toxicol 54: 165–84, 2014

Wood M, Rymarchyk S, Zheng S, Cen Y. Trichostatin A inhibits deacetylation of histone H3 and p53 by SIRT6. Arch Biochem Biophys 638: 8–17, 2018

Wright DW, Hall BA, Kenway OA, Jha S, Coveney PV. Computing clinically relevant binding free energies of HIV-1 protease inhibitors. J Chem Theory Comput 10: 1228–41, 2014

Xia YQ, Hua RJ, Juan C, Zhong ZH, Tao CS, Fang R, et al. SIRT6 depletion sensitizes human hepatoma cells to chemotherapeutics by downregulating MDR1 expression. Front Pharmacol 9: 194, 2018

Xu W, Lucke AJ, Fairlie DP. Comparing sixteen scoring functions for predicting biological activities of ligand for protein targets. J Mol Graph Model 57: 76–88, 2015a

Xu Z, Zhang L, Zhang W, Meng D, Zhang H, Jiang Y, et al. SIRT6 rescues the age related decline in base excision repair in PARP1-dependent manner. Cell Cycle 14: 269–76, 2015b

Yamanaka M, Inaka K, Furubayashi N, Matsushima M, Takahashi S, Tanaka H, et al. Optimization of salt concentration in PEG-based crystallization solutions. J Synchrotron Radiat 18: 84–7, 2011

Yang C-Y, Delproposto J, Chinnaswamy K, Brown WC, Wang S, Stuckey JA, et al. Conformational sampling and binding site assessment of suppression of tumorigenicity 2 ectodomain. PLoS One 11: e0146522, 2016

Yang C-Y, Qin C, Bai L, Wang S. Small-molecule PROTAC degraders of the bromodomain and extra yerminal (BET) proteins – a review. Drug Discov Today Technol 31: 43–51, 2019c

Yang T, Zhou R, Yu S, Yu S, Cui Z, Hu P, et al. Cytoplasmic SIRT1 inhibits cell migration and invasion by impeding epithelial–mesenchymal transition in ovarian carcinoma. Mol Cell Biochem 459: 157–69, 2019a

Yang Z, Yik JHN, Chen R, He N, Jang MK, Ozato K, et al. Recruitment of P-TEFb for stimulation of transcriptional elongation by the bromodomain protein Brd4. Mol Cell 19: 535–45, 2005

Yang Z, Yu W, Huang R, Ye M, Min Z. SIRT6/HIF-1α axis promotes papillary thyroid cancer progression by inducing epithelial-mesenchymal transition. Cancer Cell Int 19: 17, 2019b

Yasuda M, Wilson DR, Fugmann SD, Moaddel R. Synthesis and characterization of SIRT6 protein coated magnetic beads: identification of a novel inhibitor of SIRT6 deacetylase from medicinal plant extracts. Anal Chem 83: 7400–7, 2011

Yee A, Chang X, Pineda-Lucena A, Wu B, Semesi A, Le B, et al. An NMR approach to structural proteomics. Proc Natl Acad Sci U S A 99: 1825–30, 2002

Yee AA, Savchenko A, Ignachenko A, Lukin J, Xu X, Skarina T, et al. NMR and X-ray crystallography, complementary tools in structural proteomic of small proteins. J Am Chem Soc 127: 16512–7, 2005

You W, Rotili D, Li T-M, Kambach C, Meleshin M, Schutkowski M, et al. Structural basis of Sirtuin 6 activation by synthetic small molecules. Angew Chem Int Ed Engl 56: 1007–11, 2017

You W, Steegborn C. Structural basis of Sirtuin 6 inhibition by the hydroxamate trichostatin A: implications for protein deacylase drug development. J Med Chem 61: 10922–8, 2018

You W, Zheng W, Weiss S, Chua KF, Steegborn C. Structural basis for the activation and inhibition of Sirtuin 6 by quercetin and its derivatives. Sci Rep 9: 19176, 2019

Yu J, Zhou Y, Tanaka I, Yao M. Roll: a new algorithm for the detection of protein pockets and cavities with a rolling probe sphere. Bioinformatics 26: 46–52, 2010

Yu W, Yang Z, Huang R, Min Z, Ye M. SIRT6 promotes the Warburg effect of papillary thyroid cancer cell BCPAP through reactive oxygen species. Onco Targets Ther 12: 2861–8, 2019

Zhang C, Yu Y, Huang Q, Tang K. SIRT6 regulates the proliferation and apoptosis of hepatocellular carcinoma via the ERK1/2 signaling pathway. Mol Med Rep 20: 1575–82, 2019a

Zhang F, Ma S. Disrupting acetyl-lysine interactions: recent advance in the development of BET inhibitors. Curr Drug Targets 19: 1148–65, 2018

Zhang G, Liu Z, Qin S, Li K. Decreased expression of SIRT6 promotes tumor cell growth correlates closely with poor prognosis of ovarian cancer. Eur J Gynaecol Oncol 36: 629–32, 2015

Zhang P, Tu B, Wang H, Cao Z, Tang M, Zhang C, et al. Tumor suppressor p53 cooperates with SIRT6 to regulate gluconeogenesis by promoting FoxO1 nuclear exclusion. Proc Natl Acad Sci U S A 111: 10684–9, 2014

Zhang Y, Nie L, Xu K, Fu Y, Zhong J, Gu K, et al. SIRT6, a novel direct transcriptional target of FoxO3a, mediates colon cancer therapy. Theranostics 9: 2380–94, 2019b

Zhao J, Cao Y, Zhang L. Exploring the computational methods for protein-ligand binding site prediction. Comput Struct Biotechnol J 18: 417–26, 2020

Zhao K, Harshaw R, Chai X, Marmorstein R. Structural basis for nicotinamide cleavage and ADP-ribose transfer by NAD^+-dependent Sir2 histone/protein deacetylases. Proc Natl Acad Sci U S A 101: 8563–8, 2004

Zhao K, Zhou Z. Post-translational modifications of nuclear sirtuins. Genome Instab Dis 1: 34–45, 2020

Zhao X, Allison D, Condon B, Zhang F, Gheyi T, Zhang A, et al. The 2.5 Å crystal structure of the SIRT1 catalytic domain bound to nicotinamide adenine dinucleotide (NAD+) and an indole (EX527 analogue) reveals a novel mechanism of histone deacetylase inhibition. J Med Chem 56: 963–9, 2013

Zhao Z, Raman MA, Chen ZG, Shin DM. Multiple biological functions of Twist1 in various cancers. Oncotarget 8: 20380–93, 2017

Zhong L, D'Urso A, Toiber D, Sebastian C, Henry RE, Vadysirisack DD, et al. The histone deacetylase Sirt6 regulates glucose homeostasis via Hif1α. Cell 140: 280–93, 2010

Zhou J, Wu A, Yu X, Zhu J, Dai H. SIRT6 inhibits growth of gastric cancer by inhibiting JAK2/STAT3 pathway. Oncol Rep 38: 1059–66, 2017

Zhu B, Yan Y, Shao B, Tian L, Zhou W. Downregulation of *SIRT6* is associated with poor prognosis in patients with non-small cell lung cancer. J Int Med Res 46: 1517–27, 2018

Zhu D, Sun C, Qian X. MST1 suppresses viability and promotes apoptosis of glioma cells via upregulating SIRT6 expression. J Integr Neurosci 18: 117–26, 2019

Ziarek JJ, Peterson FC, Lytle BL, Volkman BF. Binding site identification and structure determination of protein-ligand complexes by NMR a semiautomated approach. Methods Enzymol 493: 241–75, 2011

JONNA TENHUNEN

Human sirtuins (SIRT1-7) are promising drug targets in many diseases. Depending on the disease sirtuins should be either activated or inhibited. In this thesis, novel small molecule inhibitors and activators for SIRT6 were discovered among natural compounds and their derivatives. The binding of these modulators was examined with computational modelling tools. Additionally, regulation of sirtuin expression was investigated as an alternative method to control sirtuin activity. Altogether, this thesis provides new insights to the regulation of sirtuins.

UNIVERSITY OF
EASTERN FINLAND

uef.fi